Aus dem Centrum für Muskuloskeletale Chirurgie

der Medizinischen Fakultät Charité – Universitätsmedizin Berlin

DISSERTATION

Interrelationship of periarticular muscle status,
electromyographic activity, electromechanical delay and
in vivo knee joint loads after total knee arthroplasty

Zusammenhang von periartikulärem Muskelstatus,
Elektromyographie, elektromechanischer Verzögerung und
in vivo Kniebelastungen nach
Knietotalendoprothesen-Implantation

zur Erlangung des akademischen Grades
Doctor medicinae (Dr. med.)

vorgelegt der Medizinischen Fakultät
Charité – Universitätsmedizin Berlin

von

Louisa Bell

aus Hanau

Datum der Promotion: 4. März 2022

Preface

Partial results of this thesis have been previously presented at a conference:

1   Bell L, Damm P, Baur ADJ, Winkler T. The effect of knee muscle status on *in vivo* measured joint loadings after total knee arthroplasty: long-term results. Deutscher Kongress für Orthopädie und Unfallchirurgie (DKOU), Berlin, 2019.

2   Bell L, Winkler T, Baur ADJ, Perka C, Duda GN, Damm P. Einfluss des allgemeinen Muskelstatus auf die Belastung des Kniegelenks. 13. Endoprothetikkongress Berlin (EKB2020), Berlin, 2020.

3   Bell L, Damm P, Baur ADJ, Perka C, Duda GN, Winkler T. Effect of periarticular skeletal muscle status on *in vivo* knee joint loads – an analysis after total knee arthroplasty. 1st Virtual EFORT Congress (VEC), 2020.

Table of Contents

3

Index of Abbreviations

ACL	Anterior Cruciate Ligament
ADL	Activity of Daily Living
AMI	Arthrogenic Muscle Inhibition
BF	Biceps Femoris
BMI	Body Mass Index
BW, %BW	Times Body Weight, Percent Body Weight
CHS	Contralateral Heel Strike
CI	Confidence Interval
CR	Cruciate Retaining
CSA, %CSA	Cross-Sectional Area, Percent Cross-Sectional Area
CT	Computed Tomography
CTO	Contralateral Toe-Off
DICOM	Digital Imaging and Communications in Medicine
DLS	Double-Limb Support
EMD	Electromechanical Delay
EMG	Electromyography
FCSA	Fat Cross-Sectional Area
F, Fres	Force, Resultant Joint Contact Force
GBD	Global Burden of Disease
GL	Gastrocnemius Lateralis
GM	Gastrocnemius Medialis
GR	Gracilis
GRF	Ground Reaction Force
H:Q	Hamstrings to Quadriceps
HL	Lateral Hamstrings
HM	Medial Hamstrings
HU	Hounsfield Units
LCSA	Lean Cross-Sectional Area
M	Moment
MIS	Minimally Invasive Surgery
MPP	Medial Parapatellar
ms	Milliseconds

MRI	Magnetic Resonance Imaging
MU	Motor Unit
MV	Midvastus
N	Newton (load)
NMES	Neuromuscular Electrical Stimulation
OA	Osteoarthritis
OECD	Organisation for Economic Co-operation and Development
OLS	One-Legged Stance
PACS	Picture Archiving and Communication System
PCL	Posterior Cruciate Ligament
PE	Polyethylene
PS	Posterior Stabilized
RF	Rectus Femoris
ROI	Region of Interest
ROM	Range of Motion
SD	Standard Deviation
SLS	Single-Limb Support
SM	Semimembranosus
SR	Sartorius
ST	Semitendinosus
SV	Subvastus
3D	Three-Dimensional
THA	Total Hip Arthroplasty
TKA	Total Knee Arthroplasty
TT	Tibial Tuberosity/ Tubercle
VI	Vastus Intermedius
VL	Vastus Lateralis
VM	Vastus Medialis
YLD	Years Lived with Disability

Abstract (English)

Objectives: The functional status of the periarticular musculature is pivotal for the long-term surgical outcome of total knee arthroplasty (TKA). Increasing rates of TKA implantations in younger, active patients emphasize the importance of implant longevity and postoperative muscle function. Skeletal muscle contractions are considered to affect the loads acting in the knee joint. Synchronized data of *in vivo* knee joint loads and electromyography (EMG) have not been available so far. The aim of this thesis was to analyze the interrelationship between periarticular muscle status, muscle activation patterns and *in vivo* knee joint loads after TKA.

Methods: The retrospective analysis included eight patients (3w, 5m; 69 years [60-75], BMI 29.7 kg/m2 [25-36]) with knee osteoarthritis, who received an instrumented implant (89) in unilateral TKA. All patients underwent computed tomography (CT) and clinical examinations prior to surgery and at a mean follow-up of 30 months (range: 8-48). *In vivo* knee joint loads were measured in all patients at a mean of 26 months (range: 8-45) postoperatively. Surface EMG was recorded synchronously in six patients. Distal femoral muscle volume, cross-sectional area (CSA) and fatty infiltration of periarticular muscles was analyzed by manual segmentation of axial CT-scans using Amira-Avizo and ImageJ software. EMG of the medial and lateral vastus (VM, VL), hamstring (HM, HL) and gastrocnemius (GM, GL) muscles was monitored during activities of daily living. Electromechanical delay (EMD) was quantified using a cross-correlation method.

Results: The average peak knee joint loads were highest during stair descent (3.41 times body weight [BW]), compared to stair ascent (3.05 BW), walking (2.67 BW), sit-to-stand (2.75 BW), stand-to-sit (2.64 BW) and one-legged-stance (2.89 BW). The intramuscular fat ratio of the quadriceps (–2.8±2.9%CSA, $p<0.05$) and hamstrings (-4.1±3.2%CSA, $p<0.01$) decreased after TKA. Distal quadriceps volume decreased by –9.6±5.7% ($p<0.01$). Fatty infiltration of the hamstrings (r=0.77, $p<0.05$) and VL (r=0.75, $p<0.05$) correlated with increased knee joint loads during walking. VM (23-30% load cycle) and GM (64-73% load cycle) muscle activity contributed to the peak knee joint loads during walking (r=0.94, $p<0.01$) and stair ascent (r=0.87, $p<0.05$), respectively. The mean EMD of VM and VL ranged from 33.7 to 137.4 ms during the ADLs. VL fatty infiltration correlated with lower peak activity levels (r=–0.92, $p<0.01$) and joint loading rates (r=–0.83, $p<0.05$) during stair climbing.

Conclusion: The results suggest that fatty infiltration of the joint stabilizing musculature increases the magnitude and rate of knee joint loads. The EMG data indicate that phasic muscle activity patterns are associated with the generation of peak knee joint loads. Improvements in periarticular muscle status and inter-muscular coordination could contribute to reduced knee joint loads and thus to improved long-term outcomes after TKA.

Abstract (German)

Fragestellung: Der periartikuläre Muskelstatus ist entscheidend für das Langzeitergebnis nach Knie-Totalendoprothesen (K-TEP) Implantation. Durch die steigende Zahl implantierter K-TEPs bei jüngeren, aktiven Patientinnen und Patienten werden Implantatbelastbarkeit und postoperative Muskelfunktion zunehmend wichtiger. Es wird angenommen, dass Muskelkontraktionen die Belastung im Kniegelenk beeinflussen. Bisher waren synchronisierte Daten der *in vivo* Kniebelastung und Elektromyographie (EMG) nicht verfügbar. Ziel dieser Arbeit war es den Zusammenhang zwischen periartikulärem Muskelstatus, Muskelaktiviät und *in vivo* Kniebelastung nach K-TEP zu analysieren.

Methodik: Die retrospektive Analyse umfasste acht Arthrose-Patienten (3w, 5m; 69 Jahre [60-75], BMI 29,7 kg/m2 [25-36]), die eine instrumentierte K-TEP (89) erhielten. Bei allen Patienten wurde präoperativ und 30 Monate (Spanne: 8-48) eine klinische Untersuchung und Computertomografie (CT) durchgeführt. *In vivo* Belastungen im Kniegelenk wurden bei allen Patienten 26 Monate (Spanne: 8-45) postoperativ gemessen. Das EMG wurde synchron bei sechs Patienten erfasst. Distal femorales Volumen, Querschnittsfläche (CSA) und fettige Infiltration der periartikulären Muskeln wurde durch manuelle Segmentierung axialer CT-Schichten mit Amira-Avizo und ImageJ-Software analysiert. Das EMG des medialen und lateralen M. vastus (VM, VL), ischiokruraler Muskulatur (HM, HL) und M. gastrocnemius (GM, GL) wurde bei Alltagsaktivitäten gemessen. Die elektromechanische Verzögerung (EMD) wurde mit einer Kreuzkorrelationsmethode quantifiziert.

Ergebnisse: Am höchsten war die Kniebelastung beim Treppabgehen (3,41-faches Körpergewicht [KG]), im Vergleich zum Treppaufgehen (3,05 KG), Gehen (2,67 KG), Aufstehen (2,75 KG), Hinsetzen (2,64 KG) und Einbeinstand (2,89 KG). Der intramuskuläre Fettgehalt des M. quadriceps femoris ($-2,8\pm2,9$%CSA; $p<0,05$), HM und HL ($-4,1\pm3,2$%CSA; $p<0,01$) nahm postoperativ ab. Das distale Quadrizepsvolumen nahm um

–9,6±5,7% (p<0,01) ab. Der intramuskuläre Fettgehalt des VL (r=0,75; p<0,05), HM und HL (r=0,77; p<0,05) korrelierte mit höheren Belastungen beim Gehen. Die Aktivität des VM (23-30% Lastzyklus) und GM (64-73% Lastzyklus) beeinflusste die Spitzenbelastung entsprechend beim Gehen (r=0,94; p<0,01) und Treppaufgehen (r=0,87; p<0,05). Das mittlere EMD des VM und VL betrug 33,7 bis 137,4 ms bei den Aktivitäten. Fettige Infiltration des VL führte zu reduzierten Spitzenaktivitäten (r=–0,92; p<0,01) und beschleunigten Lastentwicklungen (r=–0,83; p<0,05) beim Treppensteigen.

Schlussfolgerung: Die Ergebnisse deuten darauf hin, dass eine fettige Infiltration der gelenkstabilisierenden Muskulatur Belastungen im Knie erhöht. Die EMG Daten weisen einen Zusammenhang zwischen phasischer Muskelaktivität und Spitzenbelastung auf. Eine Verbesserung von periartikulärem Muskelstatus und inter-muskulärer Koordination könnte zu reduzierten Kniebelastungen und einem verbesserten Langzeitergebnis nach K-TEP beitragen.

1   Introduction and Objectives

1.1   Total knee arthroplasty

Total knee arthroplasty (TKA) is one of the most successful orthopedic interventions and one of the most common elective surgical procedures performed worldwide (1). TKA involves resection and total prosthetic replacement of damaged articular surfaces of the tibio-femoral joint, with or without patellofemoral replacement, in patients with end-stage degenerative joint disease (2). Since the initial developments of knee replacement surgery in the early 1950's (3), TKA has evolved to a reliable, cost-effective (4) treatment standard with the aim of relieving pain and restoring joint mobility and function. At present, TKA is generally related to high clinical success rates (2, 5).

In Germany, the total number of primary TKA procedures was 190,427 in 2018, according to nationwide inpatient statistic reports (6). In an international comparison by the Organization for Economic Co-operation and Development (OECD) in 2015, Germany ranked fourth place in the highest annual frequency of TKA procedures, after Switzerland, the United States and Austria (7). The international average rate of primary and revision TKA was estimated at 175 and 149 procedures per 100,000 population, respectively, by a survey of 18 countries conducted in 2011 (1). The rates of primary and revision knee replacements increased in Germany from 2005 to 2011 by 22% (27,000 cases) and 64% (6,200 cases), respectively (8). Global projections estimate a substantial increase in TKA volume in the upcoming years with rates exceeding those of total hip joint replacement (1, 9). In addition, future estimates of TKA prevalence indicate a secular trend towards a younger and more active patient population (10, 11). Patients' expectations in terms of implant longevity and rapid postoperative recovery are likewise expected to rise. Excessive joint loadings and an impaired muscle function can contribute to mechanical instability, aseptic loosening and wear of the implant and thus gain increasing importance for the long-term outcome of TKA (12, 13).

1.1.1   Indications and contraindications

The primary indication for elective TKA is end-stage knee osteoarthritis (OA), a progressive disease of the synovial knee joint with degeneration of weight-bearing articular surfaces (2, 14, 15). Besides, TKA is considered a treatment option for immune-mediated, inflammatory types of arthritis, such as rheumatoid arthritis and psoriatic arthritis (2, 5, 14). Further TKA indications include avascular necrosis (16), posttraumatic degenerative joint disease (17) and

haemophilic arthropathy (18). In general, surgical considerations are based on the patient's symptoms of persistent knee pain and physical impairment and on the radiographic evidence of structural joint damage. Patients are scheduled for TKA in case symptoms are refractory to non-surgical or other disease-specific treatment regimens.

The musculoskeletal disorder of OA accounts for the main share in TKA indications and represents a major socioeconomic burden worldwide (19, 20). The global prevalence of symptomatic knee OA was 3.8% (95% confidence interval (CI) 3.6% to 4.1%) in 2010 (19), overall affecting 9.6% of men and 18% of women of ≥60 years of age (20). Estimates indicate that the incidence of knee OA will increase exponentially in the upcoming decades due to the aging of societies and growing rates of obesity (21, 22). The rising prevalence of OA is anticipated to have major implications for future primary care and public health, as knee OA is considered a leading cause of disability worldwide (19, 22). The Global Burden of Disease (GBD) 2017 study reported a significant increase by 63.7% (95% CI 61.5% to 64.9%) from 1990 to 2007 and by 30.8% (95% CI 30.1% to 31.6%) from 2007 to 2017, in the years of life lived with disability (YLDs) due to knee OA (23). Long-term disability is mainly ascribed to functional limitations in knee range of motion (ROM), as well as pain, stiffness, swelling, and local inflammation of the affected knee joint (24). TKA is considered an effective treatment option to restore joint function, alleviate pain and thus improve patients' quality of life (14).

The pathogenesis of knee OA is multifactorial and mainly characterized by the destruction and loss of weight-bearing cartilage, bone hypertrophy with formation of bone spurs (i.e. osteophytosis), synovial inflammation and remodeling of the subchondral bone (25). Local degenerative changes are associated with prolonged biomechanical stresses, which exceed the joint load-bearing capacities (26). The main risk factors for the incidence and progression of knee OA are likewise of mechanical nature and include high body weight, physical activity, trauma, malalignment and knee joint instability (22, 27). Although several studies have related muscle weakness to the etiology of knee OA (28, 29), literature remains inconclusive on the interaction between periarticular muscle status and knee joint loading conditions.

Treatment selection for knee OA patients is based on the stage of disease severity, assessed by means of clinical evaluation and radiological examination. Radiographic grading schemes are used to classify OA severity on an ordinary scale (0 to 4, normal to severe) with regard to the formation of osteophytes, periarticular ossicles, joint space narrowing and sclerosis, cysts and

bone end deformity (30). Controversy exists on the extent to which radiographic OA features correlate with patient symptoms (31). TKA is a definitive treatment for advanced knee OA in patients with persistent disabling symptoms after exhaustion of nonsurgical treatment options. Nonoperative regimens include physical therapy, patient education, exercise, intra-articular corticosteroids, non-steroidal anti-inflammatory drugs and weight management (32).

Contraindications for TKA are acute local or systemic infection, severe peripheral vascular disease and comorbidities that confer an increased risk for severe perioperative complications (14). Obesity, defined as a body mass index (BMI) of ≥ 30 kg/m^2, does not represent a contraindication for TKA, but has been related to an elevated risk of deep infection, shortened implant survival and higher revision rates (14, 33, 34). In a review of 5088 primary TKAs, Abdel et al. (34) showed a twofold risk of revision due to aseptic tibial component loosening in patients with a BMI of ≥ 35 kg/m^2. The use of cemented tibial stem extensions with obesity has been suggested as a means to improve implant fixation and load-distribution (34, 35).

1.1.2 Surgical approaches and implant design

Several different surgical approaches exist to gain access to the knee joint in TKA, including the medial parapatellar (MPP), midvastus (MV), subvastus (SV) and the lateral approach (36). The quadriceps snip, quadriceps turndown and tibial tubercle osteotomy are extensive approaches used for joint exposure mostly in revision TKA (36, 37). Minimally invasive surgery (MIS) techniques have been developed with the aim to minimize violation of the extensor mechanism and thus achieve an earlier functional recovery (38, 39). MIS approaches include the quadriceps-sparing, mini-SV, mini-MV, and MIS lateral approach (38-40).

The MPP approach is the most widely used arthrotomy and considered a successful standard for exposure of the knee joint in TKA (36, 37). As first described by von Langenbeck in 1878 (41), the MPP approach involves an incision at the medial patellar border and the detachment of the vastus medialis (VM) tendon from its insertion onto the patella (37). The approach provides by an excellent exposure to the joint and enables an easy lateral dislocation of the patella (36). The main concern regarding potential disadvantages of the MPP approach is, however, the intraoperative violation of the knee extensor mechanism by incision of the quadriceps tendon. Long and short term impairments in quadriceps function and postoperative recovery have been reported as a result thereof (13, 42). A prospective study by Mizner et al. (42) of 2005 thus revealed a loss in quadriceps strength, failure in voluntary muscle activation

and a reduction in quadriceps cross-sectional area (CSA) by 10% in the early postoperative period. Data on the long-term changes in the status of the periarticular musculature and their relative impact on muscle activation patterns and joint loads are limited.

Highlighting the relevance of the quadriceps mechanism, Hofmann propagated the quadriceps sparing SV approach in 1991 (43). The SV approach preserves the tendinous insertion of the VM onto the patella and retains a better medial patellar blood supply (36, 37, 44). Deep subcutaneous tissues are mobilized by a full thickness flap and the VM is bluntly dissected and lifted off the medial intermuscular septum (37). The advantages of the SV approach include reduced pain, higher initial quadriceps torque, earlier straight leg raise and better knee flexion in the early postoperative period (44, 45). The SV method poses, however, constraints to the exposure of the joint and eversion of the patella. As mobile subcutaneous tissues are required to gain appropriate access to the joint, use of the SV approach is technically more demanding in obese or muscular patients, muscle contractures or a status after revision surgery with scar tissue formation (36, 44).

In order to achieve a trade-off between the MPP approach with a suitable joint exposure and the quadriceps preserving SV method, Engh developed the MV technique in 1997 (46). Though the quadriceps tendon and medial insertion of the VM remain intact, the approach involves incising and splitting the VM muscular substance in parallel direction of its muscle fibers (36, 37). Improvements over the MPP approach include a lower intraoperative blood loss and reduced need for lateral retinacular releases (47, 48), while providing a better exposure and patellar flip than the SV approach (36). Despite these advantages, there is an increased risk for iatrogenic neurovascular injury and resulting denervation of the oblique part of the VM (36). Electromyographic abnormalities in the VM were reported by Parentis et al. (47), whereby controversy exists regarding the extent to which postoperative changes in neuromuscular activity affect the long-term functional outcome of TKA (48).

Less invasive MIS approaches for TKA have gained increasing attention in recent years in an aim to preserve the extensor musculature and thus improve postoperative functional recovery. Several studies reported a better postoperative ROM, reduced pain, faster rehabilitation and shorter hospital stay for MIS TKA (38-40, 49). There is a debate on the extent to which clinical advantages are off-set by limitations in intraoperative view, longer operation time, higher risks for complications and malalignment and the need of specific instrumentation (39,

40, 50). The use of downsized MIS instruments is expected to reduce soft tissue strains, as external compression by traditional retractor devices was shown to impede local perfusion and increase intramuscular pressure (51). Müller et al. (52) determined that surgical muscle trauma and associated structural changes of fatty muscle atrophy can be reduced by the use of MIS techniques in total hip arthroplasty (THA). Von Roth et al. (53) likewise demonstrated that multiple THA revisions are associated with an increase in fatty muscle degeneration due an amplified intraoperative muscle damage. To date, there is a paucity of research on how far qualitative changes in periarticular knee musculature after TKA impact upon the internal loads acting in the knee implant.
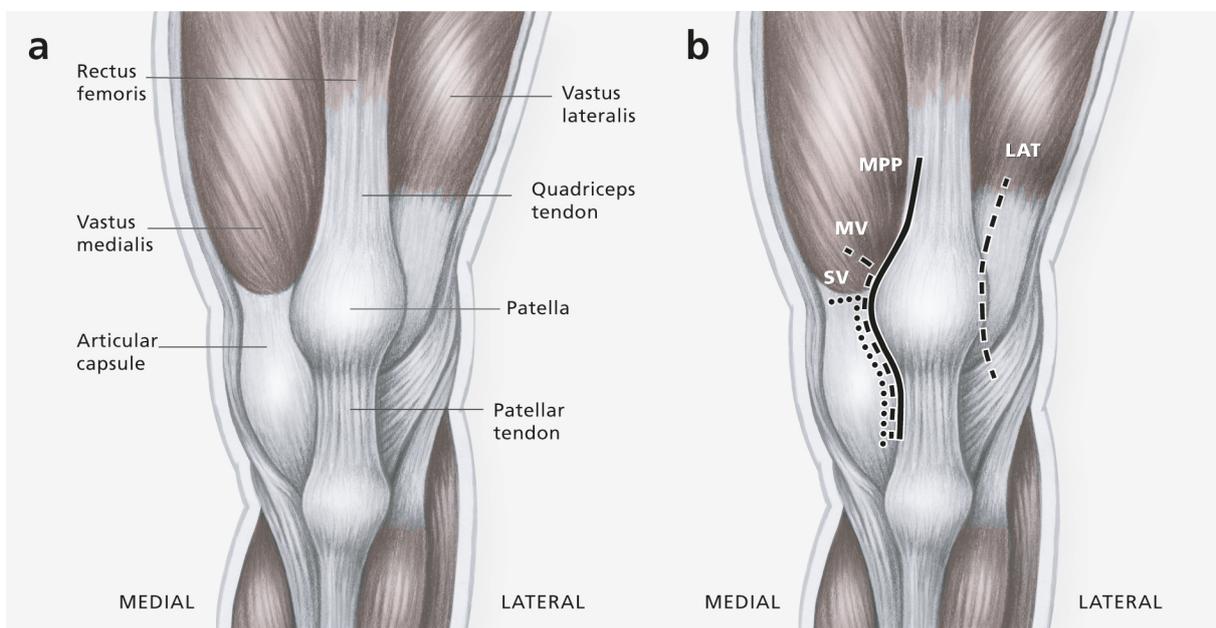
Figure 1. Surgical approaches in TKA. Overview over anatomical landmarks used for arthrotomy (**a**) and the surgical incision lines of the medial parapatellar (MPP), subvastus (SV), midvastus (MV) and lateral (LAT) approach (**b**). The illustration was adapted from Cristea et al. [36]

Implant design for TKA has to meet anatomical and mechanical requirements of restoring functional knee ROM and kinematics, secure fixation, articular congruence, biocompatibility, high wear resistance to contact stresses and homogenous load distribution. The development of total condylar knee replacement dates back to the first polycentric implant designed by Guston in 1968 (54). Early implant designs were associated with high rates in periprosthetic knee infection and mechanical failure (54). Technological advancements lead to the evolution of modern prosthesis designs and related concepts of constraint, femoral rollback and modularity (55-58). Constraint refers to the capacity of the implant to stabilize flexion-extension and varus-valgus movements (55). From contemporary implant models cruciate

retaining (CR) designs are considered the least constrained, with levels increasing for posterior stabilized (PS), unlinked constrained, rotating hinge and non-rotating hinged implants (55). Femoral rollback describes the posterior femoral translation with knee flexion. The posterior cruciate ligament (PCL) remains intact in CR implants and is replaced by a cam mechanism in PS designs. Both types of implants provide femoral rollback, while PS designs have been considered to show more predictable contact mechanics with knee flexion (56). Constrained unlinked and rotating hinge designs are indicated in difficult cases, including ligament insufficiency, hyperlaxity and bone loss (57). Modularity allows for prosthesis adjustments and involves, for example, the use of mobile-bearing designs in which the polyethylene (PE) insert is not fixed to the tibial tray (58). An advanced understanding of the *in vivo* loads acting in the artificial joint is pivotal for future optimizations in implant design.

1.1.3 Complications and soft-tissue defects

Complications of TKA encompass local wound infections, instability, malalignment, vascular or peroneal nerve injury, thromboembolic disease, periprosthetic fracture, dislocation, patellar maltracking and wear of implant bearing surfaces (14, 59). Extensor mechanism complications occur in ≤1 to 12% and include patellofemoral instability, quadriceps and patellar tendon ruptures and periprosthetic patellar fractures (60). Anterior knee pain is a common problem following TKA that results, amongst others, from functional malalignment, instability and postoperative impairments in muscular coordination (59, 61). Intraoperative muscle retraction and dissection of soft tissues may compromise blood flow of the medial genicular arteries supplying the extensor mechanism (36, 60) and potentially lead to degenerative changes in muscle architecture (51). Muscle atrophy and fatty degeneration were shown to have a negative impact on postoperative outcomes (13, 42) and mobility function (62). Pathologic and clinical aspects of structural skeletal muscle damage are further outlined in section 1.4.

1.2 Functional anatomy of the knee

The anatomy of the knee joint comprises osseous structures, cartilage, ligaments and skeletal muscles, which provide a dynamic mechanical framework for human locomotion during various loading conditions. The successful surgical reconstruction of the functional knee anatomy is thus decisive for patients to return to daily and sporting activities.

The knee is composed of three articulations, including the medial and lateral tibio-femoral joint and the patello-femoral joint (63). The articular junction of the femoral condyles with the tibial plateau functions as a modified hinge joint that allows for force transmission across the load-bearing contact surfaces. Frictionless force transfer and muscular contraction efficiency is enhanced by the gliding patello-femoral joint at the anterior distal femur, which increases the moment arm of the knee extensor mechanism (64). Active and passive knee motion occurs in six degrees of freedom of three translations (anterior-posterior, medio-lateral, compression-distraction) and three rotations (65). The rotational range of motion (ROM) occurs in the sagittal (flexion-extension), transverse (internal-external rotation) and frontal (varus-valgus rotation) plane (65). Flexion and extension movements are a combined motion of rolling and femoral gliding. Steultjens et al. (66) determined that impairments in joint ROM contribute to increased levels of self-reported and observed disability in OA patients. Preoperative ROM was also described by Ritter et al. (67) as a major predictor of both the postoperative ROM and kinematic outcome of TKA.

Joint contact stresses are minimized by articular cartilage and menisci, which increase the congruity of the tibio-femoral joint and distribute joint loads over a broad surface area (63). Degenerative changes in articular cartilage and subchondral bone remodelling have been linked to the initiation and progression of knee OA (25, 68). This association has been exemplified in a study by Cicuttini et al. (68), in which the rate of articular cartilage volume loss predicted the four-year risk of primary TKA. Frictionless movement is guided by static ligaments that function as primary knee stabilizers by posing kinematic constraint on translational and rotational joint displacement (63). The four main stabilizing ligaments are the anterior cruciate ligament (ACL), posterior cruciate ligament (PCL), medial collateral ligament and lateral collateral ligament (63). There is controversy as to whether PCL retention in TKA may restore more physiological ROMs or rather contribute to increased joint loads and PE wear in case of incorrect PCL tensioning (56, 69).

Dynamic knee stability is provided by the periarticular musculature, which generates active forces while sustaining lower limb stability during locomotion and postural tasks. The quadriceps femoris is part of the extensor mechanism at the anterior aspect of the knee and consists of the rectus femoris (RF), vastus intermedius (VI), vastus medialis (VM) and vastus lateralis (VL) muscles (63). The conventional MPP approach in TKA poses the distal oblique portion of the VM at a potential risk for surgical trauma due to its 50° angular insertion into

the superomedial border of the patella (70). Mizner et al. (42, 71) reported that postoperative muscle weakness is an important determinant for the functional outcome of TKA. Muscle weakness is generally thought to result from a loss of muscle mass, fatty infiltration or activation deficits, which have potential implications on postoperative joint contact stresses and disability (72, 73). Meier et al. (13) emphasized the need for extended rehabilitation regimens to target quadriceps impairments, as these seem to account primarily for long-term functional deficits after TKA. There has only been limited analysis of how far the knee joint loadings are affected by the long-term changes in periarticular muscle status after TKA.

The sartorius (SR) and gracilis (GR) muscles, at the medial compartment of the knee, assist knee flexion and internal rotation and insert with the ST into the pes anserinus at the anteromedial tibia (63). The gastrocnemius (G) is a biarticular muscle that has a dual action of knee flexion and plantar flexion, coupling the knee and ankle joint. Mündermann et al. (74) showed that changes in gait pattern due to severe knee OA are associated with increased axial loading rates at the foot, which can be transferred to the knee joint during level walking. The biceps femoris (BF), semimembranosus (SM) and semitendinosus (ST) muscles constitute the hamstring group at the posterior thigh and function foremost as knee flexors (63). Silva et al. (75) found a higher isometric hamstring:quadriceps (H:Q) strength ratio at an average of 2.8 years after TKA, indicating a relatively lower postoperative quadriceps isometric strength. High H:Q ratios thereby positively correlated with lower Knee Society Functional Scores and a high BMI. Evidence suggests that loads generated by muscle contraction may exceed those exerted by external forces, such as the ground reaction force (GRF) (76, 77). Knowledge on the relative impact of hamstring muscle status on *in vivo* knee joint loadings and muscle co-contraction patterns in the postsurgical course of TKA is limited.

1.3 Biomechanics of the knee joint

1.3.1 Joint loadings and moments

Given that OA can be regarded as "a disease of mechanics" (78), a profound understanding of joint loading conditions is of clinical significance for the prevention and treatment of knee OA. Joint loads result from tibio-femoral compressive forces, as well as tensile forces that are transmitted by muscles, tendons and ligaments (77). A force (F) is generally defined as mass times acceleration ($F = m*a$) expressed in the standard international unit of Newton (N). A joint moment (M), or torque, describes the turning effect about a joint axis that is produced by

a force over the perpendicular distance from the axis of rotation (i.e. lever arm). Force and moment vectors act in a three-dimensional rectangular coordinate system with components in the x, y and z direction (Figure 3a) (79). In a static equilibrium the vector sum of all forces and moments equals zero ($\Sigma F = 0$, $\Sigma M = 0$) (79). The post-arthroplasty activity levels and body weight of TKA patients are considered important determinants of joint loading and implant longevity (80, 81).

Repetitive movement patterns, such as human gait, can be described as a cyclical process, as shown in Figure 2. The gait cycle consists of a weight bearing or stance phase, which constitutes 60% of the cycle, and a non-weight bearing or swing phase of 40% during which the ipsilateral foot is lifted off the ground. During walking internal forces generated by the musculoskeletal system counteract the GRF (76, 82). Demanding tasks, such as stair climbing, have been associated with increased joint contact forces as they involve greater knee flexion angles and thus less conformity of articulating surfaces (83, 84). Andriacchi et al. (85) determined that the largest external knee flexion moments during stair descent occur at an angle of approximately 50° flexion and largely exceed those during level walking.
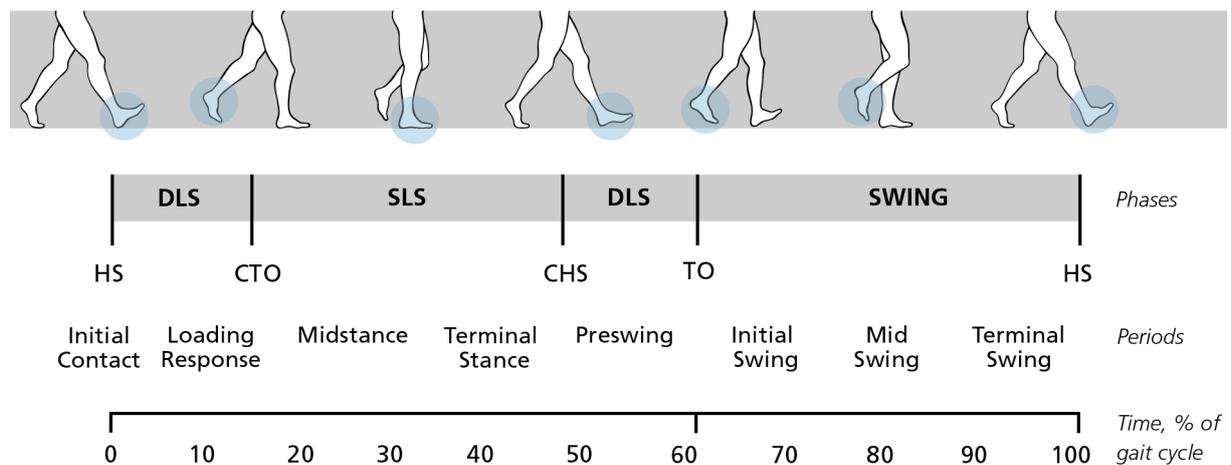
Figure 2. The gait cycle. Representation of the phases and periods of one gait cycle with right leg dominance. DLS, double-legged stance; SLS, single-legged stance; HS, heel strike; CTO, contralateral toe-off; CHS, contralateral heel strike; TO, toe-off. Graphic by Louisa Bell.

1.3.2 Measurement of joint contact forces

The measurement of *in vivo* joint contact forces during dynamic activities represents a major challenge. Computational modelling approaches have been developed in the past to estimate joint contact forces using inverse dynamics or electromyography (EMG) driven analyses (83, 86, 87). These techniques use kinematic gait data and the GRF as input parameters for

mathematical models. Calculated joint forces reported in literature show, however, considerable variations, with maximum values ranging from 190% body weight (%BW) to 720% BW during level walking (87). Challenges in mathematical modelling result from the complex nature of musculoskeletal motion and include soft tissue movement, agonist-antagonist muscle activities and biarticular muscle functions (86, 87). In order to overcome these difficulties implantable systems have been proposed to measure joint contact forces *in vivo*. The first instrumented device was implanted in the distal femur during the surgical treatment of osteosarcoma and allowed for transfer of femoral shaft forces to the knee joint (88). More recently, Heinlein et al. (89) developed an instrumented implant for TKA that enables the direct measurement of all six force and moment components acting in the knee joint (see 2.3.3). Despite major advances in the analysis of knee joint loadings, the interrelation with dynamic EMG activity and the status of the periarticular musculature after TKA remains to be established. The principle of surface EMG is outlined in section 1.5.1.
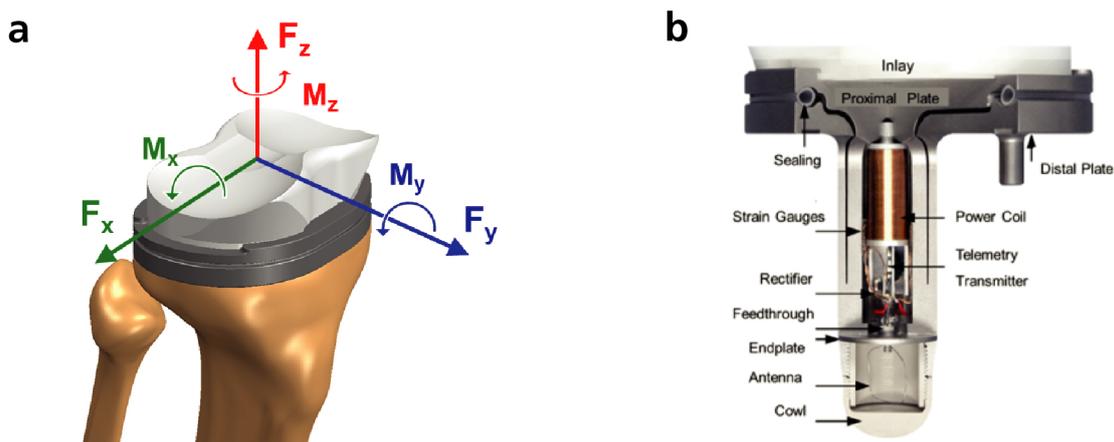
Figure 3. Instrumented knee implant. Coordinate system (**a**) of the tibial component as previously published[134]. Force (F) and moment (M) components act along the coordinate axes x, y, z. Cross-sectional view of the instrumented tibial component (**b**) developed by Heinlein et al.[89]

1.4 Skeletal muscle damage

1.4.1 Muscle atrophy and fatty degeneration

The mechanism of iatrogenic muscle damage has been generally ascribed to approach-related surgical incisions, retractor compression, tourniquet use or peripheral nerve injury (13, 51, 90, 91). Soft-tissue damage may lead to changes in muscle morphology and metabolism (91) and has been related to postoperative functional limitations (42, 52, 71). Muscle impairments have, besides, been implicated in the onset and progression of knee OA (28, 29, 92). Hence, the pathologic processes of muscle atrophy and fatty degeneration have received considerable attention in recent years regarding their impact on muscle function and recovery.

Muscle atrophy is defined as a reduction in myofiber diameter (93) and commonly assessed by means of volume or CSA measurements (94). On a molecular level, atrophic changes have been related to an activation of proteolytic signaling pathways, such as the NfκB, autophagy-lysosome or IGF1/Akt/FoxO pathway, which induce the degradation of contractile proteins (93). Histopathologic analyses of disuse and denervation atrophy have, besides, shown a selective atrophy of type I muscle fibers and a shift to type II fast-twitch fibers (95). An atrophy-related loss of muscle fibers has been linked to a replacement by fibrous-adipose tissue and a decline in muscle contraction efficiency (72). The Health, Aging and Body Composition Study (Health ABC) study, which examined 3075 non-disabled older adults (70-79 years) for over 12 years, reported that reductions in midthigh muscle CSA and increased fatty infiltration are related to an impaired lower extremity function (96).

Fatty infiltration of skeletal muscle, also referred to as myosteatosis, has been shown to correlate with a loss of functional muscle quality (97), defined as a measure of muscle strength per unit CSA. The concept of fatty infiltration is based on the accumulation of lipids between muscle fibers and has been recognized as a "novel depot" of ectopic fat (72, 98). It is now well established that adipose tissue is metabolically active, secreting proinflammatory cytokines that raise oxidative stress and impair muscular contractile performance (97, 99). Goodpaster et al. (100) found, accordingly, that muscle lipid deposition is associated with the proinflammatory states of insulin resistance and obesity, but can potentially be reversed by interventions that target weight loss. Hence, fatty infiltration seems to contribute to both metabolic and structural changes, which may consequently lead to muscle weakness and impairments in functional mobility (101, 102).

1.4.2 Grading methods

A wide array of grading methods has been proposed for the assessment of muscle function and morphology. Motor performance can be evaluated by clinical assessment and functional scores (103). Muscle damage may be indicated by an elevation of certain biochemical markers, including creatine kinase, lactate dehydrogenase, myoglobin or antioxidant enzymes, as outlined in a review by Brancaccio et al. (104). Muscle composition and morphology can be assessed using the non-invasive imaging techniques of ultrasound, magnetic resonance imaging (MRI) or computed tomography (CT) (105, 106). CT has emerged as a reliable method for the quantitative analysis of muscle atrophy and adipose tissue infiltration (94).

Measurements of muscle volume are generally computed from a series of contiguous axial muscle CSAs. Different types of tissue can be discerned by means of their attenuation characteristics measured in Hounsfield Units (HU). Mitsiopoulos et al. (106) validated CT and MRI measurements of fatty infiltration against cadaveric studies and proposed both techniques as reference methods in muscle composition studies. Goodpaster et al. (105) likewise determined that reduced muscle attenuation ranges on CT are consistent with an increased lipid content of muscle biopsy samples. Besides, CT analysis of fatty infiltration was shown to be of clinical relevance, as strong associations were found between lower muscle attenuation and reductions in muscle aerobic capacity and strength (96, 99).

1.5 Surface electromyography (EMG)

1.5.1 Signal transduction and neuromuscular patterns

Surface EMG is generally regarded as a suitable technique to analyze the phasic activity of muscles during various activities of daily living (ADLs) (107, 108). Signals in dynamic EMG analysis represent a composite of the muscle fiber action potentials at a single motor unit (MU), i.e. the muscle fibers innervated by a single alpha motor neuron (107). In response to neural stimulation, MU contraction is initiated by depolarization of the muscle fiber membrane. The ion movement involved in depolarization evokes a transmembrane electrical field that can be detected non-invasively on the skin surface above the muscle (107). Clark and Manini (73) reviewed that the degree of muscle activation and force generation is dependent on the firing rate and number of recruited MUs, as well as muscle morphology. Neuromuscular activation deficits were thereby found to have a greater impact on age-related strength loss than sole declines in muscle mass.

Recordings of EMG activity are considered to reflect the functional state of muscles, whereby muscle weakness was found to correlate with decreased MU recruitment patterns (29). In a review by Rice and McNair (109) quadriceps strength deficits observed in OA and after knee surgery were largely ascribed to the process of arthrogenic muscle inhibition (AMI). AMI is based on the concept that structural damage at the joint level may reinforce inhibitory afferent signals to supraspinal centers, which thereupon decrease voluntary muscle activation and force production. Hence, impairments in activation have been associated with radiographic OA severity and muscle weakness (92, 110, 111). The presence of anterior knee pain has been related to abnormalities in the timing pattern of VM and VL muscle activation (61). Several

studies have reported gradual improvements of voluntary quadriceps activation over a postsurgical period of three years (112, 113). The evidence that muscle status and knee loads are associated with muscle activation patterns is inconclusive.

1.5.2 Electromechanical delay (EMD)

The concept of EMD defines the temporal relationship between muscular activity measured with EMG and the onset of mechanical force generation. The time lag from muscle activation to force-time records has traditionally been based on the measurement of muscle forces (114, 115). The EMD values reported in the literature comprise the electrochemical processes required for the generation of muscle force. These include the synaptic transmission and propagation of action potentials along muscle fibers, excitation-contraction-coupling and stretching of the series elastic component to initiate joint movement (114-116). Winter et al. (117) defined EMD as the time lag between muscle activation and the onset of movement.

There is ongoing research to identify determinants of EMD, as it has been shown that changes in EMD may reflect alterations in the force generating capacity and structural properties of muscles. Bell et al. (118) determined that gender differences in muscular strength partly emerge from differences in EMD. Higher maximum strength values in men were thus associated with shorter electromechanical-response times. Muscle fatigue, on the contrary, was found to correlate with an elongated EMD (119). More recently, Hopkins et al. (120) reported a prolonged peroneus longus latency in patients with functional instability of the ankle joint. Although mechanisms of epimuscular force transmission have been extensively studied in the past (121), the temporal relation of muscle activation and joint load is largely unknown. The present thesis thus aims to provide a novel measure of the time lag between the onset of muscle activation and the onset of the *in vivo* contact forces acting in the tibio-femoral joint during dynamic ADLs.

1.6 Aim, hypothesis and objectives

The **aim** of this thesis was to analyze the status of the periarticular knee musculature, EMG data and *in vivo* tibio-femoral joint loads during dynamic ADLs in the long-term after TKA and to correlate these parameters. The increasing prevalence of TKA in younger patients, leading more active lifestyles than the elderly, highlights the importance of muscle function and implant longevity in the postoperative course. Understanding the interrelationship between biomechanical joint loads and postoperative changes in muscle morphology and electromyographic activity could contribute to future advancements in implant design, surgical technique and rehabilitation.

In the light of available data in the literature, the **hypothesis** of this thesis was that degenerative changes of periarticular knee muscle atrophy and fatty infiltration after TKA lead to consecutive activation deficits and increased knee joint loads. The VM muscle was expected to be subject to greater change than other periarticular muscles due to its potential violation in the course of the MPP approach for surgical exposure of the knee joint. Hence, this thesis was set out to quantify the size and degree of fatty infiltration of the periarticular musculature using pre- and postoperative axial CT scans. *In vivo* knee joint loads were measured across a range of ADLs via instrumented knee implants. To investigate concurrent dynamic muscle activity, surface EMG recordings were analyzed relative to the time history of the *in vivo* knee joint loads. The interrelationship between these parameters was determined in order to foster a better understanding of the impact of periarticular muscle status and function on the *in vivo* knee joint loadings after TKA.

Concluding, the **objectives** of this thesis were to analyze postoperative:

1. *in vivo* loadings of the tibio-femoral joint during ADLs
2. changes in periarticular muscle status
3. muscle activation patterns and EMD
4. associations of periarticular muscle status, EMG parameters and *in vivo* joint loads

in patients undergoing primary TKA for symptomatic knee OA.

2   Methods

2.1   Study design

This multicenter retrospective observational study was conducted at the Julius Wolff Institute for Biomechanics and Musculoskeletal Regeneration, the Center for Musculoskeletal Surgery and the Department of Radiology, Charité-Universitätsmedizin Berlin, Germany; the Department of Orthopedic Surgery at Sana Kliniken Sommerfeld, Kremmen, Germany; the Center for Sports Science and Sports Medicine Berlin (CSSB), and at the ETH Zürich Institute for Biomechanics, Switzerland. All investigations were performed in accordance with the Declaration of Helsinki. The study was approved by the local Ethics Committee of the Charité (EA4/069/06) and registered in the 'German Clinical Trials Register' (DRKS00000606). The purposes and procedures of the study were completely explained to all participants and written informed consent was obtained before enrollment.

All knee OA patients received an instrumented knee prosthesis in the course of primary TKA surgery. A comprehensive medical evaluation was performed by an orthopedic surgeon preoperatively and at the follow-up examinations. Postsurgical care and rehabilitation were performed according to a standardized protocol. Patients received CT imaging, one day prior to TKA and 30 months (range: 8-48) postoperatively. *In vivo* tibio-femoral forces were measured during six activities of daily living, an average of 26 months (range: 8-45) postoperatively. EMG signals were recorded simultaneously with the *in vivo* joint load measurements.

2.2   Patients

A total of nine (n=9) patients who were scheduled to undergo primary unilateral TKA for primary knee OA from June 2007 to May 2009 were recruited for participation. One patient was excluded, as no postoperative CT scans, eligible for analysis of muscle CSA, were available. Knee OA was evaluated on the basis of medical history, clinical examination and radiographic assessment. Eligibility criteria for OA patients were (1) symptomatic primary knee OA with indication for conventional TKA, (2) age older than 50 years, (3) bodyweight below 100kg. Exclusion criteria included (1) active implants (e.g. cardiac pacemakers), (2) inflammatory diagnosis (e.g. rheumatoid arthritis), (3) neuromuscular pathologies interfering with gait analysis. Patient characteristics were obtained from medical records and included age, gender, body weight and height.

2.3 TKA procedure

2.3.1 Surgical characteristics

The patients underwent tri-compartmental TKA through the standard MPP approach using an instrumented implant based on the Innex FIXUC system (Zimmer GmbH, Winterthur, Switzerland) (89). All TKA procedures were performed by the same two experienced, board certified orthopedic surgeons (A.M.H. and A.B.), associated with the Department of Orthopedic Surgery at the Sana Kliniken Sommerfeld, Kremmen, Germany.

Implantations of the knee prostheses were performed with patients in supine position, under general plus combined spinal-epidural anesthesia. A tourniquet was positioned as proximal as possible on the thigh to minimize thigh muscle compression and was inflated throughout surgery. The extensor mechanism was exposed by a standard anterior midline skin incision, extending from a point 5 to 7 cm proximal to the superior pole of the patella to the tibial tubercle (TT). After separation of subcutaneous tissues down to the deep fascia and the development of a medial skin flap, arthrotomy was performed. A longitudinal incision was made along the medial border of the patella, severing the medial patellar retinaculum and medial aspect of the joint capsule. Disruption of the tendinous insertion on the anterior TT was avoided. The patella was everted and dislocated laterally and the knee positioned in 90° flexion. Fat pad, ACL and PCL were excised; followed by resection of the tibial plateau and sizing of the tibial component (i.e. tibia-first technique).

An intramedullary femoral alignment guide was placed anterior of the intercondylar notch and the femoral component size was determined. Flexion and extension gaps were balanced and femoral resection was performed in anteroposterior direction. Ligament stability and femoral rotation were tested by means of a spacer. Distal femur, as well as posterior condylar facets were resected and the trochlear groove was deepened. Final preparation of the tibia was conducted by stepwise drilling and compaction of cancellous bone for tibial stem fixation. Trial implant components were placed and assessed for joint stability and balance. The instrumented tibial component (89) was cemented and the PE inlay (Innex® Fix UC Tibial Insert, GmbH, Winterthur, Switzerland) was inserted. Patellar resurfacing was performed and femoral (Innex® CR Femoral Component cemented, Zimmer, Winterthur, Switzerland) and patellar (PE Innex® Patellar Component cemented, Zimmer, Winterthur, Switzerland) components were cemented. Layered wound closure was done after irrigation, hemostasis and

inlay of intrarticular, as well as subcutaneous Redon drainages. Absorbable sutures were used for closure of the joint capsule and careful adaptation of subcutaneous tissues. The skin incision was closed by skin stapling and a sterile compression dressing was applied. Correct implant positioning was confirmed with X-ray and joint mobility was manually tested.

2.3.2 Clinical examination and rehabilitation

Patients were clinically assessed preoperatively and 3, 6 and 30 months postoperatively. The same standardized postsurgical management and rehabilitation protocol was used for all patients. Rehabilitation started from the first postoperative day with continuous passive ROM exercises up to 90° flexion, as tolerated by the patient. Progressive weight-bearing on the operated leg was supported by the use of crutches for at least six to eight weeks. All patients continued the standard inpatient rehabilitation regimen after discharge at the rehabilitation center at the Sana Rehabilitationsklinik Sommerfeld, Kremmen, Germany for four weeks. Physical therapy sessions included isometric, long-lever-arm, non-weight-bearing and weight-bearing exercises and were supervised by a physical therapist. Patients were encouraged to perform home exercises thereafter.

2.3.3 Instrumented knee implant

The commercially available, cemented Innex FIXUC Total Knee System (Zimmer GmbH, Winterthur, Switzerland), featuring an ultra congruent, fixed bearing, cruciate sacrificing PS design, was modified in its tibial component to allow for *in vivo* joint load measurements. Performance and safety requirements for clinical application of the instrumented implant were evaluated and met prior to implantation. Details on prosthesis design, mechanics and external measuring devices have been previously published (89, 122, 123).

Load-dependent strains acting on the implant were sensed by six semiconductor strain gauges (KSP 1-350-E4, Kyowa, Japan), which were installed in the tibial component (122). *In vivo* contact load measurements encompassed real-time recordings of the three-contact force and three-moment components acting on the tibial tray. The resultant tibio-femoral contact force (F_{res}) was calculated as the vector sum of the three force components F_x, F_y, F_z (Figure 3a), using external equipment. Signals of the strain gauges were transmitted via an inductively powered, nine-channel telemetry unit at a sampling rate of approximately 125 Hz (122). The mean measuring error of the recordings was less than 2% according to device calibration (89).

2.4 *In vivo* joint load measurements

In vivo knee joint loadings were measured 26±14.7 months postoperatively in the gait laboratory at CSSB, Berlin and the Laboratory for Movement Biomechanics at ETH Zürich Institute for Biomechanics. At the time of investigation, all patients had resumed functional ADLs and there was no clinical evidence of any apparent knee pain or physical impairments.

Tibio-femoral contact forces and moments were recorded during six ADLs according to a standardized protocol. Activities with single-limb support (SLS), in which one leg supports the body weight during the loading phase, included walking along a level 10 m walkway at a self-selected speed (3-4 km/h), ascending and descending a four-step staircase (step height 20 cm, step tread 26 cm, no handrail support) and one-legged stance (OLS) with no or minimal balance aid at the fingertip. Double-limb support (DLS) exercises were sit-to-stand and stand-to-sit activities on a chair (seat height 45 cm, no armrest support). Patients were made acquainted with the experimental set-up and performed several practice trials before measurement recordings. All activities were executed in the same order and patients received verbal instructions during motion sequences. For each patient, at least six repetitions were recorded per activity and sufficient rest periods were allowed between consecutive trials to minimize fatigue effects. A power coil and antenna, which transmitted signals to an external amplifier and receiver, were fastened to patient's proximal shank during measurements (89). Movement patterns of the patients were recorded and stored in video format synchronously with the *in vivo* load data (Figure 4a).
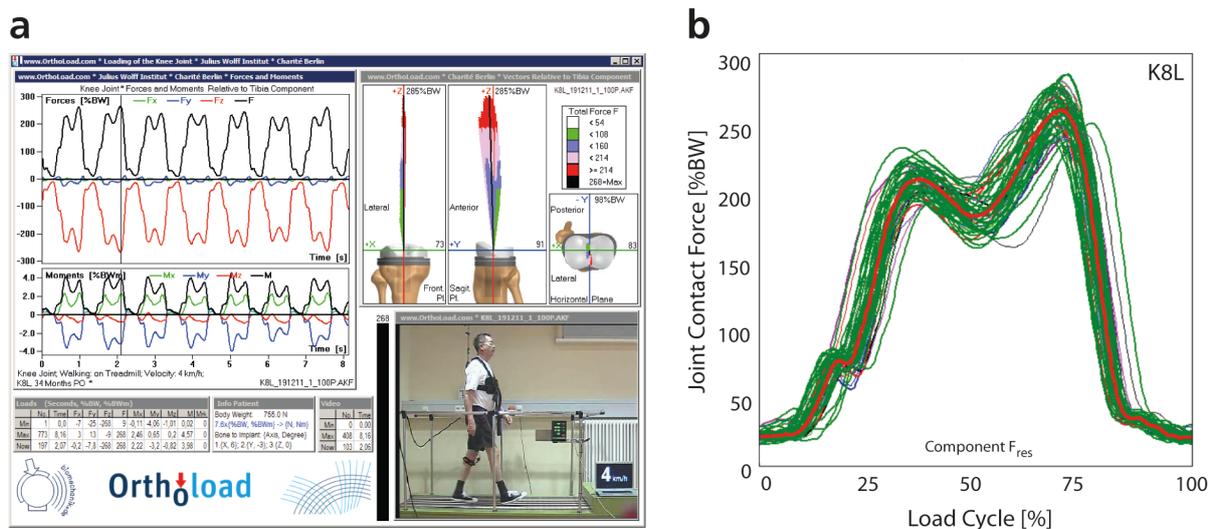
Figure 4. Measurement set-up. An example of force and moment recordings for patient K8L during level walking at 4km/h as available in the Orthoload databank[124] (**a**). The averaging process of the resultant force (F_{res}) in % body weight (%BW) for patient K8L (**b**). Thin lines: time course of F_{res} in %BW per trial. Thick red line: average curve of F_{res} in %BW across multiple trials during one load cycle.

Load-dependent signals were recorded as a function of the coordinate system fixed to the right-sided tibial component (Figure 3a). Joint force and moment data were visualized and processed using a custom-written MATLAB R2016b (The Mathworks, Natick, MA, USA) program. The resultant joint load, used for further analyses, was calculated from the three force components F_x, F_y and F_z, which act in the lateral, anterior and superior direction of the tibial plateau. The mean time course of F_{res} was calculated as the average of repeated trials per activity using a dynamic time warping procedure (123). Hence, patient-specific load patterns presented within the scope of this thesis are the arithmetic mean of several trial recordings. Figure 4b plots the averaging procedure of F_{res} over multiple trial repetitions for the example of level walking. The time course of F_{res} was normalized and presented as a percentage of the total load cycle for all activities examined.

The average load cycles were calculated and analyzed with regard to the temporal pattern of knee joint loadings and peak force values (Figure 5). For activities with a "double peak" load pattern the maxima of F_{res} were computed at two distinct instants of the load cycle and are referred to as first and second peak in the following (Figure 5a-c). Regarding activities with a "single peak" force curve, the absolute maximum load value was evaluated (Figure 5d-f). All measurements of F_{res} were normalized to the patient's body weight (BW).
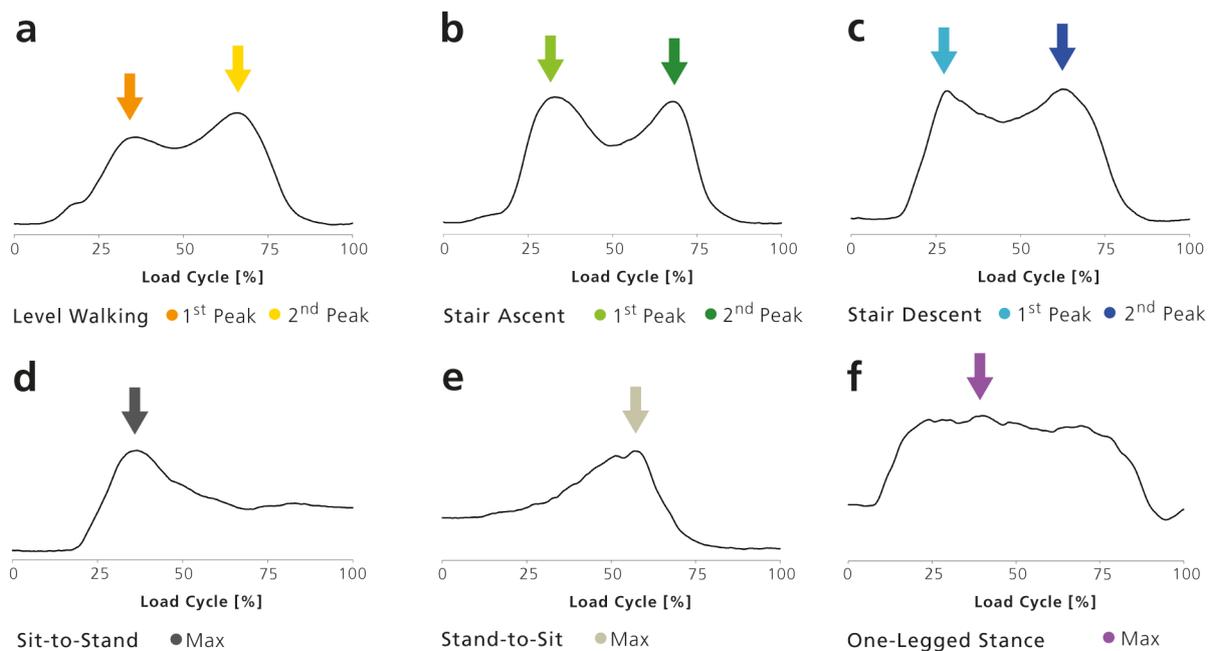
Figure 5. Loading patterns in the knee joint. The curves represent the resultant knee joint contact force F_{res} acting during one load cycle [%] during activities of daily living (**a**: level walking; **b**: stair ascent; **c**: stair descent; **d**: sit-to-stand; **e**: stand-to-sit; **f**: one-legged stance). Peak values used for analysis are marked by colored arrows.

2.5   Radiological assessment

Radiological imaging was performed at the Department of Radiology Charité Berlin, Campus Virchow Clinic and Campus Benjamin Franklin Clinic. A standing radiograph with an antero-posterior projection was obtained from each patient two days before and 9.4 ± 1.7 days after TKA. All patients underwent CT imaging one day prior to surgery and after a follow-up time of 30 ± 11.5 months.

CT was performed on one of four commercially available, multi-slice scanners: Siemens Somatom Sensation 64, SOMATOM Definition Flash (both Siemens Healthcare, Erlangen, Germany) and LightSpeed VCT, LightSpeed Pro 16 (both GE Healthcare, Milwaukee, WI, USA). Axial images were acquired with patients in a feet first, supine position. Scanning parameters included 120 kV, 100 to 200 mA, FOV 200 to 400 mm, pitch 1.0, slice thickness range of 0.6 to 4.8 mm. CT-scans were reconstructed and standardized to the thinnest possible slice thickness of 4.8 mm for all CT-scans. The analyzed scan area in the axial plane was consistent among patients. An automated dose modulation algorithm was applied to control tube voltage. CT scans were stored in Digital Imaging and Communications in Medicine (DICOM) format in the departments Picture Archiving and Communication System (PACS). DICOM-images were anonymized for analysis purposes.

2.5.1 Volumetric measurements of skeletal muscle

The distal volumes of periarticular thigh muscles were measured by manual segmentation of muscle tissues on a series of contiguous axial CT scans. Scans were analyzed using the three-dimensional (3D) image visualization and analysis software program Amira-Avizo Software version 6 (Thermo Scientific, Waltham, MA, USA) for Microsoft Windows®. Preoperative and postoperative image datasets of the operated leg were evaluated for each patient. The distal volume analyzed spanned a section of 87.7 ± 2.8 mm (18 ± 0.57 slices) proximal to the superior patellar pole. To account for inter-individual differences in body height, slice locations were selected relative to the patient's femur length. The length of the femur was defined as the distance between the lower border of the lateral femoral condyle and the tip of the greater trochanter. The regions of interests (ROIs) of the periarticular musculature included the heads of the quadriceps (VM, VL, RF, VI) and hamstrings (BF, SM, ST), as well as the GR, SR muscles. The BF muscle was segmented as a whole and not differentiated into its respective long and short head.

For analysis, individual muscle ROIs were manually traced on each slice using a Wacom Cintiq 21UX pen display (Wacom Technology Corporation, Vancouver, WA, USA). Each muscle was tagged with a different color. The anatomical CSA (cm^2) of the delineated muscle tissues was automatically computed on each slice by the software program, which multiplied the number of pixels of the user-defined ROI area by the pixel surface area. Distal muscle volume measurements in cm^3 were obtained by summation of the CSAs of each muscle and multiplication by the slice thickness of 4.8 mm. A three-dimensional reconstruction of the periarticular muscle volumes was generated using an interpolation function to correct for partial surface rendering effects (Figure 6b). The distal volumes of the quadriceps and hamstrings were calculated from individual measurements of the VL, VM, VI, RF muscles and of the BF, SM, ST muscles, respectively. The PA group was defined as the sum of the individual muscles SR, GR, ST, which feature a common tendinous insertion at the proximal anteromedial tibia. Postoperative changes in distal volume were calculated using MS Excel 2011 (Microsoft Corporation, Redmond, WA, USA) worksheets and were expressed as absolute changes (cm^3).
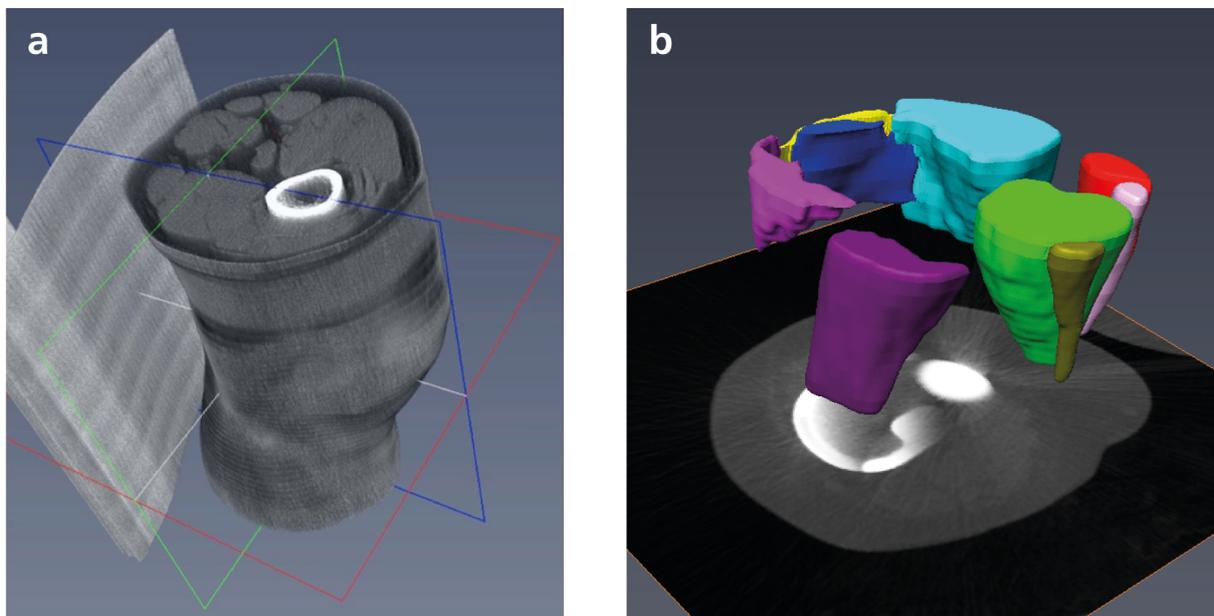
Figure 6. Three-dimensional (3D) reconstruction. 3D visualization of a preoperative CT-dataset of the right leg of one patient used for segmentation (**a**). 3D image reconstruction of the distal volumes of individual thigh muscles (**b**). Light purple: vastus lateralis; light blue: vastus medialis; yellow: rectus femoris; dark blue: vastus intermedius; red: sartorius; rose: gracilis; light green: semimembranosus; dark green: semitendinosus; dark purple: biceps femoris.

2.5.2 Quantification of muscle fat infiltration

The quantitative assessment of muscle fat infiltration was performed unilaterally on four consecutive transverse slices of the presurgical and follow-up CT scans. The superior slice was matched with the most proximal slice covered by the volumetric analyses (section 2.5.1), as CSA measurements more proximal to the respective thigh muscle belly tend to feature larger diameters and thus stronger correlations with total thigh muscle volume (125). The free image processing software NIH ImageJ 1.x (U.S. National Institutes of Health, Bethesda, MD, USA) was used for muscle composition measurements (126). The composition of muscle tissue was quantified by the analysis of muscle density, which was determined by averaging the numerical CT values within an outlined muscle ROI. The CT numbers were measured on the basis of the radiological HU scale, in which a radiodensity of 0 HU is assigned to water and -1000 HU to air. The muscle contours were manually delineated on each transverse slice (Figure 7a). Histograms showing the HU distribution within the segmented ROIs were generated for each muscle (Figure 7b). HU threshold values of -190 to -30 HU for intramuscular adipose tissue and -29 to 150 HU for skeletal muscle were used as a reference standard for segmentation (127). The anatomical CSAs of intramuscular fat (FCSA) and lean muscle (LCSA) in cm^2 were calculated by multiplying the number of pixels for a defined attenuation range by the pixel area. Measurements were averaged for each muscle over all segmented ROIs. The mean attenuation value was determined for all muscles as an inverse measure of muscle lipid content (128). The intramuscular fat ratio (FR) was computed in percent by means of the equation:

$$FR = \frac{FCSA}{FCSA + LCSA} \text{ x } 100$$

a

b
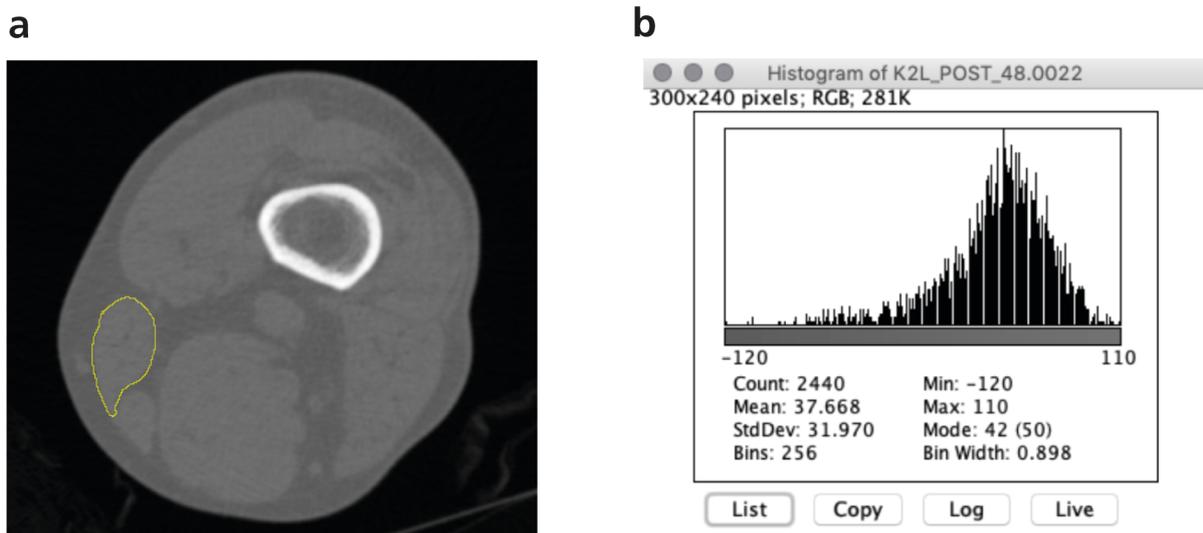
Figure 7. Segmentation of muscle tissue. Postoperative axial CT slice with manual segmentation of the sartorius muscle in yellow (**a**). The the pixel distribution is represented as a histogram (**b**).

2.6 EMG processing

2.6.1 EMG recording and analysis

Periarticular muscular activity of the operated limb was analyzed by the recording of EMG signals in six patients (K2L, K4R, K5R, K7L, K8L, K9L). The EMG signals were acquired simultaneously with the *in vivo* joint load measurements during six investigated ADLs, as outlined in section 2.4. The EMG and *in vivo* joint contact force data were synchronized and superimposed in postprocessing analyses using specialized software described hereinafter.

The surface electrodes were positioned in compliance with the Surface EMG for the Non-Invasive Assessment of Muscles (SENIAM) recommendations (129) over six muscles of the quadriceps, hamstring and triceps surae muscle groups. In particular, surface EMG signals were recorded from the VM, VL, BF (lateral hamstrings [HL]), ST (medial hamstrings [HM]), medial gastrocnemius (GM) and lateral gastrocnemius (GL) muscles. The sensors were applied above the approximate center of the palpable muscle bulks, in a longitudinal orientation to the muscle fibers to maintain correct positioning during patient movement. Prior to electrode attachment, the skin was shaved, abraded and cleaned with alcohol in order to reduce skin impedance and facilitate electrode adhesion. The ground electrode was placed on the anterior proximal tibia. Correct alignment and interference-free operation of the measuring devices were checked before the start of recording procedures. Recordings of EMG signals were sampled using a wireless 16-channel electromyographic Trigno system (Delsys Inc., Natick, MA, USA). The EMG signals were bandpass filtered with cutoff frequencies of 10 and 500 Hz using a zero-lag Butterworth filter, full wave rectified and smoothed with a 100 ms window length. Data were further processed using custom MATLAB R2009b software programs (The Mathworks, Natick, MA, USA). The surface EMG signals of each muscle were normalized to their maximum value obtained from the same patient and investigated movement task (130).

2.6.2 Cross-correlation technique

The technique of cross-correlation was used for the calculation of EMD for the six different ADLs under examination (section 2.4). EMD was defined as the temporal phase shift between the onset of muscle activation and the development of tibio-femoral joint contact forces. The cross-correlation function allows for the analysis of temporal phase shifts without a subjective definition of signal onset points (115). The concept of EMD is depicted schematically in

Figure 8. IBM SPSS Statistics 25 software (IBM Corporation, Armonk, NY, USA) was used for cross-correlating the joint contact force with the EMG linear envelope. Cross-correlation coefficients were calculated for the muscle activation of the VM, VL, HM, HL, GM and GL muscles for each trial. The delay between EMG and average tibio-femoral joint contact forces was determined by the cross-correlation coefficient with the maximal numerical value (115).
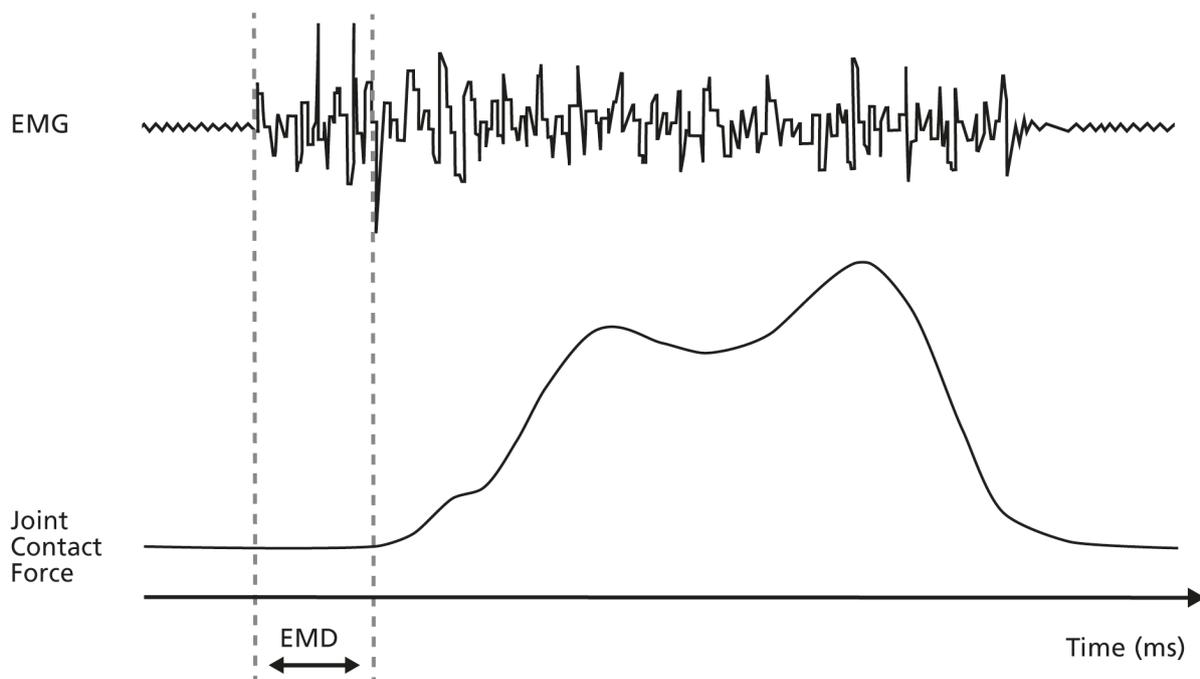
Figure 8. Graphic display of the electromechanical delay (EMD). The figure depicts the method of determining the EMD between the recording of surface electromyography (EMG; upper curve) and the average resultant knee joint contact force (F_{res}; lower curve) over time. The arrow indicates the time lag between the onset of EMG and the onset of F_{res}.

2.7 Statistical analysis

Statistical analyses were performed using IBM SPSS Statistics 25 software (IBM Corporation, Armonk, NY, USA). Descriptive statistics were determined for demographic variables, including age, body mass, height and BMI. Values were expressed as mean and standard deviation (SD) for continuous variables and as percentages for categorial data, unless stated otherwise. The changes in periarticular muscle status between the presurgical and postoperative CT examinations were assessed using paired sample t-tests. Pearson product moment correlations were calculated to analyze the association between the metric variables of interest of muscle status, *in vivo* knee joint contact force, muscular activity and EMD. Pearson correlation coefficients were considered high if $r \geq 0.7$ and moderate if $0.5 \leq r < 0.7$. The level of statistical significance was set a priori at $p \leq 0.05$.

3 Results

3.1 Patient demographics

A total of eight patients with knee OA, who matched the inclusion criteria and received an instrumented knee implant (89) in the course of unilateral TKA, were included for analysis. The mean age at baseline was 68.5 ± 5.3 years (range: 60-75) and the male-to-female ratio was 5:3. Prior to surgery, the mean BMI was 29.7±4.0 kg/m^2 (range: 25.1-36.3), whereby five (62.5%) patients had a BMI of ≥30 kg/m^2. The postoperative follow-up at 26±14.7 months (range: 8-45) showed an increase in mean BMI of 1.3±1.5 kg/m^2 (4.49%) from presurgical measurements. Implantation of the instrumented prosthesis was performed on the left and right side in five (62.5%) and three (37.5%) cases, respectively. One patient (K2L) underwent previous TKA surgery of the contralateral leg, which was asymptomatic at the time of left-sided TKA. None of the patients required revision surgery. From nine eligible TKA patients with an instrumented knee implant, one patient (K1L) was excluded, as no CT scans were available. Baseline descriptive data for the study participants are shown in Table 1.

Table 1. Preoperative patient demographics and clinical characteristics.

Patient ID	K2L	K3R	K4R	K5R	K6L	K7L	K8L	K9L	Average (SD)
Preoperative demographics									
Age (y)	71	70	63	60	65	74	70	75	**68.5 (5.3)**
Sex	m	m	f	m	f	f	m	m	-
Body weight (kg)	93	95	92	94	76	70	77	100	**87.1 (11)**
Body height (cm)	171	175	170	175	174	166	174	166	**171.4 (3.8)**
BMI (kg/m^2)	31.8	31.0	31.8	30.7	25.1	25.4	25.4	36.3	**29.7 (4.0)**
Preoperative motion and alignment									
Knee flexion (°)	130	100	90	130	100	100	120	120	**1.3 (6.4)**
Knee extension (°)	0	0	0	10	10	0	-10	0	**111.3 (15.5)**
FTA (°)[a]	5.0	3.5	-4.5	1.0	-4.0	6.5	4.0	7.0	**2.3 (4.5)**
Posterior tibial slope (°)	6.5	8	0	3	4	5	6	6	**4.8 (2.5)**

Average values are arithmetic means (standard deviation [SD]). [a] Negative angle values represent valgus alignment as obtained from standing radiographs two days prior to surgery. BMI, body mass index; FTA, femorotibial angle, m, male; f, female; ID, Identification; K, knee; R, right side of implantation; L, left side of implantation.

3.2 *In vivo* knee joint loadings

The *in vivo* knee joint loadings during dynamic ADLs consistently exceed the patients' body weight and showed high inter-individual variability in peak load magnitude (Figure 9). The highest peak loads were measured during stair descent with an average of 3.41±0.62 times body weight (BW). The activity of stand-to-sit showed the lowest magnitude (2.64±0.68 BW)

in average peak joint load of all investigated ADLs. Patient-specific measurements of the average peak knee joint loads during the respective ADLs are given in Table 2.

Table 2. Patient-specific *in vivo* knee joint loadings during activities of daily living.

Activity	K2L	K3R	K4R	K5R	K6L	K7L	K8L	K9L	Average (SD)
Level Walking 1P	218 [1964]	202 [1936]	180 [1785]	206 [1940]	268 [2184]	249 [1691]	208 [1619]	198 [2115]	**216 (29) [1904 (196)]**
Level Walking 2P	253 [2282]	249 [2390]	325 [3235]	245 [2310]	291 [2372]	342 [2321]	258 [2009]	176 [1882]	**267 (52) [2350 (401)]**
Stairs Up 1P	344 [3108]	257 [2468]	269 [2669]	325 [3059]	348 [2835]	295 [2001]	315 [2454]	229 [2446]	**298 (43) [2630 (367)]**
Stairs Up 2P	349 [3154]	240 [2305]	293 [2910]	325 [3064]	430 [3501]	354 [2401]	263 [2054]	187 [2002]	**305 (76) [2674 (557)]**
Stairs Down 1P	417 [3766]	300 [2884]	340 [3381]	359 [3383]	366 [2977]	318 [2157]	272 [2123]	208 [2230]	**323 (64) [2863 (634)]**
Stairs Down 2P	392 [3536]	231 [2221]	321 [3195]	424 [3997]	374 [3045]	377 [2558]	317 [2473]	293 [3130]	**341 (62) [3019 (587)]**
Sit Down Max	257 [2322]	233 [2233]	248 [327]	327 [3076]	378 [3073]	264 [1791]	265 [2067]	143 [1532]	**264 (68) [2320 (552)]**
Stand Up Max	292 [2632]	265 [2542]	262 [2600]	297 [2800]	385 [3137]	266 [1800]	267 [2086]	164 [1750]	**275 (61) [2418 (492)]**
One-legged Stance Max	301 [2719]	271 [2602]	285 [2836]	278 [2622]	263 [2145]	343 [2327]	362 [2823]	205 [2197]	**289 (49) [2534 (275)]**

Values indicate joint loads in percent body weight and Newton (%BW [N]). The arithmetic mean and standard deviation (SD) are provided for both unit measures. 1P, 1st load peak; 2P, 2nd load peak; Max, maximum load; K2L-K9L, patient identifier.

The activity of **level walking** showed a consistent double-peak pattern of F_{res} with a first load peak at contralateral toe-off (CTO) and a second peak at the contralateral heel-strike (CHS). The average peak values during late stance (2.67±0.52 BW) exceeded those recorded at CTO during early stance (2.16±0.29 BW) (Table 2). The inter-individual variation in peak joint load was 1.66 BW with a range from 1.76 BW (K9L) to 3.42 BW (K7L). The time course of F_{res} recorded for each patient during the gait cycle, as well as the inter-individual variation in peak load values, are shown in Figure 9a.

The highest knee joint loads were observed during **stair climbing**, with average peak values of 3.41±0.62 BW and 3.05±0.76 BW during stair descent and stair ascent, respectively. The activity of stair climbing likewise showed the highest individual peak loads of all ADLs, with values of 4.24 BW (K5R) during stair descent and of 4.3 BW (K6L) during stair ascent (Table 2). The time course of F_{res} exhibited a double peak pattern, whereby the first peak occurred at CTO and the second after the contralateral foot made contact with the next step. The average loads at the second peak were relatively higher compared to the first peak for both climbing directions (Table 2). The inter-individual variation of F_{res} during stair climbing was 53.3±4.6%. In specific, stair descent showed an inter-individual variation in peak load of 1.93 BW (range: 2.31-4.24) (Figure 9d). The highest inter-individual difference of F_{res} over all ADLs was measured during stair ascent with 2.43 BW (range: 1.87-4.3) (Figure 9c).

The double-limb exercises of **sit-to-stand** (2.75±0.61 BW) and **stand-to-sit** (2.64±0.68 BW) showed lower average peak knee joint loads than **OLS** with single leg balance (2.89±0.49 BW). The time course of F_{res} showed a maximum load peak that was associated with the instant of seat-off during sit-to-stand (Figure 9e) and chair contact during stand-to sit (Figure 9f). The lowest individual peak load of 1.43 BW was recorded in patient K9L during sitting down (Table 2). The inter-individual variation of F_{res} was higher during DLS activities with high knee flexion (mean 2.28 BW), compared to the static exercise of OLS (1.57 BW) (Figure 9b). The activity of stand-to-sit showed the second highest inter-individual variation of F_{res} of all ADLs (2.34 BW), ranging from 1.43 BW (K9L) to 3.78 BW (K6L) (Table 2).
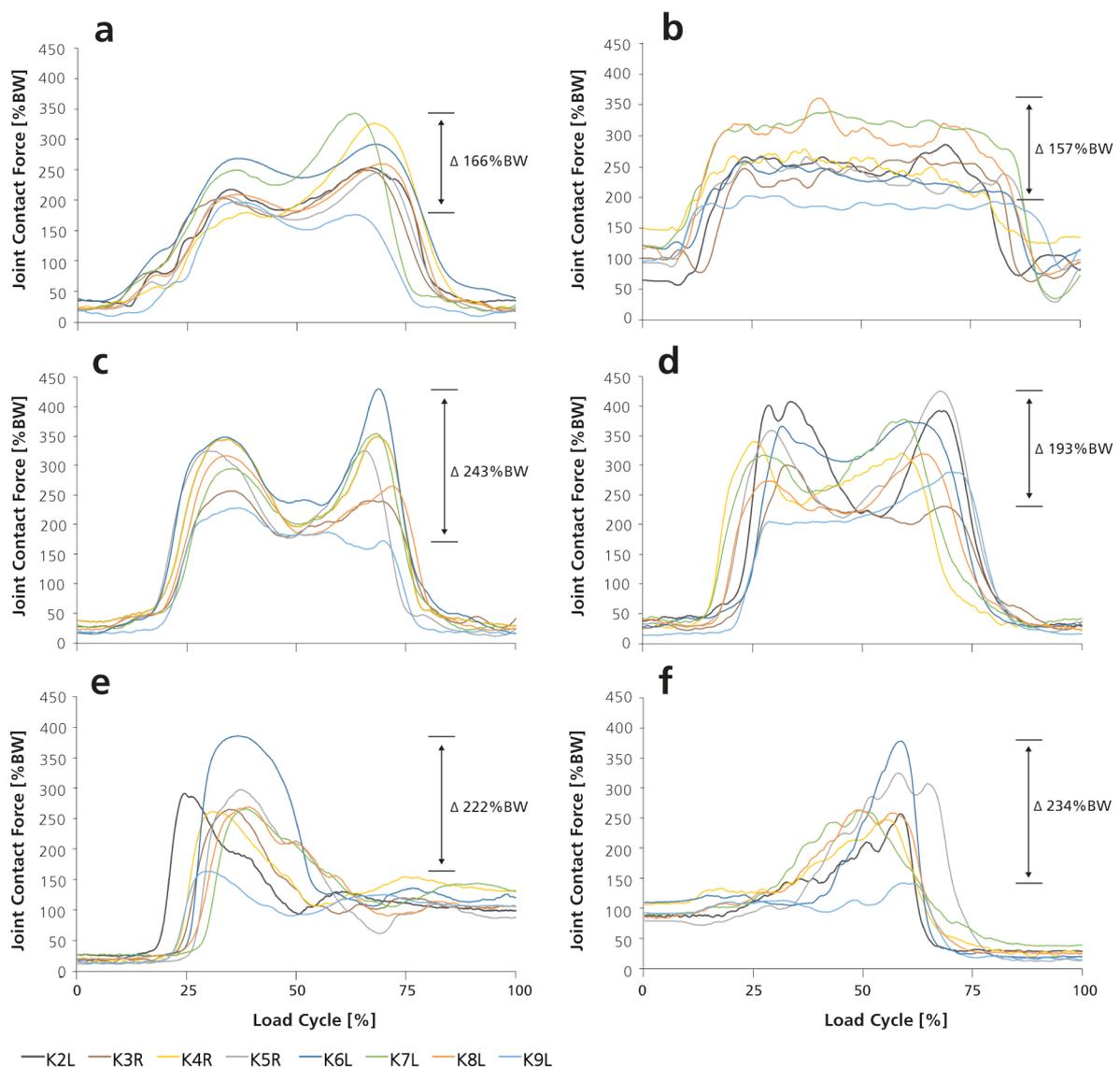
**Figure 9. Individual load patterns during activities of daily living.** Resultant knee joint contact force (F_{res}) measurements in % body weight (%BW) for each patient (K2L-K9L) during one load cycle of **a**: level walking; **b**: one-legged stance; **c**: stair ascent; **d**: stair descent; **e**: standing up; **f**: sitting down. The arrows show the inter-individual difference between peak force values in %BW.

3.3 Periarticular muscle status

3.3.1 Distal muscle volumes and cross-sections

The preoperative **distal volume** of the quadriceps femoris was 89 ± 28.7 cm^3 and decreased by $-9.6\pm5.7\%$ ($p<0.01$) in the postoperative course (Figure 10a). The absolute decrease in distal volume was significantly higher for the VM muscle (-4.5 ± 4.9 cm^3, $p<0.05$), compared to the VL muscle (-3.4 ± 2.8 cm^3, $p<0.05$) (Table 3). The relative proportion of the VM muscle to the mean reduction in distal quadriceps volume was by 12.09% higher than that of the VL. There were no significant volume changes of the other periarticular muscles over time (Figure 10).
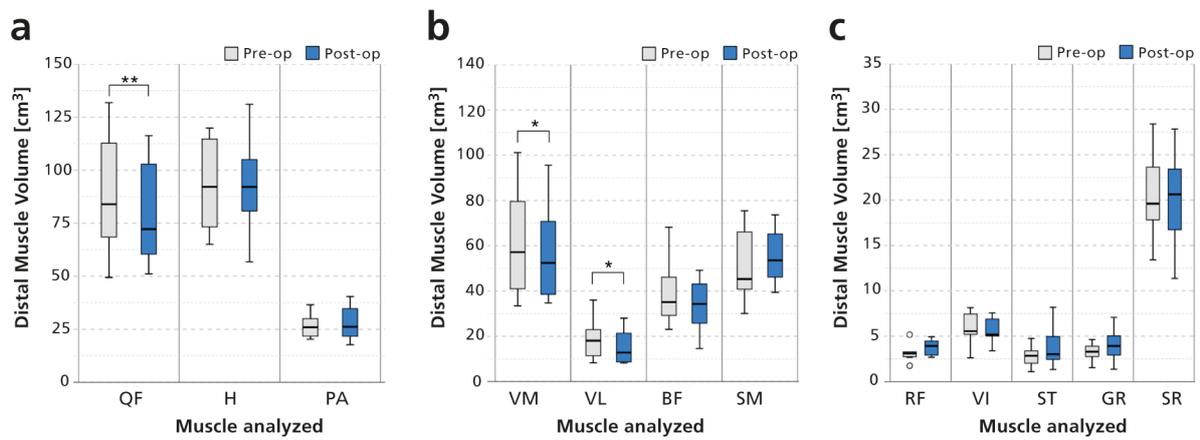
Figure 10. Boxplots of changes in distal muscle volume. Absolute change in distal muscle volume in [cm^3] of muscle groups (**a**) and of larger (**b**) and smaller (**c**) measurements of individual muscles. The horizontal, upper and lower lines of the box represent the median (50th percentile), upper (75th percentile) and lower (25th percentile) quartiles, respectively. The whiskers extend to the minimum and maximum values. Outliers are depicted as points outside the whiskers. QF, quadriceps femoris; H, hamstrings; PA, pes anserinus group; VM, vastus medialis; VL, vastus lateralis; BF, biceps femoris; SM, semimembranosus; RF, rectus femoris; VI, vastus intermedius; ST, semitendinosus; GR, gracilis; SR, sartorius muscle. Paired sample t-test, *p≤0.05, **p≤0.01.

Table 3. Postoperative changes in distal muscle volume per patient.

Patient ID	K2L	K3R	K4R	K5R	K6L	K7L	K8L	K9L	Average (SD)	p-value
QF	-8.2	-6.9	-11.6	-14.9	-9.2	-8.5	1.6	-15.5	**-9.1 (5.4)**	0.002**
RF	1	1	-0.4	1.9	-1.1	0.6	0.3	2.0	**0.6 (1.1)**	0.13
VI	0.8	-0.2	-3.0	1.5	-2.1	-0.9	0.2	1.9	**-0.2 (1.7)**	0.696
VL	-1.8	-4.3	-8	-4	-1.2	-6.8	0	-1.3	**-3.4 (2.8)**	0.011*
VM	-8.1	-3.4	-0.1	-14.2	-4.7	-1.4	1.2	-5.6	**-4.5 (4.9)**	0.035*
H	11.2	-9.4	26.7	-10	-12.1	-12.3	6.3	-1.9	**-0.2 (14)**	0.972
BF	0.8	-6.9	5.1	-19.4	-8.5	-4.4	-5.4	-3.6	**-5.3 (7.2)**	0.076
SM	6.9	-2.6	17.4	8.7	-2.8	-8	11.4	1.7	**4.1 (8.5)**	0.214
ST	3.5	0.1	4.2	0.7	-0.8	0.1	0.2	0	**1 (1.8)**	0.158
PA	3.9	0	10	3	-2.9	-1.3	-2.6	0.8	**1.4 (4.2)**	0.391
GR	1	-0.2	4	0.9	0	-0.6	-0.2	1.3	**0.8 (1.5)**	0.179
SR	-0.5	0.1	1.9	1.5	-2.1	-0.8	-2.6	-0.6	**-0.4 (1.6)**	0.495
ALL	0.4	-1.8	2.3	-2.5	-2.6	-2.5	0.6	0.5	**-0.8 (5.0)**	0.166

Values are given in [cm^3]. Average values are arithmetic means (standard deviation [SD]). ALL is the total change in distal volume of individual muscles (RF, rectus femoris; VI, vastus intermedius; VL, vastus lateralis; VM, vastus medialis; BF, biceps femoris; SM, semimembranosus; ST, semitendinosus; GR, gracilis; SR, sartorius). The pes anserinus group (PA) comprises the ST, GR and SR muscles. QF, quadriceps femoris; H, hamstrings; ID, identification; K2L-K9L, patient identifier. P values were obtained using the paired t-test. Significance level *p≤0.05, **p≤0.01.

The average periarticular **muscle CSA** showed minor changes at postoperative follow-up examinations (Table 4). There was a slight increase in mean CSA of the RF and VI muscles of 0.5 ± 0.3 cm^2 and 0.7 ± 0.3 cm^2 (both p<0.01), respectively. The CSA of the medial hamstring muscle SM increased by 1.1 ± 1.0 cm^2 (p<0.05). The lateral hamstring muscle BF showed a decrease in CSA of -1.4 ± 1.5 cm^2 (p<0.05), like the SR muscle (-0.2 ± 0.2 cm^2, p=0.05). The change in muscle CSA between pre- and postoperative measurements was not statistically significant for the muscle groups in their entirety (Figure 11a). The changes in muscle CSA of individual periarticular muscles are displayed in Figure 11b-c.
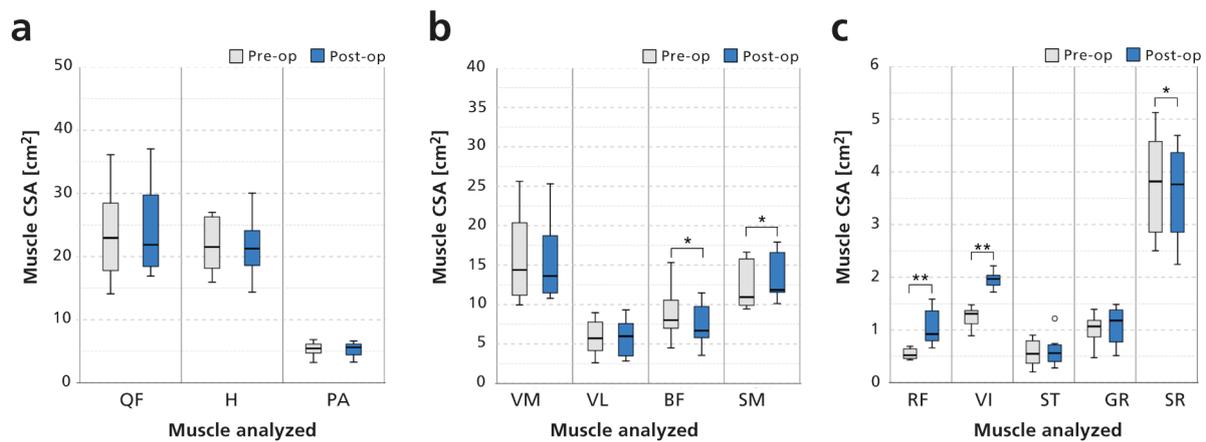
Figure 11. Boxplots of changes in muscle cross-sectional area (CSA). Absolute change in muscle CSA in [cm^2] of muscle groups (**a**) and of larger (**b**) and smaller (**c**) measurements of individual muscles. The horizontal, upper and lower lines of the box represent the median (50th percentile), upper (75th percentile) and lower (25th percentile) quartiles, respectively. The whiskers extend to the minimum and maximum values. Outliers are depicted as points outside the whiskers. QF, quadriceps femoris; H, hamstrings; PA, pes anserinus group; VM, vastus medialis; VL, vastus lateralis; BF, biceps femoris; SM, semimembranosus; RF, rectus femoris; VI, vastus intermedius; ST, semitendinosus; GR, gracilis; SR, sartorius muscle. Paired sample t-test, *p≤0.05, **p≤0.01.

Table 4. Postoperative changes in muscle cross-sectional area per patient.

Patient ID	K2L	K3R	K4R	K5R	K6L	K7L	K8L	K9L	Average (SD)	p-value
QF	2.5	0.7	-2.9	0.1	-0.5	1.8	2.8	0.9	**0.7 (1.8)**	0.366
RF	0.9	0.9	0.5	0.6	0	0.4	0.4	0.2	**0.5 (0.3)**	0.003**
VI	0.9	0.8	0.5	0.6	0.5	1.2	0.8	0.4	**0.7 (0.3)**	<0.001**
VL	1.7	-1.2	-2.3	1.1	-0.1	-0.6	0.2	0.6	**-0.1 (1.3)**	0.884
VM	-1	0.2	-1.6	-2.3	-0.9	0.8	1.4	0.3	**-0.5 (1.2)**	0.318
H	3	-1.9	1.1	-2.8	-1.5	-0.2	0.6	-0.8	**-0.3 (1.9)**	0.65
BF	0.8	-1.8	-1	-4.5	-1	-0.9	-1.7	-1.5	**-1.4 (1.5)**	0.028*
SM	2.2	0.1	1.7	1.6	-0.4	0.7	2.2	0.6	**1.1 (1)**	0.016*
ST	0.1	-0.1	0.3	0.1	-0.2	0	0.1	0.1	**0 (0.2)**	0.489
PA	-0.2	-0.2	0.5	0.2	-0.6	0	0.1	-0.2	**0 (0.3)**	0.727
GR	0.2	-0.1	0.3	0.2	-0.1	-0.1	0	0.1	**0.1 (0.2)**	0.239
SR	-0.4	0	-0.1	-0.1	-0.3	0.1	-0.1	-0.4	**-0.2 (0.2)**	0.05*
ALL	0.6	-0.1	-0.2	-0.3	-0.3	0.2	0.4	0	**0.03 (1.1)**	0.799

Values are given in [cm^2]. Average values are arithmetic means (standard deviation [SD]). ALL is the total change in cross-sectional area of individual muscles (RF, rectus femoris; VI, vastus intermedius; VL, vastus lateralis; VM, vastus medialis; BF, biceps femoris; SM, semimembranosus; ST, semitendinosus; GR, gracilis; SR, sartorius). The pes anserinus group (PA) comprises the ST, GR and SR muscles. QF, quadriceps femoris; H, hamstrings; ID, identification; K2L-K9L, patient identifier. P values were obtained using the paired t-test. Significance level *p≤0.05, **p≤0.01.

3.3.2 Muscular fatty infiltration

The postoperative change in **muscle attenuation**, a measure inversely related to the muscular fat content (128), is shown in Figure 12. Only the mean change across all periarticular muscle groups reached statistical significance with an average increase of 6.6±13.5 HU (p<0.01). The attenuation values of individual muscles showed an increase from preoperative data in a range from 2.1±16.2 HU to 11.2±15.4 HU that was not statistically significant. The change in muscle attenuation between presurgical and 2.5-year follow-up measurements of each muscle and patient are summarized in Table 5.
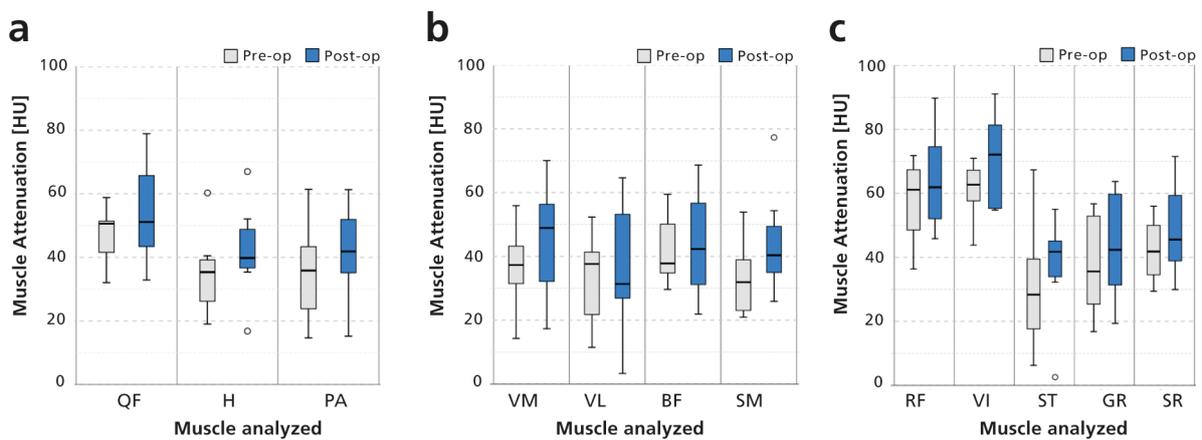

Figure 12. Boxplots of changes in muscle attenuation. Absolute change in muscle attenuation in [HU] of muscle groups (**a**) and of larger (**b**) and smaller (**c**) measurements of individual muscles. The horizontal, upper and lower lines of the box represent the median (50th percentile), upper (75th percentile) and lower (25th percentile) quartiles, respectively. The whiskers extend to the minimum and maximum values. Outliers are depicted as points outside the whiskers. QF, quadriceps femoris; H, hamstrings; PA, pes anserinus group; VM, vastus medialis; VL, vastus lateralis; BF, biceps femoris; SM, semimembranosus; RF, rectus femoris; VI, vastus intermedius; ST, semitendinosus; GR, gracilis; SR, sartorius muscle. Paired sample t-test, *p≤0.05, **p≤0.01.

Table 5. Postoperative changes in muscle attenuation per patient.

Patient ID	K2L	K3R	K4R	K5R	K6L	K7L	K8L	K9L	Average (SD)	p-value
QF	-4.6	0.1	9.4	5	0	17	26.8	0.8	**6.8 (10.5)**	0.11
RF	-2.3	0	-8.6	-2.7	9.5	20.3	27.3	7.1	**6.3 (12.4)**	0.191
VI	-6.1	-6.4	25.1	11.3	12.3	15.9	20.1	1.2	**9.2 (11.8)**	0.063
VL	-8.9	6.3	9.3	0.6	-15.2	12.8	28.7	-8.2	**3.2 (14.2)**	0.546
VM	-1.3	0.3	11.9	10.9	-6.7	19	30.9	3.1	**8.5 (12.3)**	0.091
H	0.1	7.4	17.1	11.6	-22.3	12.6	29.1	-2.2	**6.7 (15.3)**	0.254
BF	-4.8	2.5	8.6	5.5	-26.1	7.6	30.8	-7.7	**2.1 (16.2)**	0.732
SM	4.1	7.3	22.7	15.7	-14.9	12	38.1	4.9	**11.2 (15.4)**	0.078
ST	1.1	12.4	20.2	13.6	-25.8	18.3	18.5	-3.7	**6.8 (15.7)**	0.259
PA	-0.3	5.2	17.5	10.2	-19.6	13.4	25.5	0.5	**6.5 (13.6)**	0.217
GR	-4	-5.2	20.4	3.3	-18.1	8.7	34.6	9	**6.1 (16.3)**	0.325
SR	0.6	1.1	9.2	10.2	-8.7	8.5	29.5	0.5	**6.4 (11.2)**	0.152
ALL	-2.4	2.0	13.2	7.6	-10.4	13.7	28.7	0.7	**6.6 (13.5)**	<0.001**

Values are given in [HU]. Average values are arithmetic means (standard deviation [SD]). ALL is the total change in muscle attenuation of individual muscles (RF, rectus femoris; VI, vastus intermedius; VL, vastus lateralis; VM, vastus medialis; BF, biceps femoris; SM, semimembranosus; ST, semitendinosus; GR, gracilis; SR, sartorius). The pes anserinus group (PA) comprises the ST, GR and SR muscles. QF, quadriceps femoris; H, hamstrings; ID, identification; K2L-K9L, patient identifier. P values were obtained using the paired t-test. Significance level *p≤0.05, **p≤0.01.

The **lean muscle CSA** of the periarticular muscles determined preoperatively and at 2.5 years following TKA are presented in Figure 13. The change in lean CSA of the quadriceps was due to the slight increase in lean CSA of the RF (0.5 ± 0.3 cm^2, p<0.01) and VI (0.7 ± 0.3 cm^2, p<0.01) muscles, analogous to the total CSA measurements (Table 4). The VM and VL muscles did not show a significant postoperative change in lean muscle CSA (Table 6). The lean muscle CSA of the medial hamstring muscle SM increased from 11.5 ± 2.9 cm^2 (range: 8.3-16.0) to 13.2 ± 3.0 cm^2 (range: 10.0-17.6) (p<0.01). There was no significant change in lean muscle CSA identified for the other periarticular muscles (Table 6).
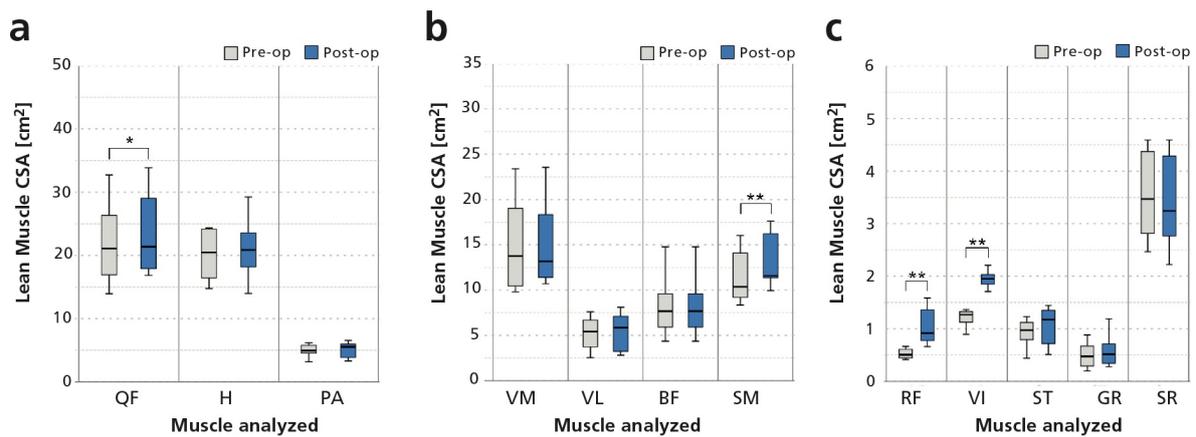

Figure 13. Boxplots of changes in lean muscle cross-sectional area (CSA). Absolute change in lean muscle CSA in [cm^2] of muscle groups (**a**) and of larger (**b**) and smaller (**c**) measurements of individual muscles. The horizontal, upper and lower lines of the box represent the median (50th percentile), upper (75th percentile) and lower (25th percentile) quartiles, respectively. The whiskers extend to the minimum and maximum values. QF, quadriceps femoris; H, hamstrings; PA pes anserinus group; VM, vastus medialis; VL, vastus lateralis; BF, biceps femoris; SM, semimembranosus; RF, rectus femoris; VI, vastus intermedius; ST, semitendinosus; GR, gracilis; SR, sartorius muscle. Paired sample t-test, *p≤0.05, **p≤0.01.

Table 6. Postoperative changes in lean muscle cross-sectional area per patient.

Patient ID	K2L	K3R	K4R	K5R	K6L	K7L	K8L	K9L	Average (SD)	p-value
QF	4.3	1.7	-0.8	1	-0.4	2	2.9	1.1	**1.5 (1.7)**	0.039*
RF	1	1	0.6	0.6	0	0.4	0.4	0.2	**0.5 (0.3)**	0.003**
VI	1	0.8	0.6	0.6	0.5	1.2	0.8	0.4	**0.7 (0.3)**	<0.001**
VL	2.2	-0.8	-1.2	1.4	-0.2	-0.5	0.3	0.3	**0.2 (1.1)**	0.646
VM	0.2	0.7	-0.7	-1.6	-0.7	0.9	1.5	0.2	**0.1 (1)**	0.889
H	5.1	0	4.3	-1.7	-1.5	0.2	1	-0.1	**0.9 (2.5)**	0.341
BF	1.6	-1.4	1	-4	-1	-0.9	-1.5	-1.4	**-0.9 (1.7)**	0.158
SM	3.4	1.4	2.9	2.3	-0.4	1	2.4	1.1	**1.8 (1.2)**	0.004**
ST	0.1	0	0.5	0.1	-0.2	0.1	0.1	0.1	**0.1 (0.2)**	0.289
PA	0.4	-0.8	1.1	0.3	-0.6	0.1	0.1	0.1	**0.1 (0.6)**	0.685
GR	0.3	0	0.5	0.2	-0.1	0	0.1	0.2	**0.1 (0.2)**	0.11
SR	0	-0.7	0.1	0.1	-0.2	0.1	0	-0.2	**-0.1 (0.3)**	0.255
ALL	1.1	0.1	0.5	0	-0.3	0.3	0.4	0.1	**0.27 (1.08)**	0.039*

Values are given in [cm^2]. Average values are arithmetic means (standard deviation [SD]). ALL is the total change in lean cross-sectional area of individual muscles (RF, rectus femoris; VI, vastus intermedius; VL, vastus lateralis; VM, vastus medialis; BF, biceps femoris; SM, semimembranosus; ST, semitendinosus; GR, gracilis; SR, sartorius). The pes anserinus group (PA) comprises the ST, GR and SR muscles. QF, quadriceps femoris; H, hamstrings; ID, identification; K2L-K9L, patient identifier. P values were obtained using the paired t-test. Significance level *p≤0.05, **p≤0.01.

There was a general decrease in **intramuscular fat CSA** across all investigated periarticular muscle groups from preoperative measurements following TKA (Figure 14a). The change in intramuscular fat CSA was slightly more pronounced for the hamstrings than for the quadriceps muscles (-1 ± 0.7 cm^2 versus -0.7 ± 0.8 cm^2, $p<0.05$, respectively) (Table 7). The greatest mean reduction in CSA of intramuscular fat was determined for the hamstring muscle SM (-0.6 ± 0.4 cm^2, $p<0.01$). The intramuscular fat CSA of the RF and VM decreased from 1.3 ± 0.9 mm^2 and 0.9 ± 0.8 cm^2 to 0.5 ± 0.6 mm^2 and 0.4 ± 0.6 cm^2 ($p\leq0.01$), respectively. The changes in intramuscular fat CSA of individual muscles are shown in Figure 14b-c.
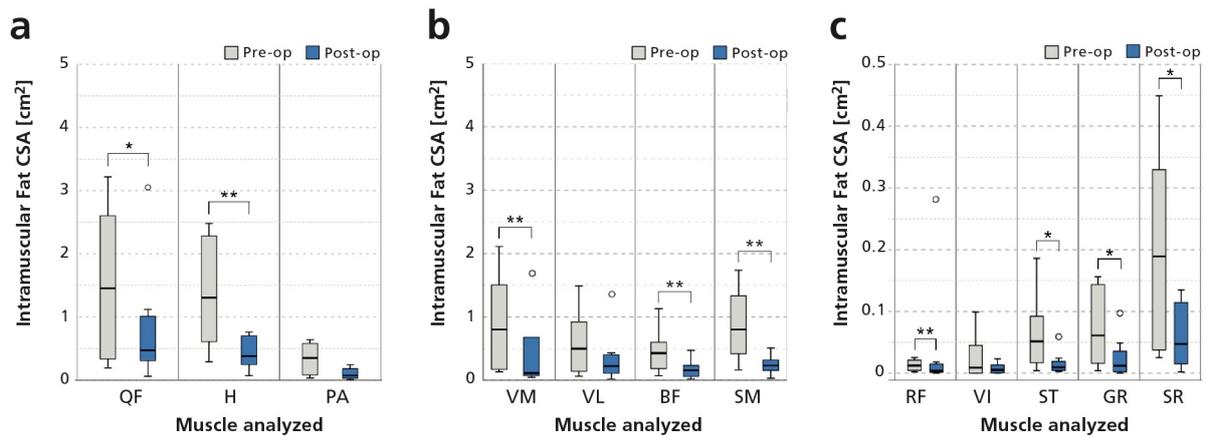
Figure 14. Boxplots of changes in intramuscular fat cross-sectional area (CSA). Absolute change in intramuscular fat CSA in [cm^2] of muscle groups (**a**) and of larger (**b**) and smaller (**c**) measurements of individual muscles. The horizontal, upper and lower lines of the box represent the median (50th percentile), upper (75th percentile) and lower (25th percentile) quartiles, respectively. The whiskers extend to the minimum and maximum values. Outliers are depicted as points outside the whiskers. QF, quadriceps femoris; H, hamstrings; PA, pes anserinus group; VM, vastus medialis; VL, vastus lateralis; BF, biceps femoris; SM, semimembranosus; RF, rectus femoris; VI, vastus intermedius; ST, semitendinosus; GR, gracilis; SR, sartorius muscle. Paired sample t-test,*$p\leq0.05$, **$p\leq0.01$.

Table 7. Postoperative changes in intramuscular fat cross-sectional area per patient.

Patient ID	K2L	K3R	K4R	K5R	K6L	K7L	K8L	K9L	Average (SD)	p-value
QF	-1.5	-1	-2	-0.7	0	0.1	-0.1	-0.2	**-0.7 (0.8)**	0.041*
RF	0	0	0	0	0	0	0	0	**0 (0)**	0.005**
VI	-0.1	0	-0.1	0	0	0	0	0	**0 (0)**	0.144
VL	-0.3	-0.5	-1.1	-0.2	0.1	-0.1	0	0.3	**-0.2 (0.4)**	0.171
VM	-1.1	-0.5	-0.8	-0.5	-0.1	-0.1	-0.1	-0.4	**-0.5 (0.4)**	0.01**
H	-1.7	-1.7	-1.7	-1.1	0.1	-0.4	-0.5	-0.6	**-1 (0.7)**	0.006**
BF	-0.7	-0.4	-0.4	-0.4	0.1	-0.1	-0.2	-0.1	**-0.3 (0.2)**	0.012*
SM	-1	-1.2	-1.1	-0.6	0	-0.4	-0.2	-0.5	**-0.6 (0.4)**	0.005**
ST	0	-0.1	-0.2	-0.1	0	0	0	0	**0 (0.1)**	0.05*
PA	-0.4	-0.3	-0.5	-0.2	0	0	-0.1	-0.2	**-0.2 (0.2)**	0.011*
GR	-0.1	0	-0.1	0	0	0	0	-0.1	**-0.1 (0)**	0.02*
SR	-0.4	-0.2	-0.2	-0.1	0	0	0	-0.1	**-0.1 (0.1)**	0.018*
ALL	-0.4	-0.3	-0.5	-0.2	0	-0.1	-0.1	-0.1	**-0.2 (0.3)**	<0.001**

Values are given in [cm^2]. Average values are arithmetic means (standard deviation [SD]). Values of <0.05 cm^2 are stated as zero because of rounding. ALL is the total change in intramuscular fat cross-sectional area of individual muscles (RF, rectus femoris; VI, vastus intermedius; VL, vastus lateralis; VM, vastus medialis; BF, biceps femoris; SM, semimembranosus; ST, semitendinosus; GR, gracilis; SR, sartorius). The pes anserinus group (PA) comprises the ST, GR and SR muscles. QF, quadriceps femoris; H, hamstrings; ID, identification; K2L-K9L, patient identifier. P values were obtained using the paired t-test. Significance level *$p\leq0.05$, **$p\leq0.01$.

The **intramuscular fat ratio** of all investigated muscle groups decreased significantly in the long-term after TKA (p<0.05). The change in intramuscular fat ratio of the quadriceps muscle (–2.8±2.9%CSA, p<0.05) was less pronounced than that of the hamstrings or pes anserinus group (both –4.1±3.2%CSA, p<0.05). The RF (–1.7±1.1%CSA, p<0.01) and VM muscles (–2.8±1.9%CSA, p<0.05) showed a relatively modest improvement in fatty infiltration, in comparison with the medial hamstring, GR and SR muscles (–6.9±6.5%CSA, –4.9±4.1%CSA and –3.2±2.7%CSA, p<0.05, respectively) (Table 8). Longitudinal changes in intramuscular fat ratio of periarticular muscle groups and individual muscles are presented in Figure 15.
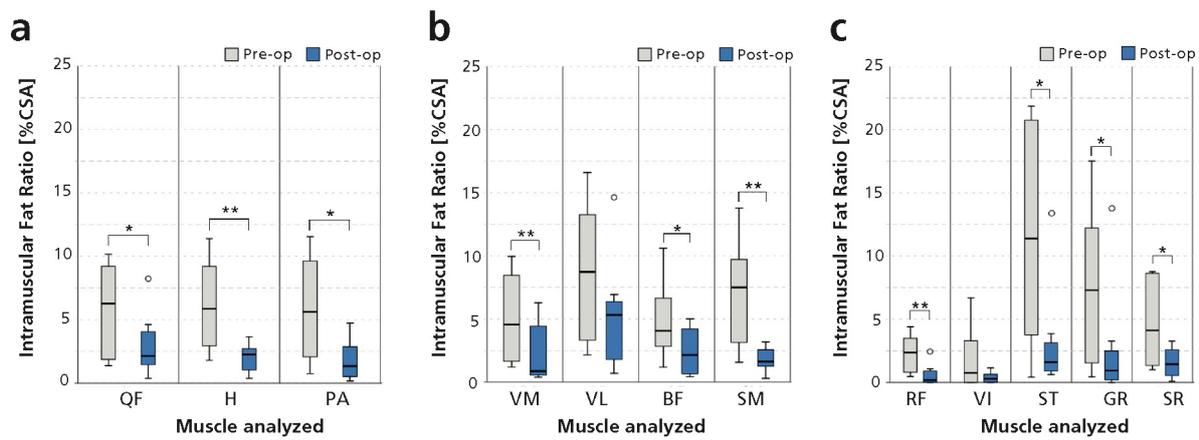

Figure 15. Boxplots of changes in intramuscular fat ratio. Percent change in intramuscular fat ratio in [% cross-sectional area (CSA)] of muscle groups (**a**) and of larger (**b**) and smaller (**c**) measurements of individual muscles. The horizontal, upper and lower lines of the box represent the median (50th percentile), upper (75th percentile) and lower (25th percentile) quartiles, respectively. The whiskers extend to the minimum and maximum values. Outliers are depicted as points outside the whiskers. QF, quadriceps femoris; H, hamstrings; PA, pes anserinus group; VM, vastus medialis; VL, vastus lateralis; BF, biceps femoris; SM, semimembranosus; RF, rectus femoris; VI, vastus interme-dius; ST, semitendinosus; GR, gracilis; SR, sartorius muscle. Paired sample t-test, *p≤0.05, **p≤0.01.

Table 8. Postoperative changes in intramuscular fat ratio per patient.

Patient ID	K2L	K3R	K4R	K5R	K6L	K7L	K8L	K9L	Average (SD)	p-value
QF	-5.4	-5.5	-7.2	-2.7	0.1	0.1	-1	-0.7	**-2.8 (2.9)**	0.041*
RF	-3.1	-2.5	-3.3	-1	-1.2	-0.5	-0.6	-1.3	**-1.7 (1.1)**	0.005**
VI	-4.6	-0.1	-5.5	-1.3	-0.6	0	0	0.3	**-1.5 (2.3)**	0.144
VL	-5.9	-8.1	-11	-3.6	-2.6	-1.5	-1.6	2	**-3.4 (4.8)**	0.171
VM	-5.2	-4.5	-5.0	-2.7	-0.4	-1.3	-0.9	-2	**-2.8 (1.9)**	0.01**
H	-6.7	-6.3	-9.3	-4	0.7	-1.9	-2.5	-3	**-4.1 (3.2)**	0.006**
BF	-6.5	-3.7	-5.3	-2.2	2.4	-0.8	-2.6	-0.8	**-2.4 (2.8)**	0.012*
SM	-6.9	-7.1	-11.6	-6.2	0.1	-2.2	-2.5	-4.5	**-5.2 (3.7)**	0.005**
ST	-4.1	-16.4	-19.2	-19.5	0.8	-5.8	-1.6	-3	**-8.6 (8.4)**	0.05*
PA	-6.5	-6.3	-9.7	-3.3	0.1	-1	-2.3	-3.6	**-4.1 (3.2)**	0.011*
GR	-6.2	-3.7	-11.9	-2.3	0.1	-0.4	-6.7	-7.9	**-4.9 (4.1)**	0.02*
SR	-6.8	-5.4	-6.6	-2.2	-0.1	-0.1	-1.6	-2.6	**-3.2 (2.7)**	0.018*
ALL	-5.5	-5.8	-8.8	-4.6	0.4	-1.4	-2.0	-2.2	**-3.7 (4.4)**	<0.001**

Values are given in [% cross-sectional area (CSA)]. Average values are arithmetic means (standard deviation [SD]). ALL is the total change in intramuscular fat ratio of individual muscles (RF, rectus femoris; VI, vastus intermedius; VL, vastus lateralis; VM, vastus medialis; BF, biceps femoris; SM, semimembranosus; ST, semitendinosus; GR, gracilis; SR, sartorius). The pes anserinus group (PA) comprises the ST, GR and SR muscles. QF, quadriceps femoris; H, hamstrings; ID, identification; K2L-K9L, patient identifier. P values were obtained using the paired t-test. Significance level *p≤0.05, **p≤0.01.

3.4 EMG activity

3.4.1 Muscle activation patterns

The average peak values of normalized muscle activation are shown for each muscle and ADL in Figure 16. The greatest inter-individual variation in peak activation was observed for the GM muscle during the static balancing exercise of OLS (61.9%). The lowest variations among patients occurred during the activities of stair descent (6.2%) and level walking (8.4%) for the VM muscle. Peak muscle activation levels obtained during the ADLs were used for the correlation analyses with periarticular muscle status (Table 21), *in vivo* knee joint load (Table 23) and EMD (Table 24). Muscle activation patterns, in relation to synchronized recordings of the *in vivo* tibio-femoral joint loads, are depicted for each ADL in Figures 17-22.
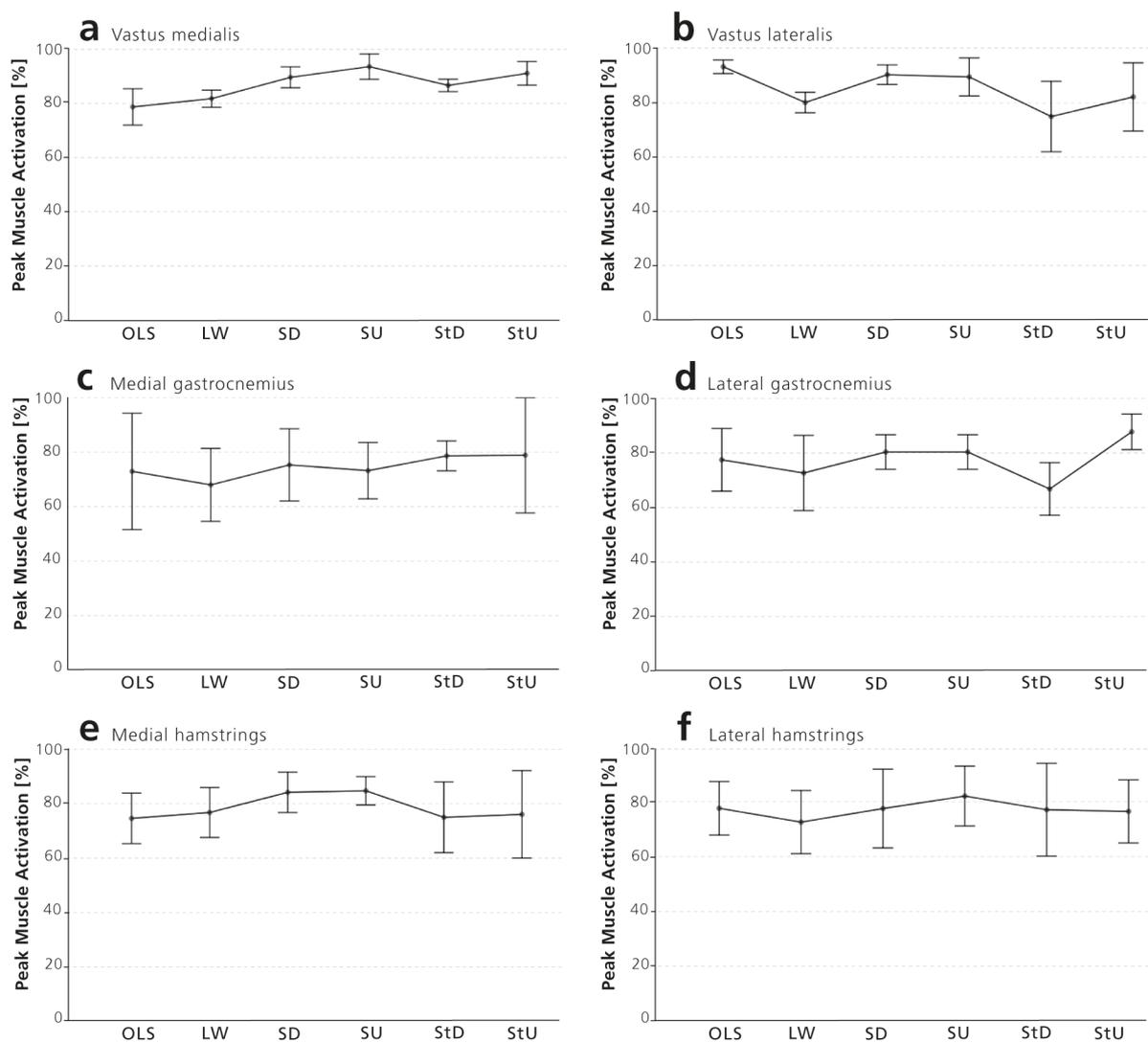
Figure 16. Peak muscle activation during functional activities. Line graph showing the average peak muscle activation and standard deviation for each of the investigated activities (OLS, one-legged stance; LW, level walking; SD, sit down; SU, stand up; StD, stairs down; StU, stairs up). Peak activation values are shown for the vastus medialis (**a**), vastus lateralis (**b**), medial gastrocnemius (**c**), lateral gastrocnemius (**d**), medial hamstring (**e**) and lateral hamstring (**f**) muscles.

The EMG profiles of the periarticular muscles and synchronized recordings of the average knee joint contact forces during **level walking** are presented in Figure 17. The VM and VL muscles showed an average peak in EMG activity during early stance phase in a range of 23 to 33% of the gait cycle and primarily contributed to the 1st peak of the knee joint contact forces (Figure 17a-b). The average peak activity of the VM (26.1±2.5% load cycle) thereby occured shortly before the VL muscle (28.15±2.9% load cycle). The plantarflexors showed a minor activity peak during the early single leg stance phase and reached a maximum during late stance at 58.6±13.7% of the gait cycle (GM: 63.5±6.7% load cycle; GL: 53.6±16.7% load cycle) (Figure 17c-d). The hamstrings foremost supported early stance at 22.8±4.1% of the gait cycle (HM 22.8±4.5% load cycle; HL 23.0±2.1% load cycle) and showed a second minor peak in activity during the late swing phase (Figure 17e-f).
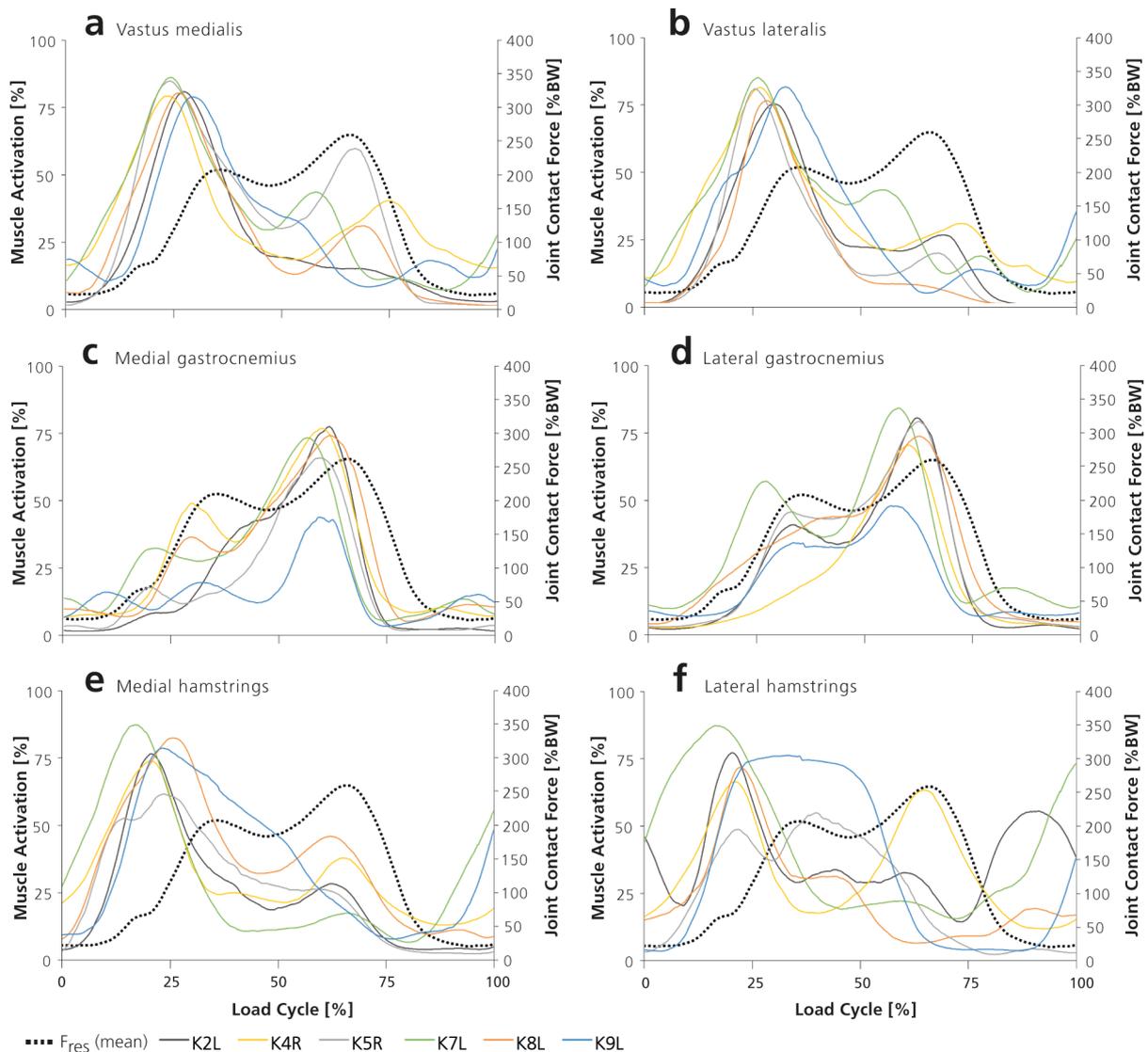
Figure 17. Electromyography (EMG) profiles and knee joint contact force during level walking. Direct comparison of the EMG signals (solid lines) normalized by the maximum per activity and patient with the resultant knee joint contact force (F_{res}) in % body weight (%BW) averaged over all patients (dashed line) throughout one load cycle. The EMG profiles represent the vastus medialis (**a**), vastus lateralis (**b**), medial gastrocnemius (**c**), lateral gastrocnemius (**d**), medial hamstring (**e**), lateral hamstring (**f**) muscles.

44

The EMG profiles of the VM and VL during **stair ascent** were similar to level walking with an activity peak during early loading response from 18 to 30% load cycle (mean 26.0±2.9%) (Figure 18a-b). The average peak in muscle activity of the VM (25.0±3.6% load cycle) shortly preceded the VL muscle (26.9±1.7% load cycle). The knee extensors showed a slight increase in activity in late stance around the second peak of the knee joint contact forces. This second peak was dominated by the gastrocnemius, which showed an average peak in EMG activity prior to swing initiation at 68.7±3.5% load cycle (range: 62-74). The average peak activity of the GM coincided with the GL muscle (68.9±3.4% load cycle versus 68.4±3.9% load cycle, respectively). The hamstrings showed high inter-individual differences in the timing of peak EMG activity (range: 0-79% load cycle) (Figure 18e-f). The tracings of EMG and the average knee joint loads during one load cycle of stair ascent are plotted in Figure 18.
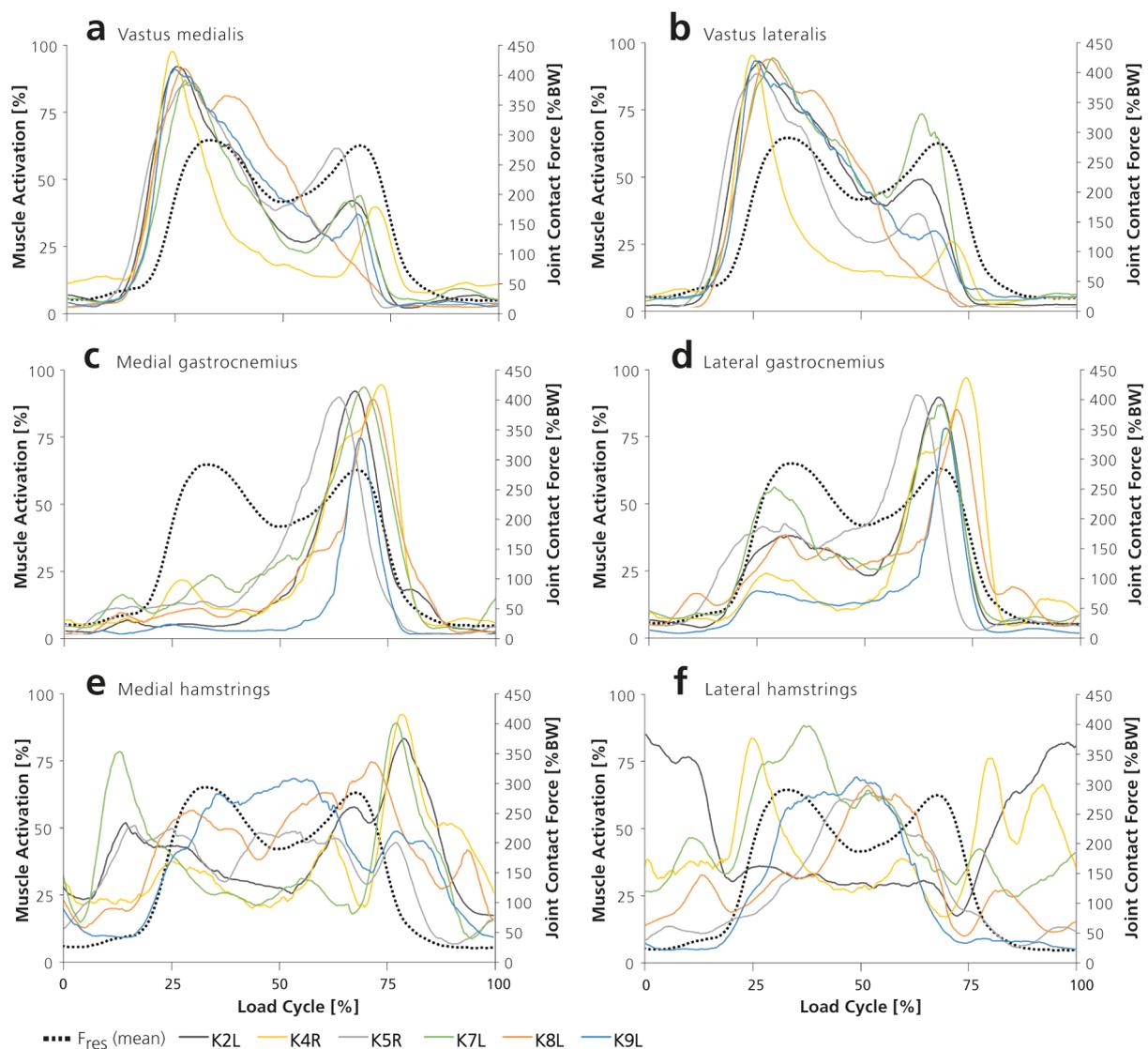

Figure 18. Electromyography (EMG) profiles and knee joint contact force during stair ascent. Direct comparison of the EMG signals (solid lines) normalized by the maximum per activity and patient with the resultant knee joint contact force (F$_{res}$) in % body weight (%BW) averaged over all patients (dashed line) throughout one load cycle. The EMG profiles represent the vastus medialis (**a**), vastus lateralis (**b**), medial gastrocnemius (**c**), lateral gastrocnemius (**d**), medial hamstring (**e**), lateral hamstring (**f**) muscles.

45

Stair descent showed a burst in activity of the GM muscle (18.6±1.9% load cycle) and, to a lesser extent, of the GL (32.0±22.7% load cycle) during weight acceptance (Figure 19c-d). The knee extensors VM and VL supported the early loading response and dominated the knee joint contact forces during late stance at 54.3±12.6% load cycle and 54.4±14.6% load cycle, respectively (Figure 19a-b). The hamstrings showed a wide inter-individual range in peak activity from 16 to 77% load cycle (HM: 38.1±29.6% load cycle; HL: 48.6±26.7% load cycle). The EMG profile of the HM and HL indicated a biphasic activity pattern with an increase in muscle activity before and after the first and second peak in joint contact force, respectively (Figure 19e-f). The time plot of periarticular muscle activity and average knee joint contact forces during stair descent are outlined in Figure 19.
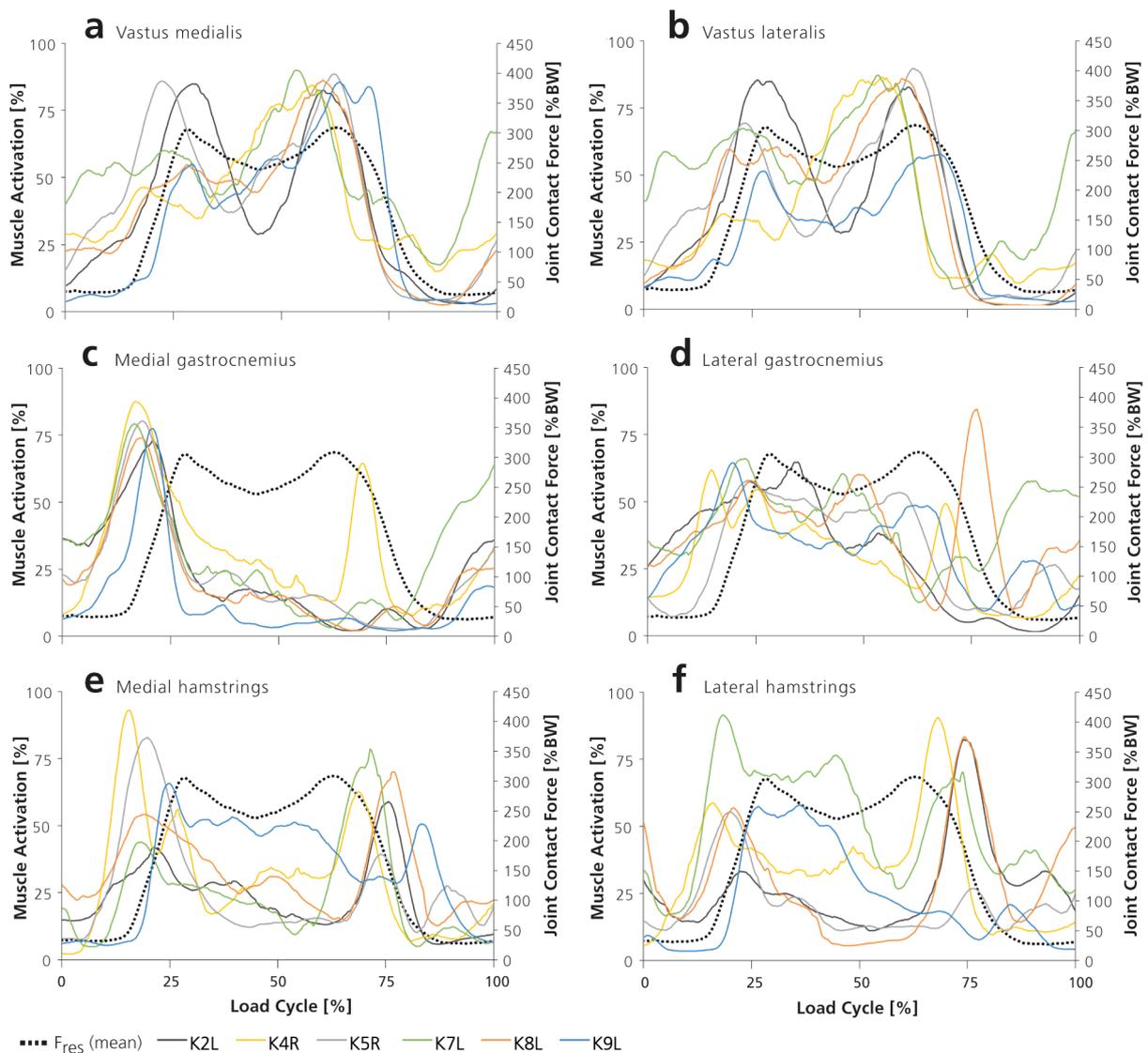

Figure 19. Electromyography (EMG) profiles and knee joint contact force during stair descent. Direct comparison of the EMG signals (solid lines) normalized by the maximum per activity and patient with the resultant knee joint contact force (F_{res}) in % body weight (%BW) averaged over all patients (dashed line) throughout one load cycle. The EMG profiles represent the vastus medialis (**a**), vastus lateralis (**b**), medial gastrocnemius (**c**), lateral gastrocnemius (**d**), medial hamstring (**e**), lateral hamstring (**f**) muscles.

The exercise of **sit-to-stand** was dominated by the activity of the VM (32.1±7.7% load cycle) and VL (44.0±14.5% load cycle) muscles during early motion at lift-off from the chair. Inter-individual variation in peak knee extensor activity ranged from 22 to 60% of the load cycle (Figure 20a-b). The plantarflexors GM (45.3±24.1% load cycle) and GL (62.2±11.2% load cycle) followed knee extensor activation and showed a wide range (9-81% load cycle) in peak activity between patients (Figure 20c-d). The hamstrings mostly supported hip and trunk extension during the straightening motion after the maximum knee joint contact force at seat-off (Figure 20e-f). The average peak activity of the HM and HL occurred at 65.2±12.5% load cycle and 48.3±14.5% load cycle (range: 22-81), respectively. Figure 20 shows the EMG curves of each patient and average knee joint contact forces during the activity of sit-to-stand.
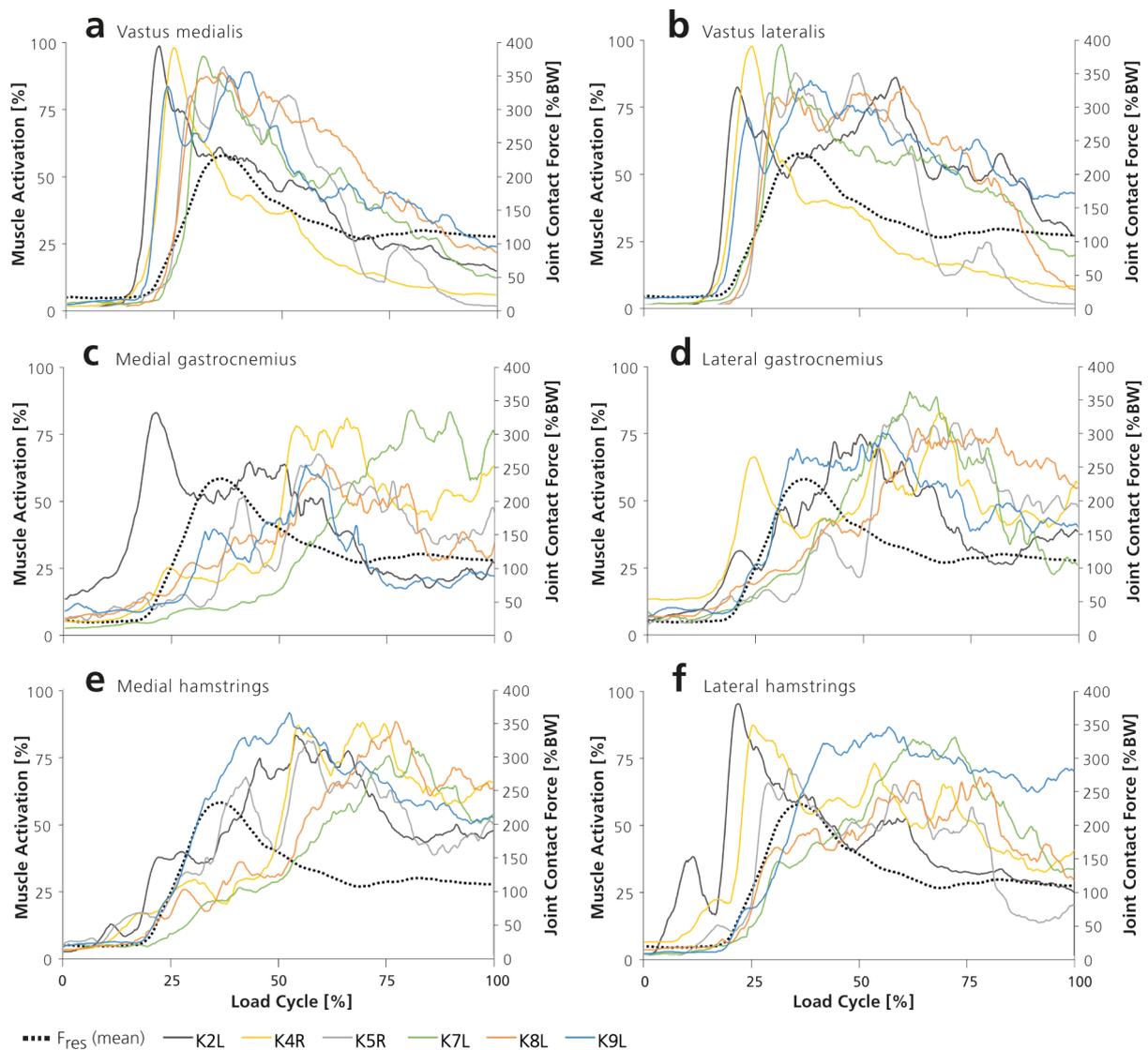
Figure 20. Electromyography (EMG) profiles and knee joint contact force during sit-to-stand. Direct comparison of the EMG signals (solid lines) normalized by the maximum per activity and patient with the resultant knee joint contact force (F_{res}) in % body weight (%BW) averaged over all patients (dashed line) throughout one load cycle. The EMG profiles represent the vastus medialis (**a**), vastus lateralis (**b**), medial gastrocnemius (**c**), lateral gastrocnemius (**d**), medial hamstring (**e**), lateral hamstring (**f**) muscles.

The VM and VL knee extensor muscles were the prime movers during the **stand-to-sit** task, showing a peak in EMG activity at 53.2±4.5% load cycle (range: 47-63) that coincided with the average peak knee joint contact force (Figure 21a-b). The average peak activity of the VM and VL muscles occurred at 52.6±5.8% load cycle and 53.7±3.2% load cycle, respectively. The hamstring (38.4±22.3% load cycle) and gastrocnemius (31.3±18.2% load cycle) muscles supported early motion and showed high inter-individual variations in peak activation timing (range: 6-78% load cycle). The HM (24.4±17.7% load cycle) and GM (19.4±9.5% load cycle) muscles showed an earlier average peak in muscle activity, compared to the HL (52.3±17.7% load cycle) and GL (43.2±17.4% load cycle) muscles. The average knee joint contact forces and the differential EMG activity of the periarticular muscles are displayed in Figure 21.
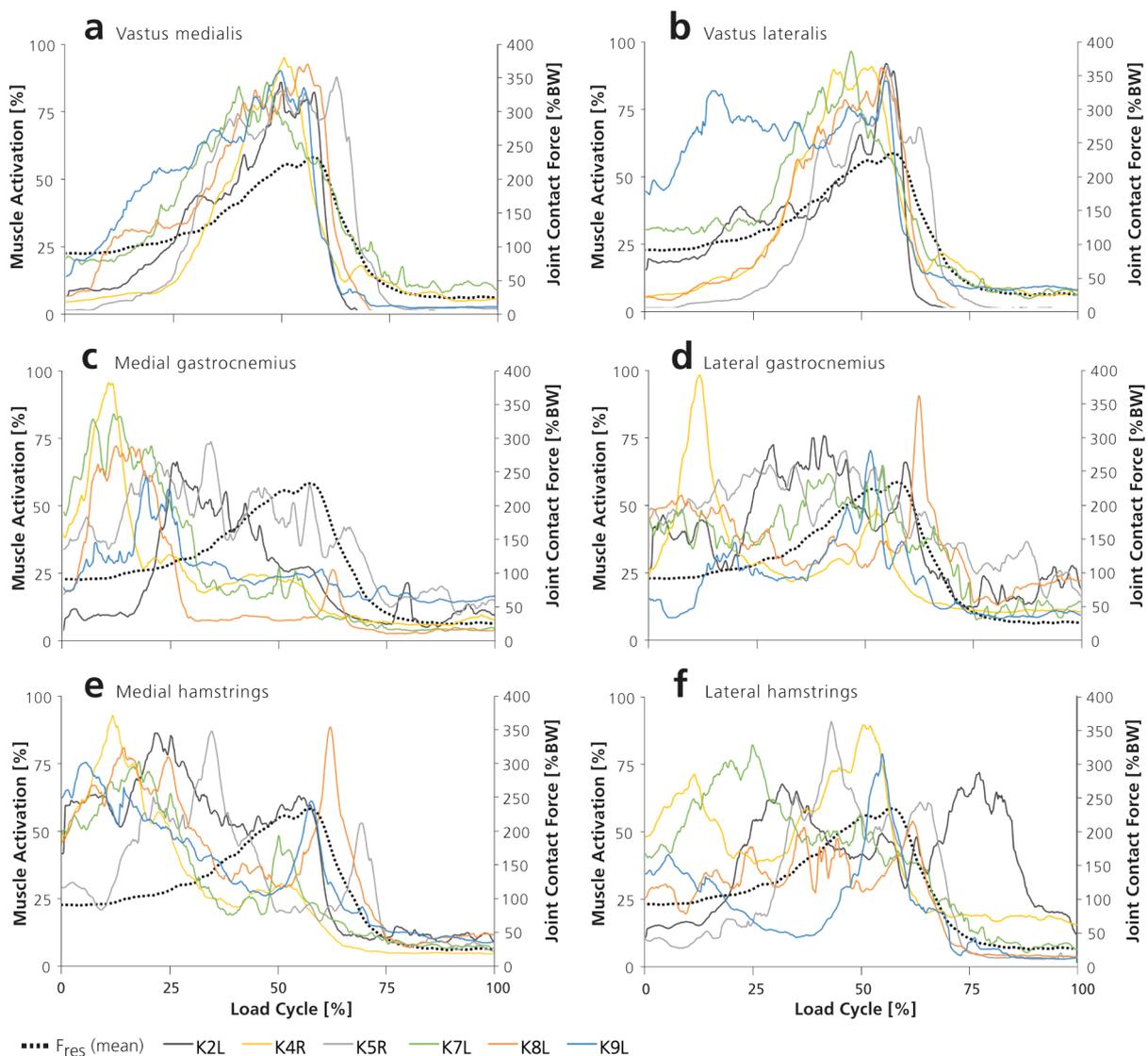

Figure 21. Electromyography (EMG) profiles and knee joint contact force during stand-to-sit. Direct comparison of the EMG signals (solid lines) normalized by the maximum per activity and patient with the resultant knee joint contact force (F_{res}) in % body weight (%BW) averaged over all patients (dashed line) throughout one load cycle. The EMG profiles represent the vastus medialis (**a**), vastus lateralis (**b**), medial gastrocnemius (**c**), lateral gastrocnemius (**d**), medial hamstring (**e**), lateral hamstring (**f**) muscles.

The EMG profiles of the periarticular muscles during the balance exercise of **OLS** are shown in relation to the average knee joint contact forces in Figure 22. The periarticular muscles reached a plateau in EMG activity, in parallel to the knee joint contact loads, after the patients achieved a balanced single-legged stance position. High inter-individual variations in the relative timing of peak EMG activity were determined for the knee extensor (21-69% load cycle), hamstring (19-81% load cycle) and gastrocnemius (20-64% load cycle) muscles. The timing in the average peak EMG activity of the medial muscles VM (38.2±17.7% load cycle), HM (47.0±23.2% load cycle) and GM (32.9±8.1% load cycle) preceded the lateral portions of VL (40.8±18.6% load cycle), HL (55.1±25.6% load cycle), GL (35.9±14.9% load cycle).
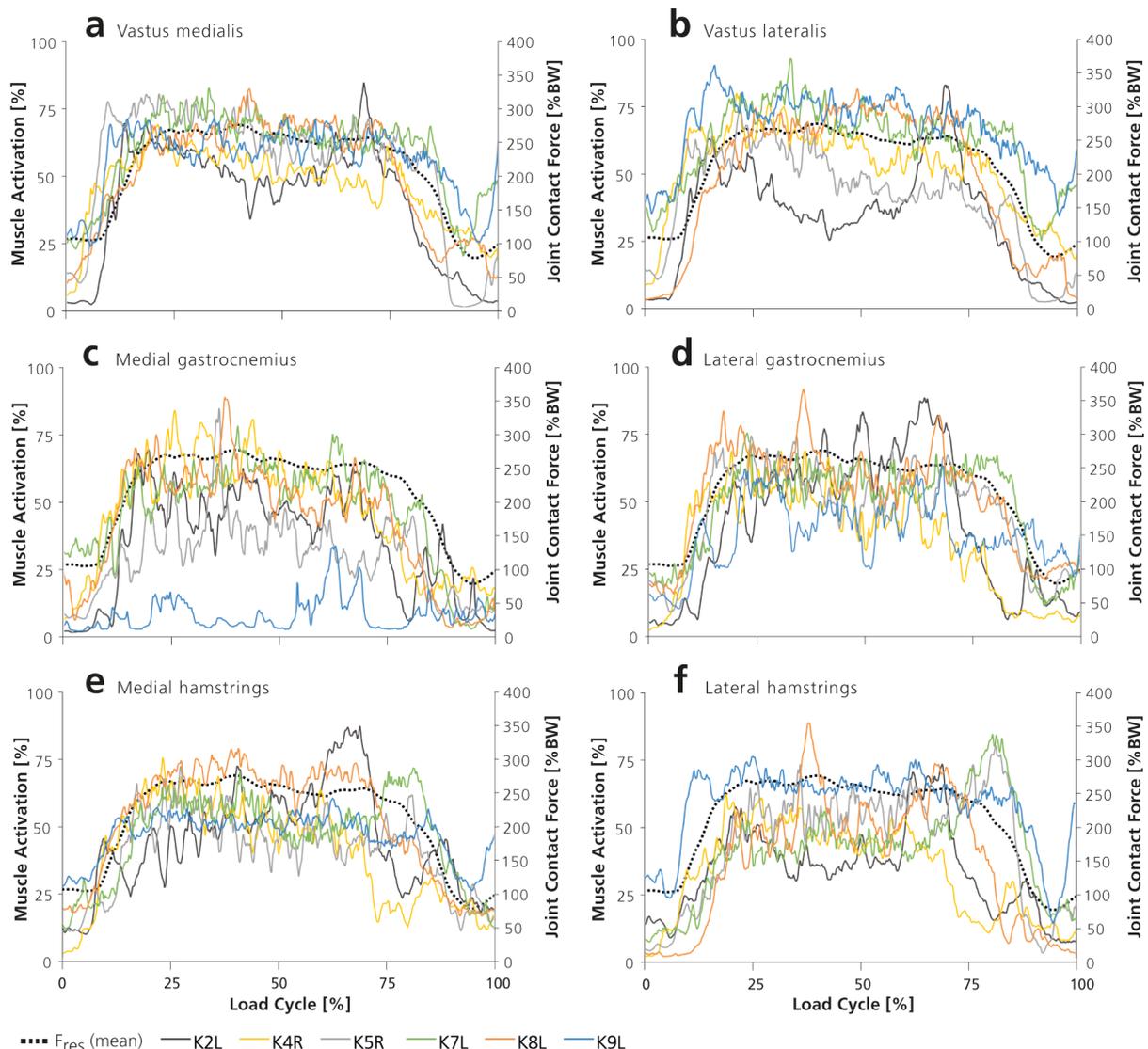

Figure 22. Electromyography (EMG) profiles and knee joint contact force during one-legged stance. Direct comparison of the EMG signals (solid lines) normalized by the maximum per activity and patient with the resultant knee joint contact force (F$_{res}$) in % body weight (%BW) averaged over all patients (dashed line) throughout one load cycle. The EMG profiles represent the vastus medialis (**a**), vastus lateralis (**b**), medial gastrocnemius (**c**), lateral gastrocnemius (**d**), medial hamstring (**e**), lateral hamstring (**f**) muscles.

3.4.2 EMD of periarticular muscles

The results of the cross-correlation analysis are summarized for the activity of **level walking** in Table 9. The mean time lag between the onset of periarticular muscle activity and the onset of knee joint contact forces during level walking ranged from 30.4 to 56.0 ms. The mean cross-correlation coefficients were moderate to high for the VM (r=0.52), GM (r=0.77) and GL (r=0.84) muscles. The corresponding mean EMD values of the VM, GM and GL muscles were 37.0±18.3 ms, 56.0±16.0 ms and 45.8±13.0 ms, respectively. The average EMD of the VM showed higher values compared to the VL muscle (37.0±18.3 ms versus 30.4±14.4 ms).

Table 9. Electromechanical delay and cross-correlation coefficients for level walking.

ID	EMD, ms						Cross correlation coefficient					
	VM	VL	HM	HL	GM	GL	VM	VL	HM	HL	GM	GL
K2L	45.12	26.72	77.18	24.94	68.87	47.50	0.411	0.566	0.455	-0.360	0.644	0.726
K4R	5.52	13.48	60.06	52.7	66.18	70.47	0.150	0.271	0.309	0.561	0.814	0.878
K5L	37.17	42.66	49.97	105.42	73.73	42.05	0.669	0.587	0.509	0.664	0.817	0.823
K7L	45.29	49.2	-111.82	-50.88	46.4	37.46	0.638	0.637	-0.425	-0.438	0.848	0.918
K8L	29.68	34.52	55.12	90.85	47.85	43.61	0.579	0.456	0.649	0.268	0.871	0.879
K9L	59.29	15.57	90.43	91.63	32.94	33.54	0.647	0.401	0.661	0.755	0.605	0.809
X̄ (SD)	37.01 (18.31)	30.36 (14.43)	36.82 (74.36)	52.44 (58.74)	56 (15.96)	45.77 (13.04)	0.516 (0.202)	0.486 (0.137)	0.360 (0.406)	0.242 (0.523)	0.767 (0.113)	0.839 (0.068)

Values represent the cross-correlation coefficient *R* and respective electromechanical delay (EMD) in [ms] between the onset of electromyographic muscle activity and the onset of *in vivo* knee joint contact forces for each patient. Average values (X̄) are arithmetic means (standard deviation [SD]). ID, identification; K2L-K9L, patient identifier; VM, vastus medialis; VL, vastus lateralis; HM, medial hamstrings; HL, lateral hamstrings; GM, medial gastrocnemius; GL, lateral gastrocnemius.

The mean EMD of the VM was 42.3±12.9 ms during **stair ascent**, while the VL showed a lower average value of 37.2±4.5 ms. This was compatible with the comparatively later peak activity of the VL during the load cycle (Figure 18a-b). The GM and GL muscles had a mean EMD of 8.4±19.8 ms and 14.8±18.1 ms, respectively. The mean cross-correlation coefficients of the knee extensors (r> 0.76) and gastrocnemius (r> 0.68) were high to moderate (Table 10).

Table 10. Electromechanical delay and cross-correlation coefficients for stair ascent.

ID	EMD, ms						Cross correlation coefficient					
	VM	VL	HM	HL	GM	GL	VM	VL	HM	HL	GM	GL
K2L	38.31	41.64	-116.6	-48.31	17.49	19.99	0.768	0.811	0.413	-0.416	0.681	0.846
K4R	34.75	36.79	-95.05	-40.88	-13.29	-18.4	0.647	0.628	0,318	-0.232	0.643	0.617
K5L	36.92	34.34	134.8	24.9	23.18	35.2	0.932	0.837	0.344	0.249	0.657	0.798
K7L	29.86	29.86	5.12	39.25	-18.77	15.36	0.737	0.835	-0.438	0.308	0.725	0.849
K8L	65.58	40.99	25.5	150.29	12.75	12.75	0.621	0.590	0.552	0.351	0.558	0.685
K9L	48.18	39.3	91.28	-96.35	29.16	24.09	0.863	0.808	0.334	0.406	0.453	0.583
X̄ (SD)	42.27 (12.91)	37.15 (4.49)	7.51 (99.47)	4.82 (87.06)	8.42 (19.8)	14.83 (18.09)	0.761 (0.121)	0.752 (0.112)	0.254 (0.350)	0.111 (0.346)	0.620 (0.098)	0.730 (0.117)

Values represent the cross-correlation coefficient *R* and respective electromechanical delay (EMD) in [ms] between the onset of electromyographic muscle activity and the onset of *in vivo* knee joint contact forces for each patient. Average values (X̄) are arithmetic means (standard deviation [SD]). ID, identification; K2L-K9L, patient identifier; VM, vastus medialis; VL, vastus lateralis; HM, medial hamstrings; HL, lateral hamstrings; GM, medial gastrocnemius; GL, lateral gastrocnemius.

The EMD during **stair descent** showed lower mean values compared to stair ascent for the VM (35.7±8.2 ms versus 42.3±12.9 ms) and VL (35.8±7.7 ms versus 37.2±4.5 ms) muscles. The cross-correlation coefficients of the VM and VL muscles were high with mean values of r=0.73 and r=0.75, respectively. The hamstrings (mean SD 87.4 ms) and gastrocnemius (mean SD 66.9 ms) muscles showed high inter-individual variations in average EMD and relatively low cross-correlation coefficients (r<0.5) during stair descent. The individual EMD values and cross-correlation coefficients are reported for stair descent in Table 11.

Table 11. Electromechanical delay and cross-correlation coefficients for stair descent.

ID	EMD, ms						Cross correlation coefficient					
	VM	VL	HM	HL	GM	GL	VM	VL	HM	HL	GM	GL
K2L	40.67	41.5	-68.06	-59.76	3.32	46.48	0.783	0.840	0.523	0.443	-0.538	0.318
K4R	32.71	32.71	115.49	-89.94	90.96	83.81	0.596	0.612	0.440	0.350	0.409	0.315
K5L	47.11	39.49	78.29	74.13	85.91	61.66	0.888	0.842	0.446	0.424	0.608	0.784
K7L	22.78	25.63	-120.53	77.82	-32.27	62.64	0.450	0.575	0.452	0.326	-0.457	0.397
K8L	33.82	45.66	-0.85	-99.78	-27.90	-105.7	0.77	0.798	-0.309	0.268	-0.547	0.281
K9L	36.9	29.52	60.27	46.74	-1.23	124.22	0.871	0.856	0.401	0.579	-0.450	0.635
X̄ (SD)	35.67 (8.19)	35.75 (7.69)	10.77 (91.17)	-8.47 (83.57)	19.8 (55.02)	45.52 (78.84)	0.726 (0.171)	0.754 (0.126)	0.326 (0.313)	0.398 (0.109)	-0.163 (0.525)	0.455 (0.206)

Values represent the cross-correlation coefficient *R* and respective electromechanical delay (EMD) in [ms] between the onset of electromyographic muscle activity and the onset of *in vivo* knee joint contact forces for each patient. Average values (X̄) are arithmetic means (standard deviation [SD]). ID, identification; K2L-K9L, patient identifier; VM, vastus medialis; VL, vastus lateralis; HM, medial hamstrings; HL, lateral hamstrings; GM, medial gastrocnemius; GL, lateral gastrocnemius.

The **sit-to-stand** exercise showed mean EMD values of 66.2±11.0 ms (r=0.77) and 63.7 ±13.8 ms (r=0.71) for the VM and VL muscles, respectively. The cross-correlation coefficient of the HL was moderate (r=0.53) and showed a mean EMD of 7.86±110.56 ms. The high standard deviation of the mean EMD value of the HL resulted from a negative outlier, as the onset of knee joint contact forces preceded the HL activity onset in patient K9L. The values of EMD and cross-correlation coefficients during the sit-to-stand task are presented in Table 12.

Table 12. Electromechanical delay and cross-correlation coefficients for sit-to-stand.

ID	EMD, ms						Cross correlation coefficient					
	VM	VL	HM	HL	GM	GL	VM	VL	HM	HL	GM	GL
K2L	53.15	49.82	46.5	36.54	56.47	146.15	0.857	0.744	0.377	0.799	0.555	0.238
K4R	72.11	83.2	-133.12	49.92	-138.67	92.91	0.814	0.821	-0.247	0.718	-0.185	0.485
K5L	57.09	50.17	-131.8	51.9	-301.02	88.23	0.705	0.75	0.269	0.600	-0.219	-0.164
K7L	60.93	60.93	-204.79	59.24	-3.39	-338.50	0.789	0.722	-0.176	0.256	-0.17	0.241
K8L	71.71	61.22	-297.34	66.47	59.47	-304.34	0.819	0.622	-0.19	0.335	0.118	-0.109
K9L	82.21	76.96	-118.94	-216.89	-118.94	-118.94	0.631	0.586	0.379	0.445	0.211	0.399
X̄ (SD)	66.2 (10.98)	63.72 (13.75)	-139.86 (113.4)	7.86 (110.56)	-74.35 (139.96)	-72.42 (213.38)	0.769 (0.085)	0.708 (0.088)	0.069 (0.303)	0.526 (0.216)	0.052 (0.304)	0.182 (0.265)

Values represent the cross-correlation coefficient *R* and respective electromechanical delay (EMD) in [ms] between the onset of electromyographic muscle activity and the onset of *in vivo* knee joint contact forces for each patient. Average values (X̄) are arithmetic means (standard deviation [SD]). ID, identification; K2L-K9L, patient identifier; VM, vastus medialis; VL, vastus lateralis; HM, medial hamstrings; HL, lateral hamstrings; GM, medial gastrocnemius; GL, lateral gastrocnemius.

The mean EMD during the activity of **stand-to-sit** was 51.7±12.6 ms (range: 33.2-67.8) for the VM and 45.5±8.1 ms (range: 37.1-57.0) for the VL muscle. The corresponding cross-correlation coefficients of the mean EMD were r=0.68 and r=0.7 for the VM and VL muscles, respectively. The hamstring (mean SD 109.3 ms) and gastrocnemius (mean SD 192.8 ms) muscles showed high inter-individual differences in mean EMD due to variations in the performance of the movement task. Table 13 reports the individual EMD and cross-correlation coefficients during the sit-to-stand task.

Table 13. Electromechanical delay and cross-correlation coefficients for stand-to-sit.

ID	EMD, ms						Cross correlation coefficient					
	VM	VL	HM	HL	GM	GL	VM	VL	HM	HL	GM	GL
K2L	33.26	37.42	41.57	-236.97	-399.1	4.16	0.76	0.844	0.398	-0.265	-0.171	0.319
K4R	67.81	56.96	32.55	56.96	103.08	59.68	0.811	0.792	0.236	0.592	0.17	0.334
K5L	62.62	52.52	-96.96	32.32	246.44	-234.32	0.688	0.757	0.23	0.462	0.179	-0.139
K7L	52.98	42.39	164.25	-21.19	317.9	-58.28	0.454	0.542	-0.227	0.123	-0.147	0.183
K8L	43.72	37.16	192.35	-48.09	-34.97	-43.72	0.713	0.721	-0.288	0.245	-0.12	0.265
K9L	49.94	46.71	3.22	57.99	201.35	128.87	0.643	0.523	0.37	0.48	-0.121	0.357
x̄ (SD)	51.72 (12.55)	45.53 (8.08)	56.16 (107)	-26.5 (111.67)	72.45 (261.52)	-23.94 (124.07)	0.678 (0.124)	0,697 (0.133)	0.12 (0.301)	0.273 (0.314)	-0.035 (0.163)	0.22 (0.186)

Values represent the cross-correlation coefficient *R* and respective electromechanical delay (EMD) in [ms] between the onset of electromyographic muscle activity and the onset of *in vivo* knee joint contact forces for each patient. Average values (x̄) are arithmetic means (standard deviation [SD]). ID, identification; K2L-K9L, patient identifier; VM, vastus medialis; VL, vastus lateralis; HM, medial hamstrings; HL, lateral hamstrings; GM, medial gastrocnemius; GL, lateral gastrocnemius.

The longest EMD times of all investigated ADLs were determined during the activity of **OLS** with mean values ranging from 55.8 to 251.8 ms. The mean EMD of the lateral muscles was by 61.4% shorter than that of the medial musculature (p=0.064). The mean EMD values of lateral and medial muscles were 71.9±15.5 ms (range: 55.8-86.7) and 186.3±74.3 ms (range: 105.5-251.8), respectively. There were high inter-individual differences in mean EMD during the static balance exercise of OLS for all muscle groups (mean SD 139.6 ms) (Table 14).

Table 14. Electromechanical delay and cross-correlation coefficients for one-legged stance.

ID	EMD, ms						Cross correlation coefficient					
	VM	VL	HM	HL	GM	GL	VM	VL	HM	HL	GM	GL
K2L	46.35	355.35	293.55	46.35	386.25	54.08	0.386	0.291	0.293	0.363	0.142	0.373
K4R	411.07	0	58.72	50.34	58.72	58.72	0.265	0.226	0.258	0.357	0.336	0.359
K5L	111.10	8.55	-59.82	85.12	109.44	206.72	0.3	0.299	0.182	0.291	0.225	0.261
K7L	97.28	-48.64	158.08	48.64	97.28	60.80	0.214	0.207	0.178	0.243	0.239	0.25
K8L	502.36	92.54	79.32	52.88	52.88	88.13	0.257	0.25	0.264	0.391	0.408	0.347
K9L	41.35	31.01	103.38	51.69	806.36	51.69	0.293	0.247	0.336	0.486	-0.105	0.206
x̄ (SD)	201.59 (201.59)	73.14 (145.7)	105.54 (116.91)	55.84 (14.53)	251.82 (298.87)	86.69 (60.25)	0.286 (0.058)	0.253 (0.036)	0.252 (0.062)	0.355 (0.084)	0.208 (0.179)	0.299 (0.069)

Values represent the cross-correlation coefficient *R* and respective electromechanical delay (EMD) in [ms] between the onset of electromyographic muscle activity and the onset of *in vivo* knee joint contact forces for each patient. Average values (x̄) are arithmetic means (standard deviation [SD]). ID, identification; K2L-K9L, patient identifier; VM, vastus medialis; VL, vastus lateralis; HM, medial hamstrings; HL, lateral hamstrings; GM, medial gastrocnemius; GL, lateral gastrocnemius.

The cross-correlation coefficients of the EMD between the onset of muscle activity and tibio-femoral joint contact force are displayed in Figure 23. The VM (r=0.62) and VL (r=0.61) showed the highest average cross-correlation values of the periarticular muscles across all ADLs (Figure 23a-b). The balance exercise of OLS showed the lowest mean cross-correlation coefficients of the ADLs (r=0.28), as high inter-individual variations in muscle coordination timing were involved in maintaining postural stability (Figure 22, Table 14).
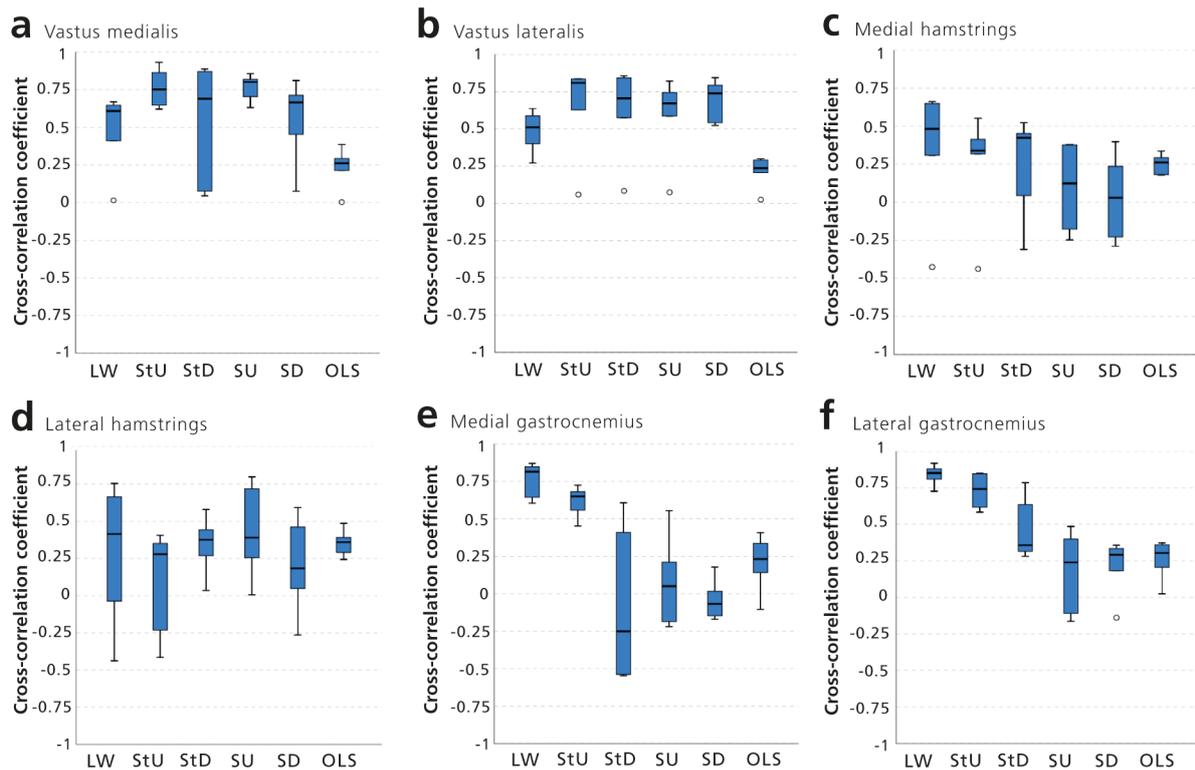

Figure 23. Cross-correlation coefficients between knee joint contact force and electromyography (EMG). Boxplots of the cross-correlations with the EMG activity of the vastus medialis (**a**), vastus lateralis (**b**), medial hamstring (**c**), lateral hamstring (**d**), medial gastrocnemius (**e**) and lateral gastrocnemius (**f**) muscles for each investigated activity (LW, level walking; StU, stairs up; StD, stairs down; SU, stand up; SD, sit down; OLS, one-legged stance). The horizontal, upper and lower lines of the box represent the median (50th percentile), upper (75th percentile) and lower (25th percentile) quartiles, respectively. The whiskers extend to the minimum and maximum values. Outliers are depicted as points outside the boxes and whiskers.

3.5   Associations with periarticular muscle status

3.5.1 Association between muscle status and *in vivo* joint loads

The correlation analysis of muscle status and *in vivo* knee joint load showed only minor effects for the parameter of **distal muscle volume** (Table 15). The only significant positive correlation of distal volume with the average peak knee joint loads was determined for the ST muscle (r=0.71, p=0.05) during the activity of stair descent. The distal ST volume had a moderate, but nonsignificant effect (r=0.52) during level walking. The distal volume of the VM muscle indicated a positive trend during level walking (r=0.51) and stair descent (r=0.6).

Table 15. Pearson correlation coefficients between distal muscle volume and joint contact force.

	Level Walking		Stairs Up		Stairs Down		Stand Up	Sit Down	One-Legged Stance
	1P	2P	1P	2P	1P	2P	Max	Max	Max
QF	0.38 (0.36)	0.13 (0.75)	0.35 (0.39)	0.08 (0.85)	0.39 (0.34)	0.61 (0.12)	-0.11 (0.79)	-0.2 (0.63)	0 (0.99)
RF	0.52 (0.19)	-0.43 (0.28)	-0.15 (0.72)	-0.21 (0.62)	-0.31 (0.45)	0.08 (0.85)	-0.14 (0.75)	-0.03 (0.95)	-0.67 (0.07)
VI	0.02 (0.97)	-0.32 (0.44)	-0.47 (0.24)	-0.47 (0.25)	-0.58 (0.13)	0.04 (0.92)	-0.54 (0.16)	-0.32 (0.45)	-0.48 (0.23)
VL	-0.03 (0.94)	-0.49 (0.21)	0.07 (0.87)	0.05 (0.91)	0.32 (0.43)	0.32 (0.44)	-0.21 (0.63)	-0.32 (0.44)	0.22 (0.61)
VM	0.51 (0.2)	-0.08 (0.85)	0.38 (0.36)	0.02 (0.97)	0.3 (0.48)	0.6 (0.12)	-0.13 (0.76)	-0.21 (0.61)	-0.12 (0.79)
H	-0.24 (0.56)	0.09 (0.83)	0.36 (0.38)	0.08 (0.86)	0.56 (0.51)	0.32 (0.43)	0.03 (0.94)	-0.03 (0.95)	0.6 (0.12)
BF	-0.11 (0.79)	0.13 (0.77)	0.59 (0.13)	0.09 (0.83)	0.64 (0.09)	0.54 (0.17)	0.17 (0.68)	0.16 (0.71)	0.69 (0.06)
SM	-0.35 (0.39)	-0.06 (0.88)	-0.02 (0.97)	-0.05 (0.92)	0.24 (0.56)	-0.04 (0.93)	-0.16 (0.7)	-0.22 (0.6)	0.33 (0.42)
ST	0.08 (0.85)	0.52 (0.19)	0.45 (0.26)	0.47 (0.24)	0.71* (0.05)	0.46 (0.26)	0.23 (0.59)	0.06 (0.9)	0.33 (0.43)
PA	0.13 (0.76)	0.29 (0.49)	0.28 (0.51)	0.07 (0.87)	0.51 (0.2)	0.42 (0.3)	-0.12 (0.79)	-0.28 (0.51)	0.25 (0.55)
GR	0.22 (0.6)	0.55 (0.16)	0.12 (0.78)	0.23 (0.59)	0.34 (0.41)	0.48 (0.23)	-0.04 (0.93)	-0.08 (0.84)	-0.07 (0.87)
SR	0.09 (0.83)	0.03 (0.95)	0.18 (0.67)	-0.18 (0.67)	0.36 (0.38)	0.26 (0.53)	-0.27 (0.52)	-0.42 (0.3)	0.26 (0.53)

Values are Pearson correlation coefficients *r* and p-values in parenthesis for the variables of postoperative distal muscle volume and average peak knee joint contact force during activities of daily living. QF, quadriceps femoris; RF, rectus femoris; VI, vastus intermedius; VL, vastus lateralis; VM, vastus medialis; H, hamstrings; BF, biceps femoris; SM, semimembranosus; ST, semitendinosus; PA, pes anserinus group; GR, gracilis; SR, sartorius muscle; OLS, One-legged stance; 1P, 1st load peak; 2P, 2nd load peak; Max, maximum load. Significance level *p≤0.05, **p≤0.01.

Only the ST muscle showed a significant association (r=0.86, p=0.01) between **muscle CSA** and increased average peak knee joint loads during late stance of level walking. In line with the correlation analyses of distal volume (Table 15), the CSA of the VM showed an effect on the knee joint loads during gait (r=0.50) and stair descent (r=0.58) that did not reach statistical significance. Pearson correlations between the BF CSA and the joint load at the first peak of stair ascent (r=0.59), stair descent (r=0.63) and the maximum of OLS (r=0.58) were moderate but nonsignificant. Table 16 shows the Pearson correlation coefficients for muscle CSA.

Table 16. Pearson correlation coefficients between muscle cross-sectional area and joint contact force.

	Level Walking		Stairs Up		Stairs Down		Stand Up	Sit Down	One-Legged Stance
	1P	2P	1P	2P	1P	2P	Max	Max	Max
QF	0.44 (0.28)	-0.21 (0.62)	0.35 (0.39)	-0.05 (0.91)	0.27 (0.52)	0.61 (0.11)	-0.21 (0.61)	-0.27 (0.52)	-0.1 (0.81)
RF	-0.4 (0.92)	0.16 (0.71)	0.46 (0.26)	0.22 (0.6)	0.66 (0.07)	0.15 (0.73)	0.35 (0.39)	0.21 (0.61)	0.55 (0.16)
VI	-0.4 (0.32)	0.3 (0.47)	0.21 (0.63)	0.31 (0.45)	0.52 (0.19)	0.18 (0.67)	0.13 (0.77)	0.09 (0.84)	0.5 (0.21)
VL	0.31 (0.45)	-0.04 (0.93)	0.26 (0.53)	0.03 (0.94)	0.29 (0.48)	0.62 (0.1)	0.21 (0.63)	-0.3 (0.93)	-0.09 (0.83)
VM	0.5 (0.21)	-0.3 (0.47)	0.35 (0.4)	-0.11 (0.8)	0.19 (0.66)	0.58 (0.14)	-0.21 (0.61)	-0.26 (0.53)	-0.15 (0.72)
H	-0.18 (0.67)	-0.01 (0.98)	0.21 (0.62)	0.02 (0.97)	0.44 (0.27)	0.16 (0.7)	-0.06 (0.9)	-0.15 (0.72)	0.41 (0.31)
BF	-0.04 (0.93)	-0.01 (0.98)	0.59 (0.13)	0.13 (0.76)	0.63 (0.1)	0.5 (0.2)	0.19 (0.65)	0.17 (0.69)	0.58 (0.13)
SM	-0.25 (0.56)	-0.09 (0.83)	-0.21 (0.62)	-0.14 (0.75)	0.1 (0.82)	-0.22 (0.6)	0.19 (0.65)	0.17 (0.69)	0.12 (0.78)
ST	-0.07 (0.87)	0.86** (0.01)	0.06 (0.88)	0.48 (0.23)	0.41 (0.31)	0.24 (0.57)	0.23 (0.59)	0.18 (0.67)	0.11 (0.79)
PA	0.23 (0.58)	0.23 (0.58)	0.33 (0.43)	0.13 (0.76)	0.54 (0.17)	0.59 (0.12)	-0.05 (0.91)	-0.11 (0.79)	0.13 (0.76)
GR	0.24 (0.57)	0.3 (0.47)	0.14 (0.74)	0.16 (0.71)	0.31 (0.45)	0.59 (0.12)	-0.05 (0.91)	-0.18 (0.67)	-0.13 (0.76)
SR	0.23 (0.58)	-0.09 (0.83)	0.36 (0.39)	-0.05 (0.91)	0.45 (0.26)	0.47 (0.24)	-0.07 (0.87)	-0.14 (0.75)	0.18 (0.66)

Values are Pearson correlation coefficients *r* and p-values in parenthesis for the variables of postoperative muscle cross-sectional area and average peak knee joint contact force during activities of daily living. QF, quadriceps femoris; RF, rectus femoris; VI, vastus intermedius; VL, vastus lateralis; VM, vastus medialis; H, hamstrings; BF, biceps femoris; SM, semimembranosus; ST, semitendinosus; PA, pes anserinus group; GR, gracilis; SR, sartorius muscle; 1P, 1st load peak; 2P, 2nd load peak; Max, maximum load. Significance level *p≤0.05, **p≤0.01.
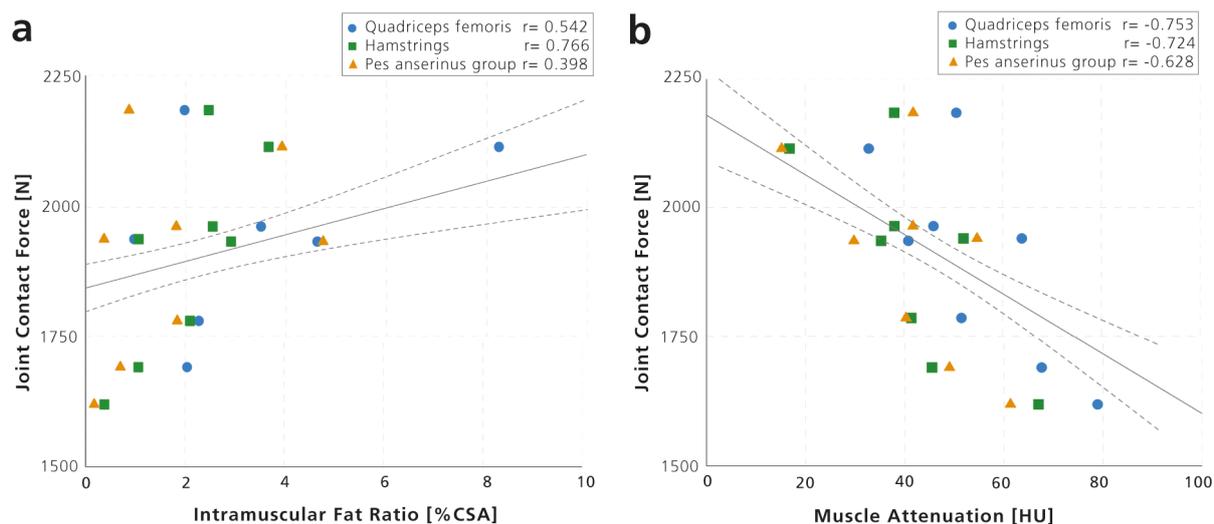
Figure 24. Scatter plot of the muscle fatty infiltration and joint contact force relationship. The peak knee joint contact force in [N] during level walking is plotted for each patient against the, **a**: intramuscular fat ratio in [% cross-sectional area (CSA)], **b**: muscle attenuation in [HU] of the quadriceps femoris, hamstring and pes anserinus group muscles. Pearson correlation coefficients *r*, linear fit (solid line) and 95% confidence interval (dashed line) are shown.

The **muscle attenuation** values of the quadriceps (r=–0.75, p<0.05) and hamstring (r=–0.72, p<0.05) muscles were significantly correlated with the *in vivo* knee joint loads in the early stance phase of level walking. The VL (r=–0.75, p<0.05), RF (r=–0.86, p=0.01) and BF (r=–0.84, p=0.01) muscles showed strong inverse associations with the first peak in joint load during walking. Moderate correlation coefficients (–0.5 ≥ r > –0.7) were not statistically significant. Table 17 summarizes the Pearson correlation coefficients of muscle attenuation and peak tibio-femoral forces for each ADL. The inverse relation between muscle attenuation and knee joint contact forces recorded at the first peak of walking is visualized in Figure 24b.

Table 17. Pearson correlation coefficients between muscle attenuation and joint contact force.

	Level Walking		Stairs Up		Stairs Down		Stand Up	Sit Down	One-Legged Stance
	1P	2P	1P	2P	1P	2P	Max	Max	Max
QF	-0.75* (0.03)	-0.04 (0.93)	-0.19 (0.66)	-0.06 (0.89)	-0.28 (0.51)	-0.11 (0.8)	-0.1 (0.82)	0.15 (0.72)	0.36 (0.38)
RF	-0.86** (0.01)	-0.19 (0.66)	-0.35 (0.4)	-0.4 (0.32)	-0.42 (0.31)	-0.12 (0.78)	-0.51 (0.19)	-0.29 (0.48)	0.43 (0.29)
VI	-0.51 (0.2)	-0.03 (0.94)	-0.25 (0.55)	0.04 (0.92)	-0.4 (0.32)	-0.16 (0.71)	-0.01 (0.95)	0.23 (0.58)	0.03 (0.94)
VL	-0.75* (0.03)	-0.07 (0.88)	-0.14 (0.74)	-0.06 (0.88)	-0.17 (0.69)	-0.16 (0.72)	-0.3 (0.95)	0.19 (0.65)	0.44 (0.27)
VM	-0.63 (0.1)	0.14 (0.74)	0 (1)	0.18 (0.66)	-0.09 (0.84)	0.03 (0.95)	0.15 (0.72)	0.39 (0.35)	0.38 (0.36)
H	-0.72* (0.04)	0.06 (0.9)	0.02 (0.96)	0.03 (0.95)	-0.07 (0.88)	-0.09 (0.84)	0.11 (0.79)	0.3 (0.47)	0.58 (0.13)
BF	-0.84** (0.01)	0.05 (0.91)	-0.32 (0.44)	-0.23 (0.44)	-0.33 (0.43)	-0.25 (0.55)	-0.17 (0.69)	0.07 (0.87)	0.45 (0.26)
SM	-0.61 (0.11)	-0.07 (0.87)	0.16 (0.71)	-0.06 (0.89)	-0.07 (0.87)	0.01 (0.99)	0.08 (0.85)	0.25 (0.56)	0.63 (0.09)
ST	-0.53 (0.18)	0.17 (0.68)	0.23 (0.59)	0.37 (0.36)	0.23 (0.59)	0.01 (0.98)	0.4 (0.33)	0.51 (0.19)	0.51 (0.2)
PA	-0.63 (0.1)	0.08 (0.85)	0.12 (0.78)	0.23 (0.58)	0.05 (0.91)	0.09 (0.84)	0.2 (0.63)	0.41 (0.31)	0.47 (0.24)
GR	-0.69 (0.06)	0.05 (0.91)	-0.07 (0.86)	0.05 (0.91)	-0.15 (0.73)	0.19 (0.66)	-0.12 (0.78)	0.17 (0.78)	0.34 (0.41)
SR	-0.58 (0.13)	-0.1 (0.81)	0.07 (0.86)	0.06 (0.89)	-0.12 (0.77)	0.11 (0.79)	0.08 (0.85)	0.35 (0.4)	0.39 (0.35)

Values are Pearson correlation coefficients *r* and p-values in parenthesis for the variables of postoperative muscle attenuation and average peak knee joint contact force during activities of daily living. QF, quadriceps femoris; RF, rectus femoris; VI, vastus intermedius; VL, vastus lateralis; VM, vastus medialis; H, hamstrings; BF, biceps femoris; SM, semimembranosus; ST, semitendinosus; PA, pes anserinus group; GR, gracilis; SR, sartorius muscle; 1P, 1st load peak; 2P, 2nd load peak; Max, maximum load. Significance level *p≤0.05, **p≤0.01.

The **intramuscular fat ratio** contributed significantly to increased knee joint loads (Table 18). There was a strong significant correlation of the intramuscular fat ratio of the hamstring group (r=0.77, p<0.05), and the VL (r=0.75, p<0.05) and BF (r=0.87, p=0.01) with increased knee joint loads at the first peak of level walking. Increased knee joint loads at the second peak of level walking correlated significantly with the intramuscular fat ratio of the VI muscle (r=0.71, p=0.05). There was a moderate, but nonsignificant association of the intramuscular fat ratio of the RF muscle and peak knee joint loads during level walking and the activity of sit-to-stand (r=0.63 and r=0.52, p>0.05, respectively). The Pearson correlation coefficients of intramuscular fat ratio of individual periarticular muscles and the knee joint loads are reported in Table 18. Figure 24a displays the positive trend between the intramuscular fat ratio of the muscle groups and increased knee joint contact forces during gait.

Table 18. Pearson correlation coefficients between intramuscular fat ratio and joint contact force.

	Level Walking		Stairs Up		Stairs Down		Stand Up	Sit Down	One-Legged Stance
	1P	2P	1P	2P	1P	2P	Max	Max	Max
QF	0.54 (0.17)	-0.3 (0.47)	-0.16 (0.7)	-0.39 (0.34)	-0.16 (0.71)	-0.07 (0.87)	-0.39 (0.38)	-0.57 (0.14)	-0.44 (0.27)
RF	0.63 (0.1)	0.28 (0.51)	0.21 (0.61)	0.54 (0.17)	0.14 (0.74)	0.08 (0.85)	0.52 (0.18)	0.43 (0.28)	-0.51 (0.2)
VI	-0.03 (0.95)	0.71* (0.05)	0.12 (0.77)	0 (0.1)	0.46 (0.25)	-0.02 (0.97)	0.17 (0.68)	-0.01 (0.99)	-0.49 (0.22)
VL	0.75* (0.03)	-0.18 (0.67)	0.09 (0.83)	-0.12 (0.78)	-0.02 (0.96)	0.16 (0.72)	-0.1 (0.81)	-0.26 (0.54)	-0.5 (0.21)
VM	0.47 (0.24)	-0.33 (0.42)	-0.08 (0.85)	-0.42 (0.3)	-0.06 (0.88)	-0.18 (0.68)	-0.29 (0.48)	-0.52 (0.19)	-0.24 (0.58)
H	0.77* (0.03)	-0.02 (0.96)	0.13 (0.75)	0.02 (0.96)	0.19 (0.65)	0.04 (0.93)	0.06 (0.89)	-0.2 (0.64)	-0.43 (0.29)
BF	0.87** (0.01)	-0.11 (0.8)	0.41 (0.32)	0.38 (0.35)	0.3 (0.47)	0.2 (0.63)	0.34 (0.41)	0.11 (0.8)	-0.49 (0.22)
SM	0.55 (0.16)	0.14 (0.74)	-0.09 (0.84)	-0.16 (0.71)	0.11 (0.8)	-0.13 (0.76)	-0.03 (0.95)	-0.24 (0.57)	-0.3 (0.47)
ST	0.46 (0.26)	-0.41 (0.32)	-0.19 (0.66)	-0.52 (0.19)	-0.36 (0.39)	0.03 (0.95)	-0.48 (0.23)	-0.52 (0.19)	-0.43 (0.29)
PA	0.4 (0.33)	-0.05 (0.91)	-0.16 (0.71)	-0.38 (0.35)	-0.02 (0.97)	-0.31 (0.46)	-0.18 (0.67)	-0.42 (0.31)	-0.16 (0.71)
GR	0.18 (0.67)	0.01 (0.99)	-0.17 (0.7)	-0.32 (0.44)	0.02 (0.96)	-0.5 (0.21)	-0.18 (0.67)	-0.45 (0.27)	0.04 (0.93)
SR	0.42 (0.31)	0.06 (0.88)	-0.12 (0.79)	-0.28 (0.5)	0.08 (0.85)	-0.22 (0.61)	-0.18 (0.67)	-0.45 (0.27)	-0.15 (0.72)

Values are Pearson correlation coefficients *r* and p-values in parenthesis for the variables of postoperative intramuscular fat ratio and average peak knee joint contact force during activities of daily living. QF, quadriceps femoris; RF, rectus femoris; VI, vastus intermedius; VL, vastus lateralis; VM, vastus medialis; H, hamstrings; BF, biceps femoris; SM, semimembranosus; ST, semitendinosus; PA, pes anserinus group; GR, gracilis; SR, sartorius muscle; 1P, 1st load peak; 2P, 2nd load peak; Max, maximum load. Significance level *p≤0.05, **p≤0.01.

The **lean muscle CSA** of the ST (r=0.85, p=0.01) was positively associated with the mean peak tibio-femoral contact forces at the second peak of level walking. This corresponded to the correlations of knee joint load with distal volume (Table 15) and total muscle CSA (Table 16). The lean CSA of the pes anserinus muscle group (r=0.73, p=0.04) showed a significant positive correlation with the average peak knee joint loads at the second peak of stair descent. This positive correlation during stair descent of lean muscle CSA and the knee joint contact force was mainly determined by the SR muscle (r=0.71, p=0.05). The lean CSA of all other periarticular muscles did not significantly affect the peak knee joint contact forces during the ADLs. The Pearson correlation data for lean muscle CSA are summarized in Table 19.

Table 19. Pearson correlation coefficients between lean muscle cross-sectional area and joint contact force.

	Level Walking		Stairs Up		Stairs Down		Stand Up	Sit Down	One-Legged Stance
	1P	2P	1P	2P	1P	2P	Max	Max	Max
QF	0.41 (0.32)	-0.18 (0.68)	0.4 (0.33)	0.01 (0.99)	0.32 (0.44)	0.67 (0.07)	-0.18 (0.67)	-0.22 (0.61)	-0.06 (0.9)
RF	-0.04 (0.92)	0.16 (0.71)	0.45 (0.26)	0.22 (0.61)	0.66 (0.08)	0.15 (0.72)	0.34 (0.4)	0.21 (0.63)	0.54 (0.17)
VI	-0.41 (0.32)	0.16 (0.53)	0.2 (0.64)	0.31 (0.45)	0.49 (0.22)	0.18 (0.67)	0.12 (0.79)	0.09 (0.84)	0.47 (0.24)
VL	0.24 (0.57)	0.02 (0.97)	0.29 (0.48)	0.09 (0.83)	0.36 (0.39)	0.66 (0.07)	-0.22 (0.6)	-0.24 (0.56)	-0.02 (0.96)
VM	0.49 (0.22)	-0.28 (0.51)	0.39 (0.34)	-0.06 (0.88)	0.23 (0.59)	0.63 (0.09)	-0.18 (0.67)	0.22 (0.61)	-0.13 (0.77)
H	-0.22 (0.6)	-0.01 (0.98)	0.2 (0.64)	0.02 (0.97)	0.43 (0.29)	0.16 (0.71)	-0.06 (0.89)	-0.14 (0.73)	0.43 (0.29)
BF	-0.02 (0.96)	-0.22 (0.59)	0.45 (0.26)	0.01 (0.99)	0.35 (0.4)	0.47 (0.24)	0.15 (0.72)	0.27 (0.51)	0.37 (0.37)
SM	-0.27 (0.52)	-0.1 (0.82)	-0.2 (0.63)	-0.13 (0.77)	0.09 (0.82)	-0.21 (0.61)	-0.28 (0.5)	-0.4 (0.33)	0.13 (0.76)
ST	-0.1 (0.81)	0.85** (0.01)	0.01 (0.97)	0.45 (0.26)	0.37 (0.36)	0.14 (0.74)	0.21 (0.62)	0.14 (0.75)	0.12 (0.78)
PA	0.17 (0.68)	0.22 (0.59)	0.37 (0.37)	0.23 (0.59)	0.52 (0.19)	0.73* (0.04)	-0.06 (0.88)	-0.07 (0.87)	0.12 (0.8)
GR	0.21 (0.62)	0.3 (0.46)	0.16 (0.71)	0.19 (0.65)	0.31 (0.45)	0.63 (0.1)	-0.16 (0.7)	-0.15 (0.73)	-0.12 (0.77)
SR	0.19 (0.65)	-0.11 (0.8)	0.45 (0.27)	0.08 (0.86)	0.46 (0.25)	0.71* (0.05)	-0.1 (0.82)	-0.08 (0.84)	0.16 (0.71)

Values are Pearson correlation coefficients *r* and p-values in parenthesis for the variables of postoperative lean muscle cross-sectional area and average peak knee joint contact force during activities of daily living. QF, quadriceps femoris; RF, rectus femoris; VI, vastus intermedius; VL, vastus lateralis; VM, vastus medialis; H, hamstrings; BF, biceps femoris; SM, semimembranosus; ST, semitendinosus; PA, pes anserinus group; GR, gracilis; SR, sartorius muscle; 1P, 1st load peak; 2P, 2nd load peak; Max, maximum load. Significance level *p≤0.05, **p≤0.01.

The **intramuscular fat CSA** of the VI muscle showed a significant positive correlation with increased peak knee joint loads during the late stance phase of level walking (r=0.72, p<0.05). The CSA of the quadriceps (r=0.51) and hamstrings (r=0.56) muscles had a moderate effect on the average peak knee joint load in early stance of level walking that was not statistically significant. Statistical trends that did not reach significance were determined for the muscular fat CSA of the BF at the first load peak of walking (r=0.57), stair ascent (r=0.54) and descent (r=0.55). Table 20 shows the correlations of intramuscular fat CSA with peak joint loads.

Table 20. Pearson correlation coefficients between intramuscular fat cross-sectional area and joint contact force.

	Level Walking		Stairs Up		Stairs Down		Stand Up	Sit Down	One-Legged Stance
	1P	2P	1P	2P	1P	2P	Max	Max	Max
QF	0.51 (0.19)	-0.38 (0.36)	-0.09 (0.83)	-0.39 (0.34)	-0.18 (0.67)	0.09 (0.84)	-0.46 (0.26)	-0.58 (0.13)	-0.42 (0.31)
RF	0.57 (0.14)	0.43 (0.29)	0.25 (0.55)	0.58 (0.13)	0.26 (0.54)	0.08 (0.85)	0.57 (0.14)	0.44 (0.27)	-0.37 (0.36)
VI	-0.05 (0.91)	0.72* (0.04)	0.13 (0.75)	0.12 (0.98)	0.48 (0.23)	-0.03 (0.95)	0.19 (0.66)	0 (1)	0.52 (0.19)
VL	0.57 (0.14)	-0.28 (0.5)	0.03 (0.94)	-0.27 (0.53)	-0.10 (0.81)	0.25 (0.56)	-0.35 (0.4)	-0.44 (0.27)	-0.4 (0.32)
VM	0.45 (0.28)	-0.13 (0.77)	0.23 (0.58)	-0.19 (0.66)	0.27 (0.52)	0.26 (0.54)	-0.2 (0.64)	-0.4 (0.33)	0 (0.99)
H	0.56 (0.15)	-0.02 (0.96)	0.22 (0.6)	0.01 (0.98)	0.37 (0.37)	0.06 (0.9)	0.04 (0.92)	-0.24 (0.57)	-0.13 (0.76)
BF	0.57 (0.14)	-0.1 (0.81)	0.54 (0.17)	0.28 (0.51)	0.55 (0.16)	0.33 (0.42)	0.21 (0.62)	-0.05 (0.91)	-0.02 (0.97)
SM	0.37 (0.36)	0.08 (0.85)	-0.14 (0.74)	-0.21 (0.61)	0.13 (0.76)	-0.26 (0.54)	-0.09 (0.84)	-0.32 (0.44)	-0.17 (0.69)
ST	0.43 (0.29)	-0.14 (0.74)	-0.16 (0.71)	-0.41 (0.32)	-0.24 (0.56)	0.11 (0.79)	-0.41 (0.31)	-0.46 (0.25)	-0.37 (0.37)
PA	0.4 (0.32)	-0.06 (0.88)	-0.12 (0.78)	-0.39 (0.34)	0.01 (0.99)	-0.21 (0.61)	-0.23 (0.58)	-0.47 (0.24)	-0.14 (0.74)
GR	0.28 (0.5)	-0.03 (0.94)	-0.16 (0.71)	-0.38 (0.35)	0.01 (0.99)	-0.41 (0.31)	-0.09 (0.83)	-0.22 (0.6)	-0.03 (0.95)
SR	0.4 (0.33)	-0.04 (0.92)	-0.06 (0.88)	-0.32 (0.44)	0.1 (0.82)	-0.16 (0.7)	-0.22 (0.61)	-0.05 (0.91)	-0.1 (0.81)

Values are Pearson correlation coefficients *r* and p-values in parenthesis for the variables of postoperative intramuscular fat cross-sectional area and average peak knee joint contact force during activities of daily living. QF, quadriceps femoris; RF, rectus femoris; VI, vastus intermedius; VL, vastus lateralis; VM, vastus medialis; H, hamstrings; BF, biceps femoris; SM, semimembranosus; ST, semitendinosus; PA, pes anserinus group; GR, gracilis; SR, sartorius muscle; 1P, 1st load peak; 2P, 2nd load peak; Max, maximum load. Significance level *p≤0.05, **p≤0.01.

3.5.2 Association between muscle status and EMG parameters

The relationship between muscle status and **EMG activity** revealed that a fatty infiltration of the VL contributed to muscle impairments during dynamic ADLs. The CSA of intramuscular fat of the VL muscle was significantly correlated with a reduction in the peak activity levels during stair descent (r=–0.95, p <0.01). This significant negative correlation of the VL muscle during stair descent, was also apparent for the parameter of intramuscular fat ratio (r=–0.92, p<0.01). The intramuscular fat ratio of the VL muscle was, moreover, negatively associated with peak activity levels during the stand-to-sit exercise (r=–0.81, p=0.05). No statistical association was determined between the magnitude of muscle activation of the periarticular muscles and the parameters of distal muscle volume and total or lean CSA. The computed Pearson correlation coefficients are shown for each muscle and activity in Table 21.

Table 21. Pearson correlation coefficients between peak muscle activity and muscle status.

		Level Walking	Stairs Up	Stairs Down	Stand Up	Sit Down	One-Legged Stance
DMV	VM	-0.55 (0.26)	0.29 (0.57)	-0.57 (0.24)	0.08 (0.89)	0.01 (0.99)	-0.51 (0.3)
	VL	0.1 (0.85)	0.54 (0.27)	-0.26 (0.62)	0.44 (0.38)	-0.16 (0.77)	0.29 (0.72)
	HM	0.39 (0.44)	0.34 (0.51)	-0.34 (0.51)	-0.71 (0.12)	-0.05 (0.92)	0.67 (0.15)
	HL	-0.81 (0.05)	-0.2 (0.7)	-0.35 (0.5)	0.12 (0.83)	0.19 (0.71)	-0.36 (0.49)
CSA	VM	-0.45 (0.38)	0.06 (0.91)	-0.42 (0.41)	-0.14 (0.79)	-0.13 (0.81)	-0.36 (0.48)
	VL	0.06 (0.91)	-0.1 (0.85)	-0.59 (0.22)	-0.04 (0.94)	-0.42 (0.41)	0.2 (0.71)
	HM	0.69 (0.13)	0.52 (0.29)	-0.37 (0.47)	-0.62 (0.19)	-0.33 (0.53)	0.45 (0.37)
	HL	-0.71 (0.12)	-0.15 (0.78)	-0.36 (0.49)	0.14 (0.79)	0.14 (0.8)	-0.18 (0.74)
LCSA	VM	-0.43 (0.4)	0.05 (0.92)	-0.42 (0.41)	-0.13 (0.81)	-0.13 (0.81)	-0.35 (0.49)
	VL	0.05 (0.92)	-0.14 (0.79)	-0.45 (0.37)	0.03 (0.56)	-0.29 (0.58)	0.14 (0.79)
	HM	-0.75 (0.09)	-0.79 (0.06)	0.32 (0.55)	-0.45 (0.37)	0.17 (0.75)	-0.08 (0.88)
	HL	-0.73 (0.1)	-0.17 (0.75)	-0.36 (0.48)	0.09 (0.87)	0.15 (0.78)	-0.15 (0.77)
FCSA	VM	-0.52 (0.29)	0.11 (0.84)	-0.4 (0.43)	-0.23 (0.67)	-0.08 (0.88)	-0.37 (0.47)
	VL	0.07 (0.9)	0.06 (0.91)	-0.95** (<0.01)	-0.3 (0.56)	-0.8 (0.06)	0.35 (0.91)
	HM	0.29 (0.58)	0.14 (0.79)	-0.21 (0.69)	0.26 (0.63)	-0.5 (0.32)	-0.45 (0.38)
	HL	-0.13 (0.81)	0.25 (0.63)	-0.15 (0.78)	0.78 (0.07)	-0.03 (0.95)	-0.46 (0.36)
FR	VM	-0.54 (0.27)	0.15 (0.77)	-0.45 (0.38)	-0.11 (0.83)	-0.12 (0.82)	-0.33 (0.53)
	VL	0.07 (0.89)	0.06 (0.91)	-0.92** (<0.01)	-0.26 (0.62)	-0.81* (0.05)	0.29 (0.58)
	HM	0.2 (0.7)	0.11 (0.84)	-0.17 (0.75)	0.3 (0.56)	-0.42 (0.56)	-0.44 (0.38)
	HL	-0.04 (0.94)	0.15 (0.78)	-0.27 (0.6)	0.77 (0.07)	0.02 (0.97)	-0.51 (0.3)
MA	VM	0.45 (0.38)	-0.21 (0.7)	0.42 (0.41)	-0.11 (0.84)	0.15 (0.78)	0.44 (0.38)
	VL	-0.09 (0.87)	-0.23 (0.67)	0.79 (0.06)	-0.04 (0.95)	0.64 (0.18)	-0.31 (0.55)
	HM	0.05 (0.93)	-0.28 (0.59)	-0.23 (0.67)	0.65 (0.17)	-0.52 (0.29)	-0.8 (0.06)
	HL	-0.11 (0.84)	-0.2 (0.71)	0.33 (0.53)	-0.81 (0.05)	-0.25 (0.63)	0.58 (0.23)

Values are Pearson correlation coefficients *r* and p-values in parenthesis. Peak muscle activity during the investigated movement tasks was correlated with the postoperative measures of distal muscle volume (DMV), muscle cross-sectional area (CSA), lean muscle CSA (LCSA), intramuscular fat CSA (FCSA), intramuscular fat ratio (FR) and muscle attenuation (MA). VM, vastus medialis; VL, vastus lateralis; HM, medial hamstrings; HL, lateral hamstrings; GM, medial gastrocnemius; GL, lateral gastrocnemius. Significance level *p≤0.05, **p≤0.01.

The fatty infiltration of VL muscle correlated with a shorter **EMD** between the onset of muscle activity and the onset of *in vivo* knee joint contact forces during stair ascent. This negative relationship was significant for the ratio (r=–0.83, p<0.05) and CSA (r=–0.85, p<0.05) of intramuscular fat of the VL muscle. The total (r=–0.85, p<0.05) and lean muscle CSA (r=–0.86, p<0.05) of the HM muscle were significantly associated with a shorter EMD duration during stair descent. There was a positive association between EMD and the HM muscle CSA during OLS (r=0.82, p=0.05), which resulted from the long mean EMD of 105.5±116.9 ms involved in maintaining postural balance (Table 14). The status of the other investigated muscles did not have a significant impact upon the average EMD duration. Table 22 gives an overview over the correlations between the mean EMD during the different ADLs and the postoperative status of the periarticular musculature.

Table 22. Pearson correlation coefficients between electromechanical delay and muscle status.

		Level Walking	Stairs Up	Stairs Down	Stand Up	Sit Down	One-Legged Stance
DMV	VM	0.35 (0.5)	-0.13 (0.81)	-0.37 (0.47)	0.29 (0.58)	-0.07 (0.9)	-0.52 (0.29)
	VL	-0.59 (0.22)	-0.17 (0.74)	-0.54 (0.27)	-0.55 (0.26)	0.4 (0.43)	0.17 (0.75)
	HM	-0.34 (0.51)	-0.54 (0.27)	-0.73 (0.1)	0.53 (0.28)	0.1 (0.85)	0.71 (0.11)
	HL	0.39 (0.44)	-0.27 (0.6)	-0.19 (0.71)	-0.08 (0.89)	-0.39 (0.44)	0.48 (0.33)
CSA	VM	0.53 (0.28)	-0.01 (0.99)	-0.38 (0.46)	-0.26 (0.62)	0.26 (0.62)	-0.6 (0.2)
	VL	-0.24 (0.65)	-0.55 (0.25)	-0.64 (0.17)	0.06 (0.91)	0.24 (0.65)	0.3 (0.57)
	HM	-0.51 (0.3)	-0.55 (0.26)	-0.85* (0.03)	0.44 (0.39)	0.29 (0.58)	0.82* (0.05)
	HL	0.33 (0.53)	-0.24 (0.65)	-0.04 (0.94)	-0.25 (0.63)	-0.54 (0.27)	0.47 (0.35)
LCSA	VM	0.51 (0.3)	-0.03 (0.96)	-0.32 (0.53)	0.22 (0.67)	-0.13 (0.55)	-0.6 (0.2)
	VL	-0.22 (0.67)	-0.43 (0.39)	-0.72 (0.11)	-0.01 (0.99)	0.24 (0.65)	0.34 (0.51)
	HM	0.05 (0.92)	-0.6 (0.21)	-0.86* (0.03)	0.41 (0.42)	-0.69 (0.13)	-0.64 (0.16)
	HL	0.34 (0.51)	-0.20 (0.7)	-0.03 (0.96)	-0.22 (0.68)	-0.52 (0.29)	0.51 (0.3)
FCSA	VM	0.65 (0.16)	0.14 (0.79)	-0.72 (0.11)	-0.5 (0.31)	-0.31 (0.55)	-0.53 (0.28)
	VL	-0.25 (0.63)	-0.85* (0.03)	-0.22 (0.68)	0.33 (0.53)	0.16 (0.76)	0.06 (0.92)
	HM	0.19 (0.73)	-0.11 (0.84)	-0.1 (0.86)	0.68 (0.14)	-0.42 (0.41)	0.34 (0.51)
	HL	0.06 (0.92)	-0.67 (0.15)	-0.2 (0.71)	-0.57 (0.24)	-0.62 (0.19)	-0.31 (0.54)
FR	VM	0.64 (0.17)	0.09 (0.86)	-0.68 (0.14)	0.43 (0.4)	-0.38 (0.46)	-0.56 (0.25)
	VL	-0.25 (0.64)	-0.83* (0.03)	-0.2 (0.71)	0.23 (0.66)	0.25 (0.63)	0.04 (0.94)
	HM	0.26 (0.62)	-0.1 (0.85)	0.19 (0.72)	0.7 (0.12)	-0.48 (0.33)	0.28 (0.59)
	HL	0.14 (0.8)	-0.79 (0.06)	-0.11 (0.84)	-0.42 (0.41)	-0.31 (0.56)	-0.38 (0.46)
MA	VM	-0.53 (0.28)	0.2 (0.7)	0.64 (0.18)	-0.34 (0.51)	0.19 (0.72)	0.64 (0.17)
	VL	0.41 (0.42)	0.69 (0.13)	0.42 (0.41)	0 (1)	-0.3 (0.56)	-0.13 (0.8)
	HM	0.41 (0.43)	0.41 (0.42)	0.41 (0.43)	0.2 (0.71)	-0.38 (0.46)	-0.11 (0.84)
	HL	-0.06 (0.92)	0.91** (0.01)	-0.08 (0.89)	0.24 (0.65)	0.15 (0.77)	0.29 (0.57)

Values are Pearson correlation coefficients *r* and p-values in parenthesis. Peak muscle activity during the investigated movement tasks was correlated with the postoperative measures of distal muscle volume (DMV), muscle cross-sectional area (CSA), lean muscle CSA (LCSA), intramuscular fat CSA (FCSA), intramuscular fat ratio (FR) and muscle attenuation (MA). VM, vastus medialis; VL, vastus lateralis; HM, medial hamstrings; HL, lateral hamstrings; GM, medial gastrocnemius; GL, lateral gastrocnemius. Significance level *p≤0.05, **p≤0.01.

3.6 Associations between EMG and joint load

The interrelationship between muscle activation, EMD and *in vivo* knee joint contact forces during the dynamic ADLs is displayed as a 3D scatter plot in Figure 25. In general, higher periarticular muscle activity levels (Table 23) and concomitantly shorter EMD times (Table 24, 25) were associated with increased *in vivo* knee joint loads during functional activities.

3.6.1 Association between muscle activity and *in vivo* joint loads

Muscular activity of the VM showed a very strong positive correlation (r=0.94, p=0.01) with the average peak knee joint loads in the early stance phase of level walking (Figure 17a). The peak loads during late stance phase of level walking were primarily affected by the activity of the gastrocnemius (Figure 17c-d). The Pearson correlation coefficients were high for the GM (r=0.77, p=0.07) and moderate for the GL (r=0.69, p=0.13) muscle, albeit insignificant. In line with the patient-specific EMG profiles of Figure 18c, the activity of the GM showed a strong significant association with the average peak joint loads at the second peak of stair ascent (r=0.87, p<0.05). The results of the Pearson correlation analysis of the individual muscle activity and average peak tibio-femoral joint loads are shown in Table 23 and Figure 25.

Table 23. Pearson correlation coefficients between peak muscle activity and joint contact force.

Activity	VM	VL	HM	HL	GM	GL
Level Walking 1P	0.94** (0.01)	0.26 (0.63)	0.15 (0.78)	0 (1)	0.14 (0.79)	0.64 (0.17)
Level Walking 2P	0.44 (0.39)	0.37 (0.47)	0.22 (0.68)	0.28 (0.59)	0.77 (0.07)	0.69 (0.13)
Stairs Up 1P	-0.3 (0.57)	-0.37 (0.47)	-0.11 (0.84)	0.05 (0.93)	0.64 (0.17)	0.39 (0.45)
Stairs Up 2P	-0.28 (0.6)	-0.13 (0.8)	0.25 (0.63)	0.54 (0.27)	0.87* (0.02)	0.63 (0.18)
Stairs Down 1P	-0.02 (0.98)	0.75 (0.09)	0.08 (0.87)	0.3 (0.56)	0.03 (0.96)	-0.36 (0.48)
Stairs Down 2P	0.53 (0.28)	0.65 (0.16)	0.06 (0.92)	-0.12 (0.83)	-0.1 (0.84)	-0.44 (0.39)
Stand Up Max	0.43 (0.39)	0.17 (0.75)	-0.69 (0.18)	-0.22 (0.68)	0.43 (0.4)	0.28 (0.59)
Sit Down Max	-0.22 (0.68)	0.63 (0.18)	0.52 (0.29)	0.12 (0.82)	0.38 (0.46)	0.05 (0.93)
One-Legged Stance Max	0.65 (0.17)	-0.06 (0.92)	0.62 (0.19)	0.51 (0.3)	0.8 (0.06)	0.77 (0.07)

Values are Pearson correlation coefficients *r* and p-values in parenthesis. Peak muscle activity was correlated with the average peak knee joint contact force acting during each functional movement task. VM, vastus medialis; VL, vastus lateralis; HM, medial hamstrings; HL, lateral hamstrings; GM, medial gastrocnemius; GL, lateral gastrocnemius; 1P, 1st load peak; 2P, 2nd load peak; Max, maximum load. Significance level *p≤0.05, **p≤0.01.

3.6.2 Association between muscle activity and EMD

An inverse association between muscle activity and EMD was determined, in which the EMD shortened when muscle activity levels increased (Table 24). The increased activity levels of the GL muscle during the late stance phase of stair ascent (Figure 18d) correlated significantly with a shorter EMD (r=–0.83, p<0.05). The magnitude of HM activity was likewise inversely correlated with the EMD (r=–0.85, p<0.05) during stair ascent. The strongest association was determined for the activity of the GM muscle (r=–0.98, p<0.01) during the static task of OLS.

Table 24. Pearson correlation coefficients between peak muscle activity and electromechanical delay.

Muscle	Level Walking	Stairs Up	Stairs Down	Stand Up	Sit Down	One-Legged Stance
VM	0.2 (0.71)	0.12 (0.82)	0.06 (0.91)	-0.51 (0.31)	0.47 (0.35)	-0.2 (0.71)
VL	-0.62 (0.19)	0.12 (0.83)	0.06 (0.92)	-0.57 (0.24)	-0.2 (0.71)	-0.14 (1)
HM	-0.5 (0.31)	-0.85* (0.03)	0.5 (0.31)	-0.08 (0.88)	-0.14 (0.8)	0.48 (0.34)
HL	-0.54 (0.27)	-0.24 (0.64)	-0.53 (0.28)	-0.21 (0.69)	0.47 (0.35)	0.18 (0.73)
GM	0.26 (0.63)	-0.69 (0.13)	0.73 (0.1)	0.28 (0.56)	0.31 (0.55)	-0.98** (<0.01)
GL	0.16 (0.76)	-0.83* (0.04)	-0.73 (0.1)	-0.35 (0.49)	0.28 (0.59)	0.02 (0.98)

Values are Pearson correlation coefficients *r* and p-values in parenthesis. Peak muscle activity was correlated with the electromechanical delay between the onset of muscle activity and the onset of the *in vivo* knee joint contact force for each functional movement task. VM, vastus medialis; VL, vastus lateralis; HM, medial hamstrings; HL, lateral hamstrings; GM, medial gastrocnemius; GL, lateral gastrocnemius; 1P, 1st load peak; 2P, 2nd load peak; Max, maximum load. Significance level *p≤0.05, **p≤0.01.

3.6.3 Association between EMD and *in vivo* joint loads

The EMD was inversely correlated with the average peak knee joint loads at the second peak of level walking in response to the activation of the VM muscle (r=–0.84, p<0.05). The load magnitude of the second peak of level walking significantly correlated with a shorter EMD between HL activation and joint load (r=–0.81, p<0.05). A shortened EMD from GM muscle activation tended to affect the knee joint loads during OLS (r=–0.79, p=0.06), but did not reach statistical significance. The strongest negative correlation between the duration of EMD and the average knee joint contact forces was obtained for the GL muscle during the stand-to-sit activity (r=–0.9, p<0.05). The correlation data between EMD and the average peak tibio-femoral joint loads are summarized in Table 25 and Figure 25.

Table 25. Pearson correlation coefficients between joint contact force and electromechanical delay.

Activity	VM	VL	HM	HL	GM	GL
Level Walking 1P	0.54 (0.26)	0.16 (0.76)	-0.66 (0.15)	-0.18 (0.73)	-0.32 (0.54)	-0.59 (0.21)
Level Walking 2P	-0.84* (0.03)	-0.42 (0.4)	-0.7 (0.12)	-0.81* (0.05)	-0.21 (0.69)	0.51 (0.3)
Stairs Up 1P	-0.09 (0.86)	0.09 (0.86)	-0.23 (0.66)	0.46 (0.36)	0.04 (0.93)	-0.14 (0.8)
Stairs Up 2P	-0.63 (0.21)	-0.44 (0.39)	-0.4 (0.44)	0.21 (0.69)	-0.48 (0.34)	-0.3 (0.57)
Stairs Down 1P	0.68 (0.14)	-0.53 (0.28)	-0.23 (0.66)	-0.18 (0.73)	0.36 (0.49)	-0.29 (0.58)
Stairs Down 2P	0.47 (0.34)	-0.28 (0.59)	0.35 (0.5)	0.39 (0.44)	0.24 (0.64)	-0.23 (0.66)
Stand Up Max	-0.58 (0.23)	-0.44 (0.38)	0.04 (0.94)	-0.02 (0.98)	0.04 (0.94)	0.27 (0.6)
Sit Down Max	0.4 (0.45)	0.06 (0.91)	-0.07 (0.89)	-0.2 (0.71)	-0.03 (0.96)	-0.9* (0.02)
One-Legged Stance Max	0.7 (0.12)	0.07 (0.9)	-0.49 (0.33)	-0.17 (0.75)	-0.79 (0.06)	0 (1)

Values are Pearson correlation coefficients *r* and p-values in parenthesis. The average peak knee joint contact force was correlated with the electromechanical delay between the onset of muscle activity and *in vivo* knee joint contact force for each functional movement task. VM, vastus medialis; VL, vastus lateralis; HM, medial hamstrings; HL, lateral hamstrings; GM, medial gastrocnemius; GL, lateral gastrocnemius; 1P, 1st load peak; 2P, 2nd load peak; Max, maximum load. Significance level *p≤0.05, **p≤0.01.
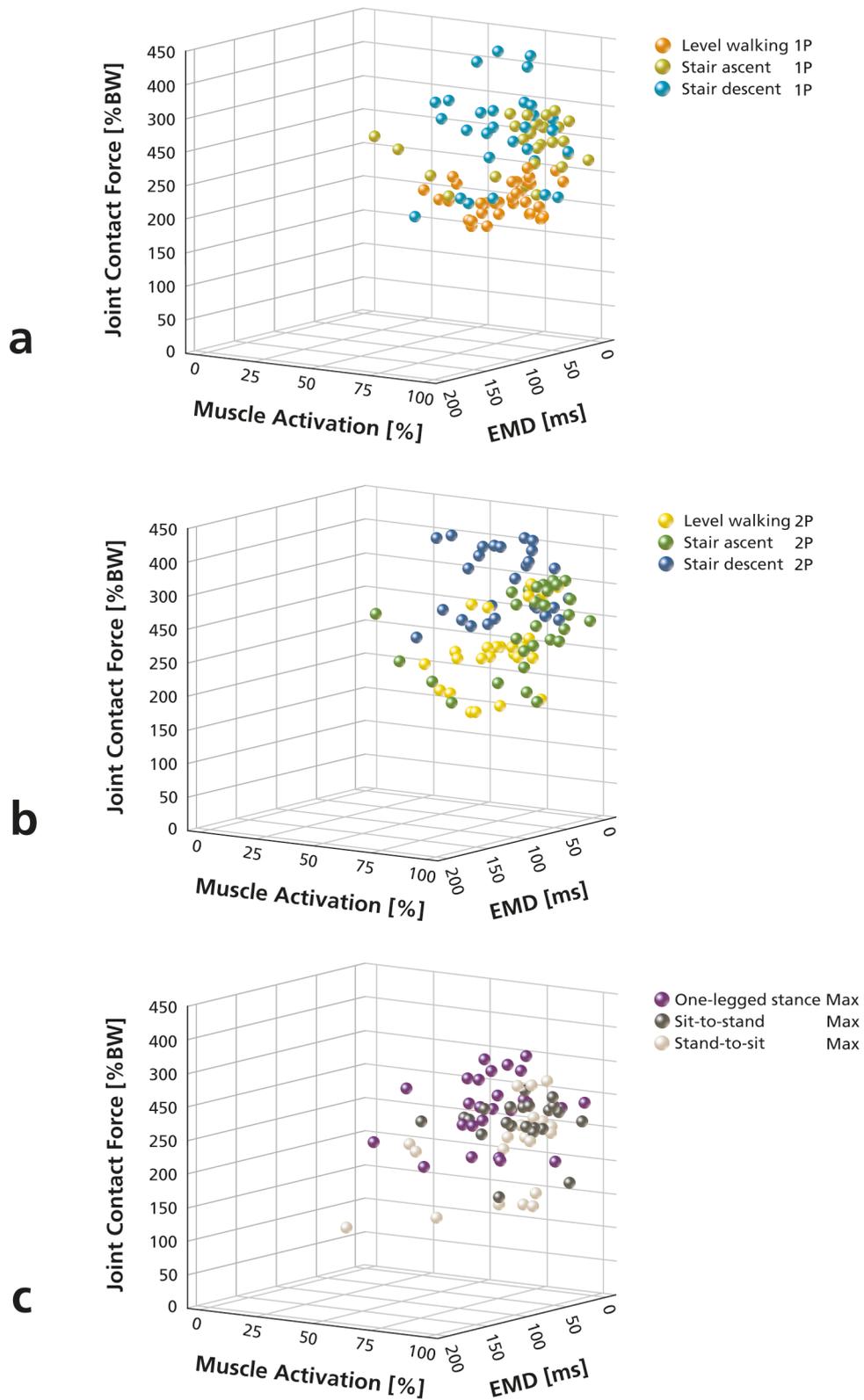
Figure 25. 3D scatter plot of muscle activation, electromechanical delay (EMD), joint contact force. A 3D scatter plot showing the interrelationship between the average peak muscle activation in [%], EMD in [ms] and the 1st peak (**a**), 2nd peak (**b**) and maximum (**c**) knee joint contact force in % body weight [%BW]. The colored dots represent the activation levels of the periarticular muscles during different activities of daily living. Muscle activation values are shown in relation to peak knee joint contact forces and the positive time latency between the onset of muscle activation and the onset of the knee joint contact force per activity. The color of the dots refers to the respective activity under investigation. 1P, 1st peak; 2P, 2nd peak; Max, maximum joint contact force.

4 Discussion

The determinants of periarticular muscle status, EMG activation pattern and mechanical knee joint load have received increasing attention in recent years with respect to the surgical outcome of TKA. The present thesis is, according to the current state of knowledge, the first to analyze both the nature and interrelationship of these determinants in the long-term follow-up of TKA. *In vivo* knee joint loads measured during different dynamic activities were correlated with synchronized EMG recordings and quantitative CT measures of muscle status. High EMG activity and impairments in periarticular muscle status in terms of fatty infiltration were associated with increased knee joint loadings in the postoperative course of TKA.

4.1 *In vivo* knee joint loadings

The tibio-femoral joint loadings were measured *in vivo* in the tibial implant component (89) across a broad spectrum of functional ADLs. In general, the knee joint loads considerably exceeded patient body weight during the ADLs and showed high inter-individual differences in relation to the involved movement patterns. The data of this investigation complement the load estimations of previous studies using instrumented knee implants (131-136) or musculoskeletal modelling techniques (77, 83, 137). Differences in peak load value between published studies originated from differences in the methodology, surgical follow-up time and activity under investigation (138).

The knee joint loads during walking showed a double-peak pattern, whereby the first peak of F_{res} approximately coincided with the CTO and the second peak with the CHS. The average peak contact force values (mean 2.67 BW) during level walking are consistent with previous *in vivo* studies, which reported loads between 2.3 to 2.8 BW in one to six subjects (131-136). The mean peak loads were marginally higher (+2.2%) than those determined previously by Kutzner et al. (134) in five patients of the same patient cohort. The measurements by Kutzner et al. were performed at an earlier postoperative time point compared to the present investigations (13.2±5.9 months versus 26±14.7 months), which could have been the reason for these small differences. In agreement with the present results, Bergmann et al. (135) observed slight increases in the *in vivo* knee joint loadings by +0.5% to +11% during most ADLs at later postoperative time points (15.8±6 months and 24.3±10.7 months), as compared to the previous measurements by Kutzner et al. (134). D'Lima et al. (133), who measured the axial tibial forces during level walking over the course of one year after TKA, likewise reported an increase in the peak force over time.

The highest tibio-femoral contact forces were measured during stair descent with maximum mean values of 3.41 BW during single limb loading. The mean peak tibio-femoral loads during stair climbing are in accord with previous *in vivo* reports in the range of 3.0 to 3.52 BW, as measured by instrumented implants in one to six patients (131-136). The increased knee joint loads during stair climbing, compared with level walking, have been attributed to the more challenging tibio-femoral contact mechanics at greater knee flexion angles (83-85, 139). Taylor et al. (83) determined higher average peak resultant knee contact forces of 5.4 BW with maximum values of up to 6.2 BW during stair climbing, using a musculoskeletal lower limb model in total hip arthroplasty patients. There are several possible explanations for this difference in peak load magnitude, compared with the present data. Previous studies have shown that gait modifications due to hip abductor weakness and lower ROMs after total hip replacement, can alter the load distribution within the lower limb joints (74). Taylor et al. thus showed that the peak tibio-femoral loads considerably exceeded those of the artificial hip joint by 116% during stair climbing. The adoption of inter-joint coordination strategies might be a potential target for rehabilitation care to redistribute loads and minimize implant stresses after total joint arthroplasty (74). Another possible explanation is that the present *in vivo* load data were measured by PS implants. PS TKA has been related to a slight anterior femoral sliding and lower external knee flexion moment at foot strike during stair climbing (140). The mechanics of post-cam engagement at low knee flexion angles may explain the lower contact forces when compared to those of the normal knee, as previously shown *in vitro* (139, 140).

The activities of sit-to-stand and stand-to-sit, during which the body weight was borne by both legs, showed slightly lower tibio-femoral joint loads, as compared to the single-limb task of OLS. Prior studies using instrumented implants to measure the *in vivo* loads during different ADLs, likewise reported that the lowest peak loads in the knee (134) and hip (141) joint occurred during stand-to-sit activities. The average peak tibio-femoral loads measured by Kutzner et al. (134) in five patients during stand-to-sit, sit-to-stand and OLS at 13 months after TKA were lower than the present data obtained about 26 months postoperatively (2.3 BW, 2.5 BW, 2.6 BW versus 2.6 BW, 2.8 BW, 2.9 BW, respectively). Consistent with the present results, Kutzner et al. determined higher inter-individual differences in peak joint load during knee bending activities, as compared to OLS. They suggested that contact forces at high knee flexion angles were mainly transferred in the lateral knee compartment, whereas adduction moments caused a rather medial force transfer during OLS. This could explain the relatively high compensatory activity of the lateral knee musculature during OLS (Figure 16).

4.2 Muscle atrophy and fatty infiltration

The long-term changes in muscle status with regard to muscle atrophy and fatty infiltration were assessed using CT imaging. The mean distal quadriceps volume showed a decrease by $-9.6\pm5.7\%$ in the postoperative course, which was not reflected by the CSA measurements. The greatest absolute change in distal quadriceps volume occurred in the VM muscle. This finding supports the hypothesis that the VM may be predominantly affected by postoperative impairments, as its anatomical insertion at the superomedial patella poses an increased risk for intraoperative muscle damage during the TKA procedure. The observed reduction in distal quadriceps volume after TKA is of comparable magnitude to the postoperative change in quadriceps muscle size reported in the literature (42, 142, 143). Mizner et al. (42) identified a decrease in the maximal anatomical CSA of the quadriceps by 10% within the early postoperative period following TKA via the MPP approach. In a study which set out to determine the effects of standard rehabilitation on muscle CSA after THA, Suetta et al. (142) found that the quadriceps anatomical CSA decreased by 13% at a follow-up of five weeks and remained below 9% of the initial CSA values after 12 weeks. This could explain remnant changes in quadriceps CSA after total joint replacement. Walls et al. (143), who determined a reduction in mid-thigh anatomical CSA of the quadriceps of 12% at 12 weeks after TKA, suggested that neuromuscular electrical stimulation (NMES) prehabilitation can limit postoperative quadriceps atrophy. This pilot study reported that muscle CSA at the mid-thigh level decreased by only 4% following preoperative NMES and was accompanied by an enhanced recovery of muscle strength and physical function. More research is required to determine the long-term clinical efficacy of NMES interventions to improve muscle status and motor function after surgery. The possible interference of aging-induced changes in muscle CSA cannot be ruled out when analyzing the long-term effect of TKA on muscle status. A 12-year longitudinal study by Frontera et al. (144) thus reported that healthy aging was related to an overall decrease in total mid-thigh muscle CSA by 14.7%, whereby the quadriceps muscle was more susceptible to change than the knee flexors. Akagi et al. (145), who investigated muscle strength declines with aging, established muscle volume as a more reliable predictor of the muscle force-generating capacity than the anatomical CSA. It has been shown that the anatomical CSA tends to underestimate muscle atrophy, as nonuniform volume changes are not covered along the longitudinal muscle axis (146). This might explain the more pronounced postoperative change in distal volume of the quadriceps muscle when compared with the measurements of anatomical muscle CSA.

An unanticipated finding was that the extent of fatty infiltration of all periarticular muscle groups was significantly decreased compared with preoperative values. However, previous studies have shown that the pathologic process of knee OA can induce the fatty replacement of muscle tissue (147, 148). Kumar et al. (147) reported, accordingly, that knee OA patients had higher proportions of quadriceps intramuscular fat than healthy age-matched controls, along with a decline in quadriceps torque and knee function. In an investigation into the progression of quadriceps recovery after TKA, Mizner et al. (113) found that such impairments in quadriceps strength and knee function can significantly improve within six months postoperatively. They showed that quadriceps strength starts to recover after an initial decline one month after TKA. The recovery of muscle strength and physical function has been formerly related to a decrease in intramuscular fat of the thigh musculature (149-151). Taaffe et al. (149) examined the effects of retraining on thigh muscle fatty infiltration and strength after a prolonged period of detraining of 24 weeks. They showed that muscle quality and strength of both the quadriceps and hamstring muscles increased after a 12-week retraining intervention. Regarding adiposity and deconditioning as important risk factors for the accumulation of intramuscular fat, Ryan et al. (150) investigated the impact of these factors on mid-thigh muscle quality. They found that weight loss and low-intensity walking activity contributed to a reduced fatty infiltration of the mid-thigh muscles and a better lipid and glucose metabolic profile. Goodpaster et al. (151) reported, moreover, that modest physical activity can even prevent the aging-associated fatty infiltration of the mid-thigh musculature, but has a reduced effect on changes in muscle CSA. The present results are thus consistent with those of previous studies indicating that muscle fatty infiltration is, to a certain extent, amenable to recovery with moderate activity.

A key finding is that the overall reduction in intramuscular fat ratio was less pronounced for the quadriceps, compared to the hamstring muscles (-2.8±2.9%CSA versus -4.1±3.2%CSA; p<0.05). The VM and RF muscles, in particular, showed a relatively modest improvement in muscular fat ratio. This seems to confirm the findings of Meier et al. (13) that the standard MPP approach with incision of the extensor mechanism can lead to residual damage of the quadriceps musculature. They highlighted that quadriceps strength deficits in the first month after TKA may improve by 10% to 20% in the postoperative course of 12 months, but rarely attain the strength levels of healthy controls of the same age or those of the contralateral non-operated leg. A study on revision THA by von Roth et al. (53) showed that the distribution and degree of muscular fatty infiltration are related to the extent of damage induced via the

surgical approach. They found that fatty infiltration of the gluteus medius increased after multiple revision THAs and was limited to the anterior and central muscle parts affected by the direct lateral approach. The present results did not reveal significant intramuscular differences in fatty infiltration of the quadriceps between the detached VM and lateral muscle portions. However, soft tissue trauma related to the MPP approach could explain the overall lower decrease in fatty infiltration of the affected quadriceps compared to the hamstrings. Silva et al. (75) reported remnant isometric strength deficits of the quadriceps relative to the hamstrings up to three years after TKA, as indicated by a higher H:Q ratio. Imbalances in H:Q co-contraction ratios have been shown to increase the external knee abduction loads (152). While indicating the regenerative capacity of the periarticular musculature, the results support the general notion that relative quadriceps impairments may persist after TKA. Quadriceps-to-hamstring muscle imbalances could be addressed by "eccentrically-biased" rehabilitation strategies in the early postoperative period to improve quadriceps function (153).

4.3   EMG activity

In the present thesis both the relative intensity and timing of muscle activation of the quadriceps, hamstrings and gastrocnemius muscles were determined during multiple ADLs. EMG can be used for the objective evaluation of coordination and allows conclusions on the functional status of periarticular muscles (107). Coordination seems to be an equally decisive component of muscle function as is muscle strength. To the current state of knowledge this is the first analysis of directly synchronized measurements of EMG activity and *in vivo* knee joint loadings during dynamic activities. The synchronized recordings revealed distinct patterns of muscle recruitment during the respective load cycles of the investigated ADLs. The differential onset and peak of muscle activity during the movement tasks affected the maximal loading response of the tibio-femoral joint.

Level walking showed consistent muscle activation patterns during the gait cycle over all subjects. Peak activation of the knee extensors in the first 33% of the gait cycle accounted for the first peak of the *in vivo* tibio-femoral loads, while the gastrocnemius contributed mostly to the second peak. The determined EMG-force patterns are in agreement with previous research on the activation and load contributions of individual muscles during walking. Anderson and Pandy (154) showed that the vertical GRF, as determined by a dynamic optimization solution, reached a maximum at approximately 38% of the gait cycle when the knee reached its peak extension. They identified that the event of foot-flat at about 10% of the gait cycle marked the

transition from initial joint support by the hamstrings and dorsiflexors to activation of the knee extensors. Consistent with these findings, HM and HL activation of the present analysis occurred at the time of weight acceptance (23% of the gait cycle), prior to the activation of the knee extensors. In line with the present results, Shelburne et al. (77) showed that the knee adduction moment during walking was mostly balanced by the quadriceps and gastrocnemius, which generated the tibio-femoral forces at the time of the CTO and CHS, respectively. The three-dimensional model of the lower limb used by Shelburne et al. showed slightly higher peak values at the CTO compared to the present *in vivo* data (2.7 BW or 2015 N versus 2.16 BW or 1904 N). The role of the gastrocnemius of providing knee joint support and initiating swing during gait was highlighted previously by Neptune et al. (155). They showed that isometric contractions during mid-stance provide vertical stability by decelerating the forward translation of the trunk, while most power was generated by concentric contractions during pre-swing. This is reflected by the present averaged EMG profiles (Figure 17c-d) of the GM and GL that showed a minor peak in activation during single leg stance and achieved a maximum at push-off. In line with previous reports by Winter et al (156), increases in hamstring activity were observed during the late swing to counter limb advancement. Differential hamstring activity showed higher amplitudes of the HL, supporting prior concepts of medial compartment off-loading (74, 82).

The EMG signals during stair ascent showed a similar pattern to that of level walking but were marked by a higher magnitude in knee extensor and plantarflexor activation values. It has been previously suggested that increased muscle activity and limb loading during the strenuous exercise of stair climbing result from the relatively higher knee flexion angles. Costigan et al. (84) thus demonstrated that peak contact forces during level walking occurred at a knee flexion angle of 20°, as compared to 60° during stair ascent. This resulted in higher contact stresses due to the limited articulating surface area and a twofold increase by 0.65 Nm/kg in the knee flexion moment. Costigan et al. argued that knee extensor activation is required to counter the initial knee flexion moment within the first 20% of the stride cycle. The present EMG recordings support this finding, as the VM and VL muscles dominated the early loading response after foot contact at 18 to 30% of the cycle. McFayden and Winter (157) likewise identified concentric knee extensor contractions during "pull-up" at 32% of the stride cycle that generated power for elevation of the body. In line with the present EMG data (Figure 18c-d), McFayden and Winter reported an onset of gastrocnemius activity prior to swing initiation and a slight increase in eccentric or isometric contractions of the knee

extensors during late stance. The latter was deemed necessary to maintain postural stability while the plantarflexors controlled push-off before the transition to the next step.

Stair descent showed a burst in GM and GL activity during weight acceptance, as all patients made step contact with the forefoot and the ankle in plantarflexion. This was followed by the activation of the VM and VL, which dominated the tibio-femoral contact forces during late stance. Prior studies have reported similar patterns of plantarflexor and quadriceps activity, controlling energy absorption at the ankle and knee (157, 158). Large knee extensor moments have been accordingly identified during late stance as a function of staircase inclination (158). Although the highest tibio-femoral loads were recorded during stair descent, the peak values of muscle activity were surprisingly lower during stair descent, as compared to stair ascent. This apparent discrepancy has been identified by several studies and was explained by differences in the kinematics and type of muscle contraction of both stair climbing directions (157-159). It has been suggested that stair descent showed less deviation of the body center of mass from center of foot contact (74), as well as lower knee and trunk flexion angles (159). McFayden and Winter (157) proposed that energy is produced by concentric contractions during stair ascent and is rather absorbed by eccentric contractions during stair descent. The present results thus confirm the general contention that relatively lower energy expenditures (160) but greater loading responses (134, 135) are involved in the deceleration of the body and impact absorption during stair descent.

The EMG and movement patterns during sit-to-stand and OLS activities have previously been used as proxy measures for functional recovery and postural control following rehabilitation (161, 162). The recorded EMG patterns during the sit-to-stand task resembled those of healthy subjects reported in the literature (163, 164). The VM and VL dominated early motion at lift-off from the chair just prior to the peak knee joint load, while the hamstrings sustained leg and trunk extension. Millington et al. (164) showed, accordingly, that the upward lifting motion at 27-36% of the activity cycle was mainly controlled by concentric quadriceps contractions, followed by the eccentric activity of the BF and gluteus maximus. These EMG patterns were obtained from healthy adults of comparable age to the present patient cohort (69±3 years versus 69±5.3 years). The potential to restore functional muscle activation patterns after TKA has been exemplified by previous studies (161, 162), which could explain the present finding of comparably normal postoperative EMG patterns. It has been reported that asymmetries in muscle activation and limb loading due to ipsilateral muscle weakness

can be largely restored within one year after TKA (161, 162). Single-leg balance during OLS was shown to recover in the course of one year after physical therapy, albeit at a slower pace than improvements in thigh muscle strength (165). Physical therapy approaches that target muscle activation deficits at an early stage and incorporate biofeedback, NMES or balance training might accelerate the functional recovery after TKA (112, 143, 165).

One aim of this thesis was to investigate the time lag between lower limb muscle activation and the mechanical loading response at the knee joint using a cross-correlation technique. The present data quantify for the first time the temporal relation of EMG activity and the initiation of *in vivo* knee joint contact forces during dynamic ADLs. The determined values of EMD (Tables 9-14) were largely within the typical range of 30-100ms reported in the literature (114-120). Direct comparisons are, however, only possible to a certain extent, as different methods and endpoints have been used to define EMD. Similar to the present analysis, Vos et al. (115) applied a cross-correlation method and determined a mean delay of 86 ±5.1 ms until submaximal isometric contractions of the VL muscle were observed. This contraction delay was higher than the present average EMD between VL activation and the onset of tibio-femoral contact forces during ADLs (range: 30 to 73 ms). The observed difference between the measurements may partly be related to disparities in the types of muscle contraction and coordination patterns. Cavanagh et al. (114) showed that eccentric contractions precipitate the rate of muscle force development and exhibit shorter EMD values than isometric or concentric contractions. They considered such shorter EMD values to be more pronounced in case of antecedent counter movements, during which the muscle is stretched before concentrically contracting. In this regard, Cavanagh et al. predicted that the activation of elbow flexors leads to shorter EMD values of less than 50 ms during rapid extension, as compared to those during rapid flexion of over 55 ms. As the present data were measured during natural locomotion, the EMD values were most certainly influenced by reciprocal agonist-antagonist muscle actions.

In line with the findings by Cavanagh et al. (114), EMD following the activation of the vastus muscles was shorter during their eccentric action during stair descent than under concentric work in stair ascent (157, 158). The mean duration of EMD was shorter during more rapid movement sequences, such as stair climbing, and longest during the static exercise of OLS. This finding is consistent with prior considerations on muscle force-velocity relationships reported in the literature. Bell et al. (118) thus determined that a shorter EMD is associated

with increases in the rate of force development and maximal voluntary contraction force. Increased movement velocies during eccentric contractions of the brachial biceps muscle were correlated with a shorter EMD, as reported by Norman and Komi (166). Winter et al. (117), who defined the endpoint of EMD as movement, found an average latency of 38±1.7 ms from activation of the soleus muscle to the movement of the heel. They proposed that this delay between EMG and the onset of movement, can be further subdivided into the interval from muscle activation to the development of muscle tension (i.e. force time) and from the generation of muscle tension to movement (i.e. elastic charge time). The present EMD data suggest that this sub-classification of Winter et al. may be complemented by an additional time interval that refers to the transmission of joint loads and could be termed joint load time. Further studies, that take these variables into account, are required to develop a comprehensive picture of the underlying mechanisms and time-relationships of EMD during dynamic movement.

An interesting finding is that the VM was activated prior to the VL muscle during gait and stair climbing and thus had a comparatively longer EMD time. Chester et al. (61) reviewed that aberrant timing patterns of the oblique VM and VL muscles during dynamic activities, such as stair climbing, are related to the incidence of anterior knee pain. In specific, this meta-analysis determined the slowed recruitment of the oblique VM, compared to the VL, as a predisposing factor for anterior knee pain. In line with the present results, Cowan et al. (167) found that the coordinated timing, in which VM EMG onset precedes the VL, can be restored by rehabilitation strategies that retrain VM motor control. Berth et al. (112) likewise showed that deficits in quadriceps voluntary activation and contraction force are partly reversible within three years after TKA. Besides, it has been suggested that voluntary activation deficits after TKA have a greater effect on quadriceps strength than atrophic changes in muscle status (42). This might explain more pronounced improvements in VM and VL muscle activation after successful TKA, as compared to measurements in muscle atrophy. In general, the present results of VM-VL activation patterns concur with those on muscle status that indicate the regenerative potential of the periarticular musculature after TKA.

4.4 Interrelationship between muscle status, EMG and joint load

4.4.1 Associations with periarticular muscle status

This thesis aimed to examine the association of the status of the periarticular musculature with *in vivo* knee joint loads and EMG activities during functional activities. The underlying hypothesis that impairments in muscle status affect the internal loads of the knee joint was generally supported by the present results. Fatty muscle infiltration contributed to increased knee joint loadings after TKA, whereas changes in muscle size had only minor effects.

An important clinically relevant finding was that an increased intramuscular fat content of the vastus and hamstring muscles contributed to higher peak knee joint loadings during gait. This outcome supports previous research on the etiology of knee OA that linked the intramuscular fat content of the quadriceps musculature to higher grades of clinical and radiographic knee OA (147, 148). The results are further in accordance with those of Damm et al. (141), showing a correlation between the fat content of the hip abductor muscles and increased hip joint loads during level walking at three months after THA. Marcus et al. (62) determined that quadriceps muscle fatty infiltration has a relatively stronger impact than lean thigh muscle tissue on the mobility performance in older adults. This could explain the subordinate effect of lean thigh muscle tissue on the magnitude of the average peak tibio-femoral joint loads.

Drawing on the measurements of muscle CSA, only the size of the ST muscle was correlated significantly with the average peak knee joint loads during level walking. This result supports previous research results on ACL reconstruction with hamstring autografts (168), that showed reduced medial knee compartment loads during gait after ST and GR tendon harvest. Based on the present results, it can be assumed that this reported decrease in medial joint load after ACL reconstruction could be largely attributed to harvest-induced reductions in ST muscle CSA (169). The overall limited correlation of joint load and muscle CSA reflects the prevailing view in the literature that muscle quality might have a greater impact on physical function than mass alone (101, 102, 147). Kumar et al. (147) found that intramuscular fat, rather than muscle CSA, contributed to muscle weakness, radiographic disease severity and physical disability in knee OA patients. They found that quadriceps strength deficits were related to a higher degree of intramuscular fat and remained unaffected by changes in lean muscle CSA. The review by Mitchell et al. (170) showed that age-related declines in muscle strength by far outpace the loss of muscle mass and have more adverse effects on physical function in older age. Goodpaster et al. (171) found that rises in muscle mass alone cannot

prevent strength declines with age. In agreement with these previous research findings, fatty infiltration could thus represent an independent risk factor for increased tibio-femoral joint loadings after TKA.

The correlation analysis of periarticular muscle status and EMG signal patterns indicated that quadriceps muscle fat infiltration contributed to reduced levels of muscle activation. Muscular atrophy and voluntary activation deficits have been previously shown to account up to 85% for the decrease in muscle strength within the first month after TKA (42). Taaffe et al. (149) determined that reductions in thigh muscle strength due to declining rates of physical activity occur in parallel to muscle fatty infiltration. Stevens et al. (110) found a strong association between quadriceps weakness and voluntary activation deficits after TKA. It seems possible that the present results may partly be explained by the process of AMI, whereby neural inhibition after TKA may induce long-term muscle atrophy and weakness (109).

A strong correlation was determined between fatty infiltration of the VL and impairments in muscle activity during stair climbing and stand-to-sit activities. Increased antagonistic muscle activity and pretension of soft tissues at the lateral aspect of the knee were shown to be relevant for counteracting the external knee adduction moment (82). External knee adduction moments are generally considered a surrogate measure for contact forces in the medial knee compartment (172) and have been related to the onset and progression of knee OA (173). Hubley-Kozey et al. (111) determined that knee OA patients show neuromuscular alterations in terms of an increased lateral muscle activity in an attempt to reduce medial contact stresses. According to Schipplein and Andriacchi (82) lateral soft tissues at the knee contribute to dynamic joint stability by producing compressive forces that resist lateral joint opening and off-load the medial compartment. Hence, the present results suggest that fatty infiltration and related changes in muscle activity of the VL may impair the protective function of the lateral musculature to counteract medial adduction moments and maintain joint stability.

Furthermore, a high degree of fatty infiltration of the VL muscle correlated with a short delay between the change in EMG activity and tibio-femoral loading during stair ascent. This result is likely related to the finding of D'Lima et al. (132) that soft tissues absorb most of the anterior shear forces at the knee joint during stair climbing. The non-contractile tissue of intramuscular fat is considered to increase a muscle's stiffness, which may impair its ability to generate forces and absorb energy of impact loads (97). Early work on muscular force transmission of Tidball et al. (174), showed that muscle disuse atrophy can increase the

stresses at the myotendinous junction during loading. Increases in musculo-tendinous stiffness and changes in tissue elasticity, have been previously related to shorter EMD times (120). In this regard, the stiff mechanical properties of intramuscular fat, may explain, to some extent, the short EMD observed in relation to the fatty infiltration of the periarticular musculature.

4.4.2 Associations between EMG and joint load

The present thesis aimed to evaluate the association between muscle activation patterns and *in vivo* tibio-femoral joint contact forces during dynamic activities. The current data support the hypothesis that the loads transferred at the knee joint respond to the unique action of the periarticular musculature. The activation onset and amplitude of the EMG signals modulated peak contact force values. Muscle activation characteristics thus explained, at least in part, the considerable inter-individual variations in knee joint loads observed during the various ADLs.

The tibio-femoral forces were sensitive to the activation of the VM at the CTO (i.e. first peak force) during level walking. The relationship between *in vivo* knee joint loads and VM muscle activity levels supports earlier simulation results of Sasaki et al. (137). They determined that the vastus muscles account for the first peak of axial knee joint forces at approximately 15% of the gait cycle. The tibio-femoral contact forces predicted in this model were slightly higher than those of the present *in vivo* data (2.8 BW or 2100 N versus 2.16 BW or 1904 N). Based on a post-hoc simulation, Sasaki et al. found that peak tibio-femoral joint forces can be reduced by the adoption of quadriceps avoidance gait patterns that require lower knee extensor torques. Anderson and Pandy (154) computed, accordingly, that muscles contribute 50 to 95% to the vertical GRF using a dynamic optimization model of gait. Skeletal structures and the muscles of the contralateral limb thereby had a subordinate load effect on the GRF of 20-50% and 15%, respectively. Kutzner et al. (134) likewise determined that muscle induced forces can add additional 60% BW to the tibio-femoral load of 44% BW that are needed for postural support during two-legged stance. In accord with prior investigations, the present findings thus indicate a modulation of joint loads in response to differential muscle activation.

The results showed a strong significant correlation of GM muscle activity and *in vivo* knee joint loads at the second peak of stair ascent and a trend for the second peak of walking. These results are in line with a recent study by Trepczynski et al. (175), who applied musculoskeletal modelling techniques to determine the effect of antagonistic muscle co-contraction on joint contact forces. The study found that co-contractions of the gastrocnemius

and quadriceps muscles increase the peak tibio-femoral joint contact forces by up to 66% in stair ascent and up to 56% in the terminal stance phase of level walking. This equated to an additional joint load of up to 100 %BW. The constrained model used by Trepczynski et al. to quantify the extent of muscle co-contraction was based on *in vivo* joint load data, which were obtained from the same patient cohort as the one included in the present investigations. The finding that peak knee joint loads during the late stance of level walking are responsive to the activation of the gastrocnemius are further consistent with data obtained by DeMers et al. (176). They analyzed tibio-femoral forces using a musculoskeletal model-based approach in relation to muscle coordination strategies during gait. In their simulations tibio-femoral joint loads during late stance were sensitive to increased gastrocnemius, RF and BF co-activation and could be decreased by compensatory activation of the gluteus medius and soleus. Sasaki et al. (137) likewise showed that co-contractions of muscles that do not span the knee, such as the gluteus maximus or soleus, can decrease peak tibio-femoral forces during late stance. The *in vivo* data obtained in the present thesis thus support previous model-based findings that gait patterns, which involve reduced gastrocnemius activity, can contribute to reduced knee joint loads. Further research is required to determine how far strengthening of the hip musculature can reduce the *in vivo* loads acting in the knee joint following TKA.

The rate of force transmission to the tibio-femoral joint, in terms of EMD, was found to accelerate when muscle activation levels increased. Hence, a short EMD was related to a greater muscle activation of the hamstrings and plantar flexors during stair climbing. This finding supports the notion of Banks et al. (58) that a high hamstring activity and reduced intrinsic knee stability may contribute to a lower efficiency of the extensor mechanism at higher muscular loads. This inference was based on the differences in intrinsic constraint that Banks et al. determined between various implant designs during stair climbing. They found a medial shift in the center of rotation of PS implants with high knee flexion, which might have implications on the medial compartment load (173). MacWilliams et al. (177) likewise suggested that hamstring co-contractions during weight-bearing knee flexion increase the quadriceps loads and compressive forces at the knee joint to sustain a joint equilibrium. The present results further support those of Yavuz et al. (178), who showed that increasing levels of muscle contraction lead to shorter EMD times, as the muscle stiffens and the tendon is stretched more rapidly. Muscle fatigue was, conversely, related to a longer EMD in this study due to decreases in fiber stiffness and muscle contractile strength. The association between short EMD times and high levels of muscle activation could, besides, be related to the

discharge frequency of the MUs. Maffiuletti et al. (179) reviewed that both the magnitude and contractile rate of force generation depend on the number and firing rate of activated MUs. They found that high-intensity resistance training can induce neuromuscular adaptations that increase EMG amplitude and the rate of force development. Heavy resistance exercises could thus improve muscle power (180) but might contribute to higher joint loads.

During the activity of OLS a short EMD duration was associated with high activation levels of the plantar flexor GM and a trend towards increased knee joint loads. These results are in accord with data on ankle stability obtained by Mora et al. (181), who reported a shortened time latency in monopedal stance between the activation of the peroneus longus (i.e. plantar flexor), and the onset of the GRF. They ascribed this reduction in EMD to the increased leg muscle tone and ankle musculotendinous stiffness required to maintain static balance during OLS. Gribble and Robinson (182) further highlighted the importance of the ankle joint for knee kinematics, showing that chronic ankle instability is associated with reduced knee flexion during single-leg jump landing and declines in dynamic stability. Rehabilitation programs following TKA should consider balance training, as proposed previously by Piva et al. (183), and the functional recovery of the ankle musculature.

The results indicated an inverse association between the magnitude of peak tibio-femoral joint loads and the duration of EMD. A shortened EMD following VM and HL muscle activation correlated with increased peak tibio-femoral load values in the late stance phase of level walking. This is in agreement with the findings of Hubley-Kozey et al. (111), who showed that increased quadriceps and hamstring co-activations during stance are related to a higher grade of knee OA. Antagonistic co-contractions supposedly maintain muscular balance and biomechanical joint stability, but can contribute to increased tibio-femoral loads and joint wear (137, 152, 175). Trepczynski et al. (175) quantified, by means of a constrained musculoskeletal model, that muscle co-contractions in the late stance phase of level walking may increase peak tibio-femoral contact forces by up to 1.0 BW ($\sim 50\%$). As determined by Bell et al. (118), the maximum forces exerted by muscular contraction are dependent on the duration of the EMD. With respect to these previous research results, the present data suggest that antagonistic muscle activity may increase the transmission of contact forces at the knee joint. Besides, this finding provides some support for the premise that antagonistic muscle co-contraction patterns should be minimized after TKA and addressed by rehabilitation strategies (152, 175). Furthermore, Benedetti et al. (184), who investigated the kinematics and kinetics

of gait at two years after TKA, showed that prolonged co-contractions are closely related to a postoperative "stiff knee gait pattern". It has been suggested that such impairments in muscle function and mobility bear the potential to be reversed in the postoperative course of four years (112, 113, 185). Hence, an early restoration of muscle coordination and on-off timing patterns seems decisive to minimize joint loads and improve the long-term outcome of TKA.

4.5   Clinical implications

The present results provide an insight into muscular properties and *in vivo* knee joint loadings following TKA and are of relevance to implant design, surgical technique and rehabilitation programs. High loads acted in the knee implant during dynamic ADL, whereby the highest peak values of 3.41 BW occurred during the activity of stair climbing. Implant designs must be adjusted in order to maximize patient satisfaction, restoration of joint function and implant longevity. A comprehensive cross-sectional study of 1703 patients undergoing primary TKA investigated patient satisfaction one year postoperatively during different ADL (186). This study showed that patient satisfaction with pain reduction and knee function was lowest for the activity of stair climbing, which is associated with increased knee joint loads. Besides functional constraints, high knee joint loadings might pose a risk for wear-related complications and limited implant survival. Vessely et al. (187), who assessed the survival rates of 1000 CR implants, reported that and tibial PE wear accounted for about one third of the revision surgeries 14.5 to 17.9 years after primary TKA. In Germany, aseptic loosening and implant wear were registered among the most common causes for revision surgery of TKA in 2018 with 25.0% and 5.7%, respectively (188). A close monitoring of current and novel TKA designs is essential to evaluate and improve implant performance. Hence, national joint registries have gained increasing importance in recent years (189) and will most likely gain further importance to ensure the long-term clinical success of TKA.

The magnitude of *in vivo* tibio-femoral joint loads appeared to be affected by the degree of fatty infiltration of the joint stabilizing musculature. Although the extent of intramuscular fat decreased in the postoperative course, the improvement in muscle status was least pronounced for the quadriceps muscle. These findings highlight the importance of minimizing surgical trauma during TKA and effectively restoring postoperative muscle function. There is a rising interest in MIS approaches for TKA, which avoid violation of the extensor mechanism and have been related to an expedited postoperative recovery (38-40, 49). Bonutti et al. (49) suggested that the reduced incision length, use of down-sized instruments and avoidance of

patellar eversion and joint dislocation during the quadriceps sparing approach can limit soft-tissue strains. This study showed that MIS TKA can thus reduce postoperative pain, rehabilitation requirements and length of hospital stay. Future studies are required to establish the long-term effectiveness of MIS TKA with regards to muscle status and function. The present results indicate that a reduced fatty infiltration of the periarticular musculature could contribute to lower knee joint loadings and thus to a reduced mechanical stress on the implant. Muscle activation timing and coordination patterns were found to modulate the average peak knee joint loads during the different ADLs. This has implications for rehabilitation, indicating that exercise programs should target muscle activation patterns and motor control in addition to strength deficits and atrophy. The improvement of voluntary muscle activation and recruitment patterns (112, 113) has been previously linked to enhanced postoperative strength gains and surgical outcomes. Compensatory training of the hip and ankle musculature may support the endeavors to increase postoperative strength and functional ability and yet reduce the loads acting in the knee joint (137). Moreover, more attention should be addressed to the preoperative optimization of muscle strength and function. Recent studies indicate that multimodal prehabilitation before TKA, including functional and strength training, NMES, and patient education can improve postoperative recovery (143, 190). As rehabilitation practices and standards differ widely among clinical institutions, there is a need for a consensus on evidence-based rehabilitation guidelines (191).

4.6   Limitations

There are limitations that must be considered when interpreting the present results. First, only a small number of patients were included for evaluation. This may have limited the ability to determine statistical significance in some of the correlation analyses. Nonetheless, the present patient cohort is the largest worldwide with instrumented implants that allow for synchronized measurements of *in vivo* knee joint loads and surface EMG. Second, the retrospective design limited the amount of CT slices available per patient. Standardized segmentation of individual muscles could be only performed at the distal thigh of the operated leg. The analyzed muscle region corresponded, however, to the distal segment of the thigh that was considered to be most affected by the MPP arthrotomy. Besides, this investigation provides a framework for the exploration of muscle status that could be transferred to the entire span of individual muscles and the contralateral leg in future studies. By definition, the contralateral leg should not be regarded as the healthy comparator to the operated leg though, as McMahon et al. (192) determined that nearly 40% of the patients progress to contralateral TKA within 10

years after unilateral knee replacement. The patients included in the present thesis had no contralateral symptoms at the time of investigation that could have influenced the outcome measurements. Third, possible inaccuracies in the measurements that deal with the timing and delay of muscular and loading events may arise from the delay inherent in the different measurement systems. Standardized and established methods of data acquisition and evaluation were applied in order to enhance the reliability of the determined metrics. Fourth, measurements of the joint load and EMG were only performed at a mean of 26 months (range: 8-45) after TKA and not on the same date as the CT examinations. The measured knee joint loads and muscle activation patterns are thus not representative of the conditions that prevail preoperatively, in the acute postoperative period or in other implant designs. The present findings are, however, coherent with those of previous studies (131-136) conducted at different time points in the postoperative continuum of care of TKA.

5 Conclusion

TKA is considered the gold standard to relieve pain and restore function in patients with end-stage knee OA (5). The number of cases is expected to rise significantly in the upcoming years, with procedures being increasingly performed in younger and more active patients (11). Higher physical demands and patient expectations emphasize the importance of postoperative muscle function and implant longevity. The aim of the present investigation was thus to assess the periarticular muscle status, EMG activation patterns and *in vivo* loads acting in the knee joint during dynamic activities. The results of this analysis provide unprecedented insight into the interrelationship between these parameters in the long-term after TKA.

The longevity of knee implants can be limited by excessive tibio-femoral joint loads, as they may accelerate PE wear and lead to early implant failure. Instrumented knee implants (89) were used to measure the knee joint loads *in vivo* during different weight-bearing ADLs. The load magnitude varied between the movement tasks, but consistently exceeded the patient's body weight, reaching average peak values of up to 3.41 BW. Dynamic loading during stair descent showed the highest peak knee joint loads, as the contact area of the articulating surfaces was reduced at high knee flexion angles. The close monitoring and benchmarking of knee implants by means of joint registries may contribute to improved long-term treatment outcomes after TKA.

The pathologic process of knee OA and intraoperative muscle damage have been associated with muscular atrophy and fatty infiltration (28, 29, 148). Postoperative changes in muscle status were assessed by manual segmentation of axial CT scans of the ipsilateral distal thigh. The postoperative course showed a significant reduction in distal quadriceps volume of about 10%. The extent of fatty infiltration overall decreased within 2.5 years following TKA, albeit improvements in intramuscular fat ratio were least pronounced for the quadriceps muscle. Attempts should be made to minimize approach-related soft-tissue damage. MIS techniques seem promising to preserve the extensor mechanism and improve short-term recovery (39), but need to be reassessed with regard to long-term clinical effectiveness and safety. The results complement those of earlier studies that fatty infiltration can recover through physical exercise (149-151) and underscore the importance of targeting relative quadriceps weakness in rehabilitation. More attention should be directed towards the concept of prehabilitation (190), as presurgical improvements in muscle status might enhance postoperative recovery.

This thesis has demonstrated, for the first time, a direct effect of muscle activation patterns on the magnitude and timing of *in vivo* knee joint loads during functional activities. Real-time measurements of *in vivo* tibio-femoral loads were synchronized with surface EMG recordings of knee flexor and extensor muscles. The temporal phase shift between the onset of EMG and the mechanical loading response in the knee joint was computed using a cross-correlation technique. Differential activation patterns of the periarticular musculature modulated both, the peak contact forces and loading rate of the knee joint. A novel time interval of "joint load time" was determined for the different ADLs, complementing previous research on EMD. The results substantiate the impact of muscle activity on the internal loadings of the knee and indicate the potential to reduce peak joint loads by altering muscle activation strategies. The restoration of functional stability and effective muscle coordination patterns may contribute to lower knee joint loads. The application of NMES (143) should be considered as a possible rehabilitation approach to resolve muscle activation deficits and facilitate functional recovery.

Muscle weakness and voluntary activation deficits are increasingly considered as important predictors for the surgical outcome after TKA (13). In the correlation analyses muscle fatty infiltration emerged as a risk factor and stronger indicator for high knee joint loads than distal volume. Besides, intramuscular fat accelerated the rate of knee joint loading, most probably due to alterations in the mechanical properties of muscle contraction and tissue stiffness (97). The increased peak values and rates of joint loading related to fatty infiltration may increase

joint degeneration in knee OA (78), implant wear and revision rates after TKA. Moreover, motion patterns with high EMG activation of antagonistic muscles contributed to increased knee joint loadings. Postoperative recovery should aim to restore an environment of enhanced mobility in which tibio-femoral joint loads are largely minimized. The compensatory strengthening of the hip and ankle musculature might present a perspective for rehabilitation to off-load the knee and redistribute loads between adjacent joints (137). Hence, multi-joint dynamics should be considered when retraining muscle activation and strength after surgery.

In conclusion, the present analysis suggests that periarticular muscle status, activation patterns and *in vivo* knee joint loads are closely interrelated. Muscular impairments of fatty infiltration and functional activation deficits can induce increased peak knee joint loads. The results highlight the importance of training or treating the joint stabilizing musculature to restore a functional muscle-joint interplay and prevent joint overloading. A good muscle status could contribute to an improved long-term outcome and quality of life for patients undergoing TKA.

Bibliography

1. **Kurtz SM, Ong KL, Lau E, Widmer M, Maravic M, Gómez-Barrena E, de Pina M, Manno V, Torre M, Walter WL, de Steiger R, Geesink RG, Peltola M, Röder C.** International survey of primary and revision total knee replacement. Int Orthop 2011; 35(12):1783-1789.

2. **Harris WH, Sledge CB.** Total hip and total knee replacement. N Engl J Med 1990; 323(11):725-731.

3. **Wallidus B.** Arthroplasty of the knee using and endoprosthesis. Acta Orthoped Scand 1957; 28(24 Suppl):1-112

4. **Losina E, Walensky RP, Kessler CL, Emrani PS, Reichmann WM, Wright EA, Holt HL, Solomon DH, Yelin E, Paltiel AD, Katz JN.** Cost-effectiveness of total knee arthroplasty in the United States: patient risk and hospital volume. Arch Intern Med 2009; 169(12):1113-1121.

5. **Carr AJ, Robertsson O, Graves S, Price AJ, Arden NK, Judge A, Beard DJ.** Knee replacement. Lancet 2012; 379(9823):1331-1340.

6. **Statistisches Bundesamt (Destatis).** Fallpauschalenbezogene Krankenhausstatistik (DRG-Statistik), Operationen und Prozeduren der vollstationären Patientinnen und Patienten in Krankenhäusern. http://www.gbe-bund.de (Search: Implantation einer Endoprothese am Kniegelenk, last accessed on June 06, 2020 at 11:18h).

7. **OECD.** Health at a Glance 2017: OECD Indicators. Hip and knee replacement. OECD Publishing 2017. https://doi.org/10.1787/health_glance-2017-65-en (last accessed on May 20, 2020 at 15:12h).

8. **Wengler A, Nimptsch U, Mansky T.** Hip and knee replacement in Germany and the USA: analysis of individual inpatient data from German and US hospitals for the years 2005 to 2011. Dtsch Arztebl Int 2014; 111(23-24):407-416.

9. **Kurtz S, Ong K, Lau E, Mowat F, Halpern M.** Projections of primary and revision hip and knee arthroplasty in the United States from 2005 to 2030. J Bone Joint Surg Am 2007; 89(4):780-785.

10. **Maradit Kremers H, Larson DR, Crowson CS, Kremers WK, Washington RE, Steiner CA, Jiranek WA, Berry DJ.** Prevalence of Total Hip and Knee Replacement in the United States. J Bone Joint Surg Am 2015; 97(17):1386-1397.

11. **Kurtz SM, Lau E, Ong K, Zhao K, Kelly M, Bozic KJ.** Future young patient demand for primary and revision joint replacement: national projections from 2010 to 2030. Clin Orthop Relat Res 2009; 467(10): 2606-2612.

12. **Sharkey PF, Lichstein PM, Shen C, Tokarski AT, Parvizi J.** Why are total knee arthroplasties failing today--has anything changed after 10 years?. J Arthroplasty 2014; 29(9):1774-1778.

13. **Meier W, Mizner RL, Marcus RL, Dibble LE, Peters C, Lastayo PC.** Total knee arthroplasty: muscle impairments, functional limitations, and recommended rehabilitation approaches. J Orthop Sports Phys Ther 2008; 38(5):246-256.

14. **NIH Consensus Panel.** NIH Consensus Statement on total knee replacement, December 8-10, 2003. J Bone Joint Surg Am 2004; 86(6):1328-1335.

15. **Lane NE, Brandt K, Hawker G, Peeva E, Schreyer E, Tsuji W, Hochberg MC.** OARSI-FDA initiative: defining the disease state of osteoarthritis. Osteoarthritis Cartilage 2011; 19(5):478-482.

16. **Mont MA, Rifai A, Baumgarten KM, Sheldon M, Hungerford DS.** Total knee arthroplasty for osteonecrosis. J Bone Joint Surg Am 2002; 84(4):599-603.

17. **Saleh H, Yu S, Vigdorchik J, Schwarzkopf R.** Total knee arthroplasty for treatment of post-traumatic arthritis: Systematic review. World J Orthop 2016; 7(9):584-591.

18. **Rodriguez-Merchan EC.** Total knee replacement in haemophilic arthropathy. J Bone Joint Surg Br 2007; 89(2):186-188.

19. **Cross M, Smith E, Hoy D, Nolte S, Ackerman I, Fransen M, Bridgett L, Williams S, Guillemin F, Hill CL, Laslett LL, Jones G, Cicuttini F, Osborne R, Vos T, Buchbinder R, Woolf A, March L.** The global burden of hip and knee osteoarthritis: estimates from the global burden of disease 2010 study. Ann Rheum Dis 2014; 73(7):1323-1330.

20. **Woolf AD, Pfleger B.** Burden of major musculoskeletal conditions. Bull World Health Organ. 2003; 81(9):646-656.

21. **Inacio MCS, Paxton EW, Graves SE, Namba RS, Nemes S.** Projected increase in total knee arthroplasty in the United States - an alternative projection model. Osteoarthritis Cartilage 2017; 25(11):1797-1803.

22. **Palazzo C, Nguyen C, Lefevre-Colau MM, Rannou F, Poiraudeau S.** Risk factors and burden of osteoarthritis. Ann Phys Rehabil Med. 2016; 59(3):134-138.

23. **GBD 2017 Disease and Injury Incidence and Prevalence Collaborators.** Global, regional, and national incidence, prevalence, and years lived with disability for 354 diseases and injuries for 195 countries and territories, 1990-2017: a systematic analysis for the Global Burden of Disease Study 2017. Lancet 2018; 392(10159):1789-1858.

24. **Hunter DJ, McDougall JJ, Keefe FJ.** The symptoms of osteoarthritis and the genesis of pain. Rheum Dis Clin North Am 2008; 34(3):623-643.

25. **Goldring MB, Goldring SR.** Articular cartilage and subchondral bone in the pathogenesis of osteoarthritis. Ann N Y Acad Sci 2010; 1192:230-237.

26. **Heijink A, Gomoll AH, Madry H, Drobnič M, Filardo G, Espregueira-Mendes J, Van Dijk CN.** Biomechanical considerations in the pathogenesis of osteoarthritis of the knee. Knee Surg Sports Traumatol Arthrosc 2012; 20(3):423-435.

27. **Englund M.** The role of biomechanics in the initiation and progression of OA of the knee. Best Pract Res Clin Rheumatol 2010; 24(1):39-46.

28. **Hurley MV.** Muscle dysfunction and effective rehabilitation of knee osteoarthritis: What we know and what we need to find out. Arthritis & Rheumatism 2003; 49:444-452.

29. **Lewek MD, Rudolph KS, Snyder-Mackler L.** Quadriceps femoris muscle weakness and activation failure in patients with symptomatic knee osteoarthritis. J Orthop Res 2004; 22(1):110-115.

30. **Kellgren JH, Lawrence JS.** Radiological assessment of osteoarthrosis. Ann Rheum Dis 1957; 16(4):494-502.

31. **Bedson J, Croft PR.** The discordance between clinical and radiographic knee osteoarthritis: a systematic search and summary of the literature. BMC Musculoskelet Disord 2008; 9:116.

32. **McAlindon TE, Bannuru RR, Sullivan MC, Arden NK, Berenbaum F, Bierma-Zeinstra SM, Hawker GA, Henrotin Y, Hunter DJ, Kawaguchi H, Kwoh K, Lohmander S, Rannou F, Roos EM, Underwood M.** OARSI guidelines for the non-surgical management of knee osteoarthritis. Osteoarthritis Cartilage 2014; 22(3):363-388.

33. **Kerkhoffs GM, Servien E, Dunn W, Dahm D, Bramer JA, Haverkamp D.** The influence of obesity on the complication rate and outcome of total knee arthroplasty: a meta-analysis and systematic literature review. J Bone Joint Surg Am 2012; 94(20):1839-1844.

34. **Abdel MP, Bonadurer GF 3rd, Jennings MT, Hanssen AD.** Increased Aseptic Tibial Failures in Patients With a BMI ≥35 and Well-Aligned Total Knee Arthroplasties. J Arthroplasty 2015; 30(12):2181-2184.

35. **Scott CE, Biant LC.** The role of the design of tibial components and stems in knee replacement. J Bone Joint Surg Br 2012; 94(8):1009-1015.

36. **Cristea S, Predescu V, Dragosloveanu Ş, Cuculici Ş, Mărăndici N.** Surgical Approaches for Total Knee Arthroplasty, Arthroplasty - A Comprehensive Review. IntechOpen 2016; 2:25-47.

37. **Anand A, Veerappa YA, Dilip N, Ravindran R, Adala R, Srinivas JV.** Surgical exposure in total knee arthroplasty (TKA). In: Affatato S (ed.). Surgical Techniques in Total Knee Arthroplasty and Alternative Procedures. Woodhead Publishing 2014; 123-134.

38. **Pipino G, Indelli PF, Graceffa A, Faaborg-Andersen C, Poli P, Marcucci M.** Mini-invasive approach in total knee arthroplasty (TKA). In: Affatato S (ed.) Surgical Techniques in Total Knee Arthroplasty and Alternative Procedures. Woodhead Publishing 2014; 167-179.

39. **Tria AJ Jr, Coon TM.** Minimal incision total knee arthroplasty: early experience. Clin Orthop Relat Res 2003; (416):185-190.

40. **Tzatzairis T, Fiska A, Ververidis A, Tilkeridis K, Kazakos K, Drosos GI.** Minimally invasive versus conventional approaches in total knee replacement/arthroplasty: A review of the literature. J Orthop 2018; 15(2):459-466.

41. **von Langenbeck B.** Zur resection des kniegellenks. Verhandlungen der Deutschen Gesellschaft fur Churg 1878; VII:23. (Cited from Affatato S (ed.) 2014, 123-134).

42. **Mizner RL, Petterson SC, Stevens JE, Vandenborne K, Snyder-Mackler L.** Early quadriceps strength loss after total knee arthroplasty. The contributions of muscle atrophy and failure of voluntary muscle activation. J Bone Joint Surg Am 2005; 87(5):1047-1053.

43. **Hofmann AA, Plaster RL, Murdock LE.** Subvastus (Southern) approach for primary total knee arthroplasty. Clin Orthop Relat Res 1991; (269):70-77. (Cited from Affatato S (ed.) 2014, 123-134).

44. **Berstock JR, Murray JR, Whitehouse MR, Blom AW, Beswick AD.** Medial subvastus versus the medial parapatellar approach for total knee replacement: A systematic review and meta-analysis of randomized controlled trials. EFORT Open Rev 2018; 3(3):78-84.

45. **Chang CH, Chen KH, Yang RS, Liu TK.** Muscle torques in total knee arthroplasty with subvastus and parapatellar approaches. Clin Orthop Relat Res 2002; (398):189-195.

46. **Engh GA, Holt BT, Parks NL.** A midvastus muscle-splitting approach for total knee arthroplasty. J Arthroplasty. 1997; 12(3):322-331.

47. **Parentis MA, Rumi MN, Deol GS, Kothari M, Parrish WM, Pellegrini VD Jr.** A comparison of the vastus splitting and median parapatellar approaches in total knee arthroplasty. Clin Orthop Relat Res 1999; (367):107-116.

48. **Kelly MJ, Rumi MN, Kothari M, Parentis MA, Bailey KJ, Parrish WM, Pellegrini VD Jr.** Comparison of the vastus-splitting and median parapatellar approaches for primary total knee arthroplasty: a prospective, randomized study. Surgical technique. J Bone Joint Surg Am 2007; 89 Suppl 2 Pt.1:80-92.

49. **Bonutti PM, Mont MA, McMahon M, Ragland PS, Kester M.** Minimally invasive total knee arthroplasty. J Bone Joint Surg Am 2004; 86-A Suppl 2:26-32.

50. **Dalury DF, Dennis DA.** Mini-incision total knee arthroplasty can increase risk of component malalignment. Clin Orthop Relat Res 2005; 440:77-81.

51. **Taylor H, McGregor AH, Medhi-Zadeh S, Richards S, Kahn N, Zadeh JA, Hughes SP.** The impact of self-retaining retractors on the paraspinal muscles during posterior spinal surgery. Spine (Phila Pa 1976) 2002; 27(24):2758-2762.

52. **Müller M, Tohtz S, Winkler T, Dewey M, Springer I, Perka C.** MRI findings of gluteus minimus muscle damage in primary total hip arthroplasty and the influence on clinical outcome. Arch Orthop Trauma Surg 2010; 130(7):927-935.

53. **von Roth P, Abdel MP, Wauer F, Winkler T, Wassilew G, Diederichs G, Perka C.** Significant muscle damage after multiple revision total hip replacements through the direct lateral approach. Bone Joint J. 2014; 96-B(12):1618-1622.

54. **Ranawat AS, Ranawat CS.** The history of total knee arthroplasty. In: Bonnin M (ed.). The Knee Joint. Surgical Techniques and Strategies. Springer 2012; 699-707.

55. **Morgan H, Battista V, Leopold SS.** Constraint in primary total knee arthroplasty. J Am Acad Orthop Surg 2005; 13(8):515-524.

56. **Most E, Zayontz S, Li G, Otterberg E, Sabbag K, Rubash HE.** Femoral rollback after cruciate-retaining and stabilizing total knee arthroplasty. Clin Orthop Relat Res 2003; (410):101-113.

57. **Rodríguez-Merchán EC.** Total knee arthroplasty using hinge joints: Indications and results. EFORT Open Rev. 2019;4(4):121-132.

58. **Banks SA, Hodge WA.** 2003 Hap Paul Award Paper of the International Society for Technology in Arthroplasty. Design and activity dependence of kinematics in fixed and mobile-bearing knee arthroplasties. J Arthroplasty 2004; 19(7):809-816.

59. **Petersen W, Rembitzki IV, Brüggemann GP, Ellermann A, Best R, Koppenburg AG, Liebau C.** Anterior knee pain after total knee arthroplasty: a narrative review. Int Orthop 2014; 38(2):319-328.

60. **Nam D, Abdel MP, Cross MB, LaMont LE, Reinhardt KR, McArthur BA, Mayman DJ, Hanssen AD, Sculco TP.** The management of extensor mechanism complications in total knee arthroplasty. AAOS exhibit selection. J Bone Joint Surg Am 2014; 96(6):e47.

61. **Chester R, Smith TO, Sweeting D, Dixon J, Wood S, Song F.** The relative timing of VMO and VL in the aetiology of anterior knee pain: a systematic review and meta-analysis. BMC Musculoskelet Disord 2008; 9:64.

62. **Marcus RL, Addison O, Dibble LE, Foreman KB, Morrell G, Lastayo P.** Intramuscular adipose tissue, sarcopenia, and mobility function in older individuals. J Aging Res 2012; 629637.

63. **Flandry F, Hommel G.** Normal anatomy and biomechanics of the knee. Sports Med Arthrosc Rev 2011; 19(2):82-92.

64. **Grelsamer RP, Klein JR.** The biomechanics of the patellofemoral joint. J Orthop Sports Phys Ther. 1998; 28(5):286-298.

65. **Strobel M, Stedtfeld HW.** Evaluation of the ligaments. Basic Principles. In: Strobel M (ed.). Diagnostic Evaluation of the Knee. Springer 1990; 100-109.

66. **Steultjens MP, Dekker J, van Baar ME, Oostendorp RA, Bijlsma JW.** Range of joint motion and disability in patients with osteoarthritis of the knee or hip. Rheumatology (Oxford) 2000; 39(9):955-961.

67. **Ritter MA, Harty LD, Davis KE, Meding JB, Berend ME.** Predicting range of motion after total knee arthroplasty. Clustering, log-linear regression, and regression tree analysis. J Bone Joint Surg Am 2003; 85(7):1278-1285.

68. **Cicuttini FM, Jones G, Forbes A, Wluka AE.** Rate of cartilage loss at two years predicts subsequent total knee arthroplasty: a prospective study. Ann Rheum Dis 2004; 63(9): 1124-1127.

69. **Banks SA, Markovich GD, Hodge WA.** In vivo kinematics of cruciate-retaining and -substituting knee arthroplasties. J Arthroplasty 1997; 12(3):297-304.

70. **Holt G, Nunn T, Allen RA, Forrester AW, Gregori A.** Variation of the vastus medialis obliquus insertion and its relevance to minimally invasive total knee arthroplasty. J Arthroplasty 2008; 23(4): 600-604.

71. **Mizner RL, Snyder-Mackler L.** Altered loading during walking and sit-to-stand is affected by quadriceps weakness after total knee arthroplasty. J Orthop Res 2005; 23(5): 1083-1090.

72. **Hamrick MW, McGee-Lawrence ME, Frechette DM.** Fatty Infiltration of Skeletal Muscle: Mechanisms and Comparisons with Bone Marrow Adiposity. Front Endocrinol (Lausanne) 2016; 7:69.

73. **Clark BC, Manini TM.** Sarcopenia =/= Dynapenia. J Gerontol A Biol Sci Med Sci 2008; 63(8): 829-834.

74. **Mündermann A, Dyrby CO, Andriacchi TP.** Secondary gait changes in patients with medial compartment knee osteoarthritis: increased load at the ankle, knee, and hip during walking. Arthritis Rheum 2005; 52(9):2835-2844.

75. **Silva M, Shepherd EF, Jackson WO, Pratt JA, McClung CD, Schmalzried TP.** Knee strength after total knee arthroplasty. J Arthroplasty 2003; 18(5):605-611.

76. **Winby CR, Lloyd DG, Besier TF, Kirk TB.** Muscle and external load contribution to knee joint contact loads during normal gait. J Biomech 2009; 42(14):2294-2300.

77. **Shelburne KB, Torry MR, Pandy MG.** Contributions of muscles, ligaments, and the ground-reaction force to tibiofemoral joint loading during normal gait. J Orthop Res 2006; 24(10):1983-1990.

78. **Felson DT.** Osteoarthritis as a disease of mechanics. Osteoarthritis Cartilage 2013; 21(1):10-15.

79. **Prendergast PJ, Van der Helm FCT, Duda GN.** Analysis of muscle and joint loads. In: Mow VC, Huiskes R (ed.) Basic Orthopaedic Biomechanics & Mechano-Biology. Lippincott Williams & Wilkins 2005; 29-84.

80. **Kuster MS.** Exercise recommendations after total joint replacement: a review of the current literature and proposal of scientifically based guidelines. Sports Med 2002; 32(7): 433-445.

81. **Gillespie GN, Porteous AJ.** Obesity and knee arthroplasty. Knee 2007; 14(2):81-86.

82. **Schipplein OD, Andriacchi TP.** Interaction between active and passive knee stabilizers during level walking. J Orthop Res 1991; 9(1):113-119.

83. **Taylor WR, Heller MO, Bergmann G, Duda GN.** Tibio-femoral loading during human gait and stair climbing. J Orthop Res 2004; 22:625-632.

84. **Costigan PA, Deluzio KJ, Wyss UP.** Knee and hip kinetics during normal stair climbing. Gait Posture 2002; 16(1):31-37.

85. **Andriacchi TP, Andersson GB, Fermier RW, Stern D, Galante JO.** A study of lower-limb mechanics during stair-climbing. J Bone Joint Surg Am 1980; 62(5):749-757.

86. **Fregly BJ, Besier TF, Lloyd DG, Delp SL, Banks SA, Pandy MG, D'Lima DD.** Grand challenge competition to predict in vivo knee loads. J Orthop Res 2012; 30(4):503-513.

87. **Komistek RD, Kane TR, Mahfouz M, Ochoa JA, Dennis DA.** Knee mechanics: a review of past and present techniques to determine in vivo loads. J Biomech 2005; 38(2):215-228.

88. **Taylor SJ, Walker PS, Perry JS, Cannon SR, Woledge R.** The forces in the distal femur and the knee during walking and other activities measured by telemetry. J Arthroplasty 1998; 13(4):428-437.

89. **Heinlein B, Graichen F, Bender A, Rohlmann A, Bergmann G.** Design, calibration and pre-clinical testing of an instrumented tibial tray. J Biomech 2007; 40 Suppl 1:S4-S10.

90. **Kam PC, Kavanagh R, Yoong FF.** The arterial tourniquet: pathophysiological consequences and anaesthetic implications. Anaesthesia 2001; 56(6):534-545.

91. **Tidball JG.** Mechanisms of muscle injury, repair, and regeneration. Compr Physiol 2011; 1(4):2029-2062.

92. **Petterson SC, Barrance P, Buchanan T, Binder-Macleod S, Snyder-Mackler L.** Mechanisms underlying quadriceps weakness in knee osteoarthritis. Med Sci Sports Exerc 2008; 40(3):422-427.

93. **Bonaldo P, Sandri M.** Cellular and molecular mechanisms of muscle atrophy. Dis Model Mech 2013; 6(1):25-39.

94. **Engelke K, Museyko O, Wang L, Laredo JD.** Quantitative analysis of skeletal muscle by computed tomography imaging-State of the art. J Orthop Translat 2018; 15:91-103.

95. **Wang Y, Pessin JE.** Mechanisms for fiber-type specificity of skeletal muscle atrophy. Curr Opin Clin Nutr Metab Care 2013; 16(3):243-250.

96. **Goodpaster BH, Carlson CL, Visser M, Kelley DE, Scherzinger A, Harris TB, Stamm E, Newman AB.** Attenuation of skeletal muscle and strength in the elderly: The Health ABC Study. J Appl Physiol (1985) 2001; 90(6):2157-2165.

97. **Rahemi H, Nigam N, Wakeling JM.** The effect of intramuscular fat on skeletal muscle mechanics: implications for the elderly and obese. R Soc Interface 2015; 12:20150365.

98. **Gallagher D, Kuznia P, Heshka S, Albu J, Heymsfield SB, Goodpaster B, Visser M, Harris TB.** Adipose tissue in muscle: a novel depot similar in size to visceral adipose tissue. Am J Clin Nutr 2005; 81(4):903-910.

99. **Shaw CS, Clark J, Wagenmakers AJ.** The effect of exercise and nutrition on intramuscular fat metabolism and insulin sensitivity. Annu Rev Nutr 2010; 30:13-34.

100. **Goodpaster BH, Thaete FL, Kelley DE.** Thigh adipose tissue distribution is associated with insulin resistance in obesity and in type 2 diabetes mellitus. Am J Clin Nutr 2000; 71(4):885-892.

101. **McGregor RA, Cameron-Smith D, Poppitt SD.** It is not just muscle mass: a review of muscle quality, composition and metabolism during ageing as determinants of muscle function and mobility in later life. Longev Healthspan 2014; 3(1):9.

102. **Visser M, Goodpaster BH, Kritchevsky SB, Newman AB, Nevitt M, Rubin SM, Simonsick EM, Harris TB.** Muscle mass, muscle strength, and muscle fat infiltration as predictors of incident mobility limitations in well-functioning older persons. J Gerontol A Biol Sci Med Sci 2005; 60(3):324-333.

103. **Scuderi GR, Bourne RB, Noble PC, Benjamin JB, Lonner JH, Scott WN.** The new Knee Society Knee Scoring System. Clin Orthop Relat Res 2012; 470(1):3-19.

104. **Brancaccio P, Lippi G, Maffulli N.** Biochemical markers of muscular damage. Clin Chem Lab Med 2010; 48(6):757-767.

105. **Goodpaster BH, Thaete FL, Kelley DE.** Composition of Skeletal Muscle Evaluated with Computed Tomography. Ann N Y Acad Sci 2000; 904:18-24.

106. **Mitsiopoulos N, Baumgartner RN, Heymsfield SB, Lyons W, Gallagher D, Ross R.** Cadaver validation of skeletal muscle measurement by magnetic resonance imaging and computerized tomography. J Appl Physiol (1985) 1998; 85(1):115-122.

107. **Konrad P.** The ABC of EMG: A Practical Introduction to Kinesiological Electromyography, Version 1.4 March 2006. Noraxon INC, USA 2006.

108. **De Luca CJ.** The Use of Surface Electromyography in Biomechanics, J Appl Biomech 1997; 13(2):135-163.

109. **Rice DA, McNair PJ.** Quadriceps arthrogenic muscle inhibition: neural mechanisms and treatment perspectives. Semin Arthritis Rheum 2010; 40(3):250-266.

110. **Stevens JE, Mizner RL, Snyder-Mackler L**. Quadriceps strength and volitional activation before and after total knee arthroplasty for osteoarthritis. J Orthop Res 2003; 21(5):775-779.

111. **Hubley-Kozey CL, Hill NA, Rutherford DJ, Dunbar MJ, Stanish WD.** Co-activation differences in lower limb muscles between asymptomatic controls and those with varying degrees of knee osteoarthritis during walking. Clin Biomech 2009; 24(5):407-414.

112. **Berth A, Urbach D, Awiszus F.** Improvement of voluntary quadriceps muscle activation after total knee arthroplasty. Arch Phys Med Rehabil 2002; 83(10):1432-1436.

113. **Mizner RL, Petterson SC, Snyder-Mackler L.** Quadriceps strength and the time course of functional recovery after total knee arthroplasty. J Orthop Sports Phys Ther 2005; 35(7):424-436.

114. **Cavanagh PR, Komi PV.** Electromechanical delay in human skeletal muscle under concentric and eccentric contractions. Eur J Appl Physiol Occup Physiol 1979; 42(3):1 59-163.

115. **Vos EJ, Mullender MG, van Ingen Schenau GJ.** Electromechanical delay in the vastus lateralis muscle during dynamic isometric contractions. Eur J Appl Physiol 1990; 60:467-471.

116. **Muraoka T, Muramatsu T, Fukunaga T, Kanehisa H.** Influence of tendon slack on electromechanical delay in the human medial gastrocnemius in vivo. J Appl Physiol (1985) 2004; 96(2):540-544.

117. **Winter EM, Brookes FB.** Electromechanical response times and muscle elasticity in men and women. Eur J Appl Physiol Occup Physiol 1991; 63(2):124-128.

118. **Bell DG, Jacobs I.** Electro-mechanical response times and rate of force development in males and females. Med Sci Sports Exerc 1986; 18(1):31-36.

119. **Zhou S, McKenna MJ, Lawson DL, Morrison WE, Fairweather I.** Effects of fatigue and sprint training on electromechanical delay of knee extensor muscles. Eur J Appl Physiol Occup Physiol 1996; 72(5-6):410-416.

120. **Hopkins JT, Brown TN, Christensen L, Palmieri-Smith RM.** Deficits in peroneal latency and electromechanical delay in patients with functional ankle instability. J Orthop Res 2009; 27(12):1541-1546.

121. **Huijing PA.** Epimuscular myofascial force transmission: a historical review and implications for new research. International Society of Biomechanics Muybridge Award Lecture, Taipei, 2007. J Biomech 2009; 42(1):9-21.

122. **Graichen F, Arnold R, Rohlmann A, Bergmann G.** Implantable 9-channel telemetry system for in vivo load measurements with orthopedic implants. IEEE Trans Biomed Eng 2007; 54(2):253-261.

123. **Bender A, Bergmann G.** Determination of typical patterns from strongly varying signals. Comput Methods Biomech Biomed Engin 2012; 15(7):761-769.

124. **Orthoload.** Loading of Orthopaedic Implants. https://orthoload.com/database/ (Search: Database, Knee Joint, last accessed on June 17, 2020 at 19:14h).

125. **Yamauchi K, Yoshiko A, Suzuki S, Kato C, Akima H, Kato T, Ishida K.** Estimation of individual thigh muscle volumes from a single-slice muscle cross-sectional area and muscle thickness using magnetic resonance imaging in patients with knee osteoarthritis. J Orthop Surg (Hong Kong) 2017; 25(3):2309499017743101.

126. **Strandberg S, Wretling ML, Wredmark T, Shalabi A.** Reliability of computed tomography measurements in assessment of thigh muscle cross-sectional area and attenuation. BMC Med Imaging 2010; 10:18.

127. **Aubrey J, Esfandiari N, Baracos VE, Buteau FA, Frenette J, Putman CT, Mazurak VC.** Measurement of skeletal muscle radiation attenuation and basis of its biological variation. Acta Physiol (Oxf) 2014; 210(3):489-497.

128. **Goodpaster BH, Kelley DE, Thaete FL, He J, Ross R.** Skeletal muscle attenuation determined by computed tomography is associated with skeletal muscle lipid content. J Appl Physiol (1985) 2000; 89(1):104-110.

129. **Hermens H, Freriks B, Merletti R, Stegeman D, Blok J, Rau G, Disselhorst-Klug C, Hägg G.** SENIAM: European recommendations for surface electromyography. Roessingh Res. Development 1999. http://www.seniam.org (last accessed on June 6, 2020 at 11:11h).

130. **Ghazwan A, Forrest SM, Holt CA, Whatling GM.** Can activities of daily living contribute to EMG normalization for gait analysis? PLoS One 2017; 12(4):e0174670.

131. **Heinlein B, Kutzner I, Graichen F, Bender A, Rohlmann A, Halder AM, Beier A, Bergmann G.** ESB Clinical Biomechanics Award 2008: Complete data of total knee replacement loading for level walking and stair climbing measured in vivo with a follow-up of 6-10 months. Clin Biomech (Bristol, Avon) 2009; 24(4):315-326.

132. **D'Lima DD, Patil S, Steklov N, Chien S, Colwell CW Jr.** In vivo knee moments and shear after total knee arthroplasty. J Biomech 2007; 40 Suppl 1:S11-S17.

133. **D'Lima DD, Patil S, Steklov N, Slamin JE, Colwell CW Jr.** The Chitranjan Ranawat Award: in vivo knee forces after total knee arthroplasty. Clin Orthop Relat Res 2005; 440:45-49.

134. **Kutzner I, Heinlein B, Graichen F, Bender A, Rohlmann A, Halder A, Beier A, Bergmann G.** Loading of the knee joint during activities of daily living measured in vivo in five subjects. J Biomech 2010; 43(11): 2164-2173.

135. **Bergmann G, Bender A, Graichen F, Dymke J, Rohlmann A, Trepczynski A, Heller MO, Kutzner I.** Standardized Loads Acting in Knee Implants. PLoS ONE 2014; 9(1): e86035.

136. **Taylor WR, Schütz P, Bergmann G, List R, Postolka B, Hitz M, Dymke J, Damm P, Duda G, Gerber H, Schwachmeyer V, Hosseini Nasab SH, Trepczynski A, Kutzner I.** A comprehensive assessment of the musculoskeletal system: The CAMS-Knee data set. J Biomech 2017; 65:32-39.

137. **Sasaki K, Neptune RR.** Individual muscle contributions to the axial knee joint contact force during normal walking. J Biomech 2010; 43(14):2780-2784.

138. **D'Lima DD, Fregly BJ, Patil S, Steklov N, Colwell CW Jr.** Knee joint forces: prediction, measurement, and significance. Proc Inst Mech Eng H 2012; 226(2):95-102.

139. **Arnout N, Vanlommel L, Vanlommel J, Luyckx JP, Labey L, Innocenti B, Victor J, Bellemans J.** Post-cam mechanics and tibiofemoral kinematics: a dynamic in vitro analysis of eight posterior-stabilized total knee designs. Knee Surg Sports Traumatol Arthrosc 2015; 23(11):3343-3353.

140. **Andriacchi TP, Dyrby CO.** Gait analysis and Total Knee Replacement. In: Bellemans J. Total Knee Arthroplasty: A Guide To Get Better Performance. Springer Science & Business Media 2005; 40-41.

141. **Damm P, Zonneveld J, Brackertz S, Streitparth F, Winkler T.** Gluteal muscle damage leads to higher in vivo hip joint loads 3 months after total hip arthroplasty. PLoS One 2018; 13(1): e0190626.

142. **Suetta C, Aagaard P, Rosted A, Jakobsen AK, Duus B, Kjaer M, Magnusson SP.** Training-induced changes in muscle CSA, muscle strength, EMG, and rate of force development in elderly subjects after long-term unilateral disuse. J Appl Physiol (1985) 2004; 97(5):1954-1961.

143. **Walls RJ, McHugh G, O'Gorman DJ, Moyna NM, O'Byrne JM.** Effects of preoperative neuromuscular electrical stimulation on quadriceps strength and functional recovery in total knee arthroplasty. A pilot study. BMC Musculoskelet Disord 2010; 11:119.

144. **Frontera WR, Hughes VA, Fielding RA, Fiatarone MA, Evans WJ, Roubenoff R.** Aging of skeletal muscle: a 12-yr longitudinal study. J Appl Physiol (1985) 2000; 88(4):1321-1326.

145. **Akagi R, Takai Y, Ohta M, Kanehisa H, Kawakami Y, Fukunaga T.** Muscle volume compared to cross-sectional area is more appropriate for evaluating muscle strength in young and elderly individuals. Age Ageing 2009; 38(5):564-569.

146. **Alway SE, Coggan AR, Sproul MS, Abduljalil AM, Robitaille PM.** Muscle torque in young and older untrained and endurance-trained men. J Gerontol A Biol Sci Med Sci 1996; 51(3):B195-B201.

147. **Kumar D, Karampinos DC, MacLeod TD, Lin W, Nardo L, Li X, Link TM, Majumdar S, Souza RB.** Quadriceps intramuscular fat fraction rather than muscle size is associated with knee osteoarthritis. Osteoarthritis Cartilage 2014; 22(2):226-234.

148. **Pedroso MG, de Almeida AC, Aily JB, de Noronha M, Mattiello SM.** Fatty infiltration in the thigh muscles in knee osteoarthritis: a systematic review and meta-analysis. Rheumatol Int 2019; 39(4): 627-635.

149. **Taaffe DR, Henwood TR, Nalls MA, Walker DG, Lang TF, Harris TB.** Alterations in muscle attenuation following detraining and retraining in resistance-trained older adults. Gerontology 2009; 55(2):217-223.

150. **Ryan AS, Nicklas BJ, Berman DM, Dennis KE.** Dietary restriction and walking reduce fat deposition in the midthigh in obese older women. Am J Clin Nutr 2000; 72(3):708-713.

151. **Goodpaster BH, Chomentowski P, Ward BK, Rossi A, Glynn NW, Delmonico MJ, Kritchevsky SB, Pahor M, Newman AB.** Effects of physical activity on strength and skeletal muscle fat infiltration in older adults: a randomized controlled trial. J Appl Physiol (1985) 2008; 105(5):1498-1503.

152. **Palmieri-Smith RM, McLean SG, Ashton-Miller JA, Wojtys EM.** Association of quadriceps and hamstrings cocontraction patterns with knee joint loading. J Athl Train 2009; 44(3): 256-263.

153. **Marcus RL, Yoshida Y, Meier W, Peters C, Lastayo PC.** An Eccentrically Biased Rehabilitation Program Early after TKA Surgery. Arthritis 2011; 2011:353149.

154. **Anderson FC, Pandy MG.** Individual muscle contributions to support in normal walking. Gait & Posture 2003; 17(2):159-169.

155. **Neptune RR, Kautz SA, Zajac FE.** Contributions of the individual ankle plantar flexors to support, forward progression and swing initiation during walking. J Biomech 2001; 34(11):1387-1398.

156. **Winter DA, Yack HJ.** EMG profiles during normal human walking: stride-to-stride and inter-subject variability. Electroencephalogr Clin Neurophysiol 1987; 67(5):402-411.

157. **McFadyen BJ, Winter DA.** An integrated biomechanical analysis of normal stair ascent and descent. J Biomech 1988; 21(9):733-744.

158. **Riener R, Rabuffetti M, Frigo C.** Stair ascent and descent at different inclinations. Gait Posture 2002; 15(1):32-44.

159. **Protopapadaki A, Drechsler WI, Cramp MC, Coutts FJ, Scott OM.** Hip, knee, ankle kinematics and kinetics during stair ascent and descent in healthy young individuals. Clin Biomech (Bristol, Avon) 2007; 22(2):203-210.

160. **Startzell JK, Owens DA, Mulfinger LM, Cavanagh PR.** Stair negotiation in older people: a review. J Am Geriatr Soc 2000; 48(5):567-580.

161. **Boonstra MC, Schwering PJ, De Waal Malefijt MC, Verdonschot N.** Sit-to-stand movement as a performance-based measure for patients with total knee arthroplasty. Phys Ther 2010; 90(2):149-156.

162. **Farquhar SJ, Reisman DS, Snyder-Mackler L.** Persistence of altered movement patterns during a sit-to-stand task 1 year following unilateral total knee arthroplasty. Phys Ther 2008; 88(5):567-579.

163. **Roebroeck ME, Doorenbosch CA, Harlaar J, Jacobs R, Lankhorst GJ.** Biomechanics and muscular activity during sit-to-stand transfer. Clin Biomech (Bristol, Avon) 1994; 9(4):235-244.

164. **Millington PJ, Myklebust BM, Shambes GM.** Biomechanical analysis of the sit-to-stand motion in elderly persons. Arch Phys Med Rehabil 1992; 73(7):609-617.

165. **Zätterström R, Fridén T, Lindstrand A, Moritz U.** The effect of physiotherapy on standing balance in chronic anterior cruciate ligament insufficiency. Am J Sports Med 1994; 22(4): 531-536.

166. **Norman RW, Komi PV.** Electromechanical delay in skeletal muscle under normal movement conditions. Acta Physiologica Scandinavica 1979, 106: 241-248.

167. **Cowan SM, Bennell KL, Hodges PW, Crossley KM, McConnell J.** Delayed onset of electromyographic activity of vastus medialis obliquus relative to vastus lateralis in subjects with patellofemoral pain syndrome. Arch Phys Med Rehabil 2001; 82(2):183-189.

168. **Konrath JM, Saxby DJ, Killen BA, Pizzolato C, Vertullo CJ, Barrett RS, Lloyd DG.** Muscle contributions to medial tibiofemoral compartment contact loading following ACL reconstruction using semitendinosus and gracilis tendon grafts. PLoS One 2017; 12(4):e0176016.

169. **Williams GN, Snyder-Mackler L, Barrance PJ, Axe MJ, Buchanan TS.** Muscle and tendon morphology after reconstruction of the anterior cruciate ligament with autologous semitendinosus-gracilis graft. J Bone Joint Surg Am 2004; 86(9):1936-1946.

170. **Mitchell WK, Williams J, Atherton P, Larvin M, Lund J, Narici M.** Sarcopenia, dynapenia, and the impact of advancing age on human skeletal muscle size and strength; a quantitative review. Front Physiol 2012; 3:260.

171. **Goodpaster BH, Park SW, Harris TB, Kritchevsky SB, Nevitt M, Schwartz AV, Simonsick EM, Tylavsky FA, Visser M, Newman AB.** The loss of skeletal muscle strength, mass, and quality in older adults: the health, aging and body composition study. J Gerontol A Biol Sci Med Sci 2006; 61(10):1059-1064.

172. **Kutzner I, Trepczynski A, Heller MO, Bergmann G.** Knee adduction moment and medial contact force--facts about their correlation during gait. PLoS One 2013; 8(12):e81036.

173. **Baliunas AJ, Hurwitz DE, Ryals AB, Karrar A, Case JP, Block JA, Andriacchi TP.** Increased knee joint loads during walking are present in subjects with knee osteoarthritis. Osteoarthritis Cartilage 2002; 10(7):573-579.

174. **Tidball JG.** Force transmission across muscle cell membranes. J Biomech 1991; 24 Suppl 1:43-52.

175. **Trepczynski A, Kutzner I, Schwachmeyer V, Heller MO, Pfitzner T, Duda GN.** Impact of antagonistic muscle co-contraction on in vivo knee contact forces. J Neuroeng Rehabil 2018; 15(1):101.

176. **Demers MS, Pal S, Delp SL.** Changes in tibiofemoral forces due to variations in muscle activity during walking. J Orthop Res 2014; 32(6):769-776.

177. **MacWilliams BA, Wilson DR, DesJardins JD, Romero J, Chao EY.** Hamstrings cocontraction reduces internal rotation, anterior translation, and anterior cruciate ligament load in weight-bearing flexion. J Orthop Res 1999; 17(6): 817-822.

178. **Yavuz SU, Sendemir-Urkmez A, Türker KS.** Effect of gender, age, fatigue and contraction level on electromechanical delay. Clin Neurophysiol 2010; 121(10):1700-1706.

179. **Maffiuletti NA, Aagaard P, Blazevich AJ, Folland J, Tillin N, Duchateau J.** Rate of force development: physiological and methodological considerations. Eur J Appl Physiol. 2016; 116(6): 1091-1116.

180. **Aagaard P, Simonsen EB, Andersen JL, Magnusson P, Dyhre-Poulsen P.** Increased rate of force development and neural drive of human skeletal muscle following resistance training. J Appl Physiol (1985) 2002; 93(4):1318-1326.

181. **Mora I, Quinteiro-Blondin S, Pérot C.** Electromechanical assessment of ankle stability. Eur J Appl Physiol 2003; 88(6):558-564.

182. **Gribble PA, Robinson RH.** Alterations in knee kinematics and dynamic stability associated with chronic ankle instability. J Athl Train 2009; 44(4):350-355.

183. **Piva SR, Gil AB, Almeida GJ, DiGioia AM 3rd, Levison TJ, Fitzgerald GK.** A balance exercise program appears to improve function for patients with total knee arthroplasty: a randomized clinical trial. Phys Ther 2010; 90(6):880-894.

184. **Benedetti MG, Catani F, Bilotta TW, Marcacci M, Mariani E, Giannini S.** Muscle activation pattern and gait biomechanics after total knee replacement. Clin Biomech 2003; 18(9):871-876.

185. **LaStayo PC, Meier W, Marcus RL, Mizner R, Dibble L, Peters C.** Reversing muscle and mobility deficits 1 to 4 years after TKA: a pilot study. Clin Orthop Relat Res 2009; 467(6):1493-1500.

186. **Bourne RB, Chesworth BM, Davis AM, Mahomed NN, Charron KD.** Patient satisfaction after total knee arthroplasty: who is satisfied and who is not? Clin Orthop Relat Res 2010; 468(1):57-63.

187. **Vessely MB, Whaley AL, Harmsen WS, Schleck CD, Berry DJ.** The Chitranjan Ranawat Award: Long-term Survivorship and Failure Modes of 1000 Cemented Condylar Total Knee Arthroplasties. Clinical Orthopaedics and Related Research 2006; 452:28-34.

188. **Grimberg A, Jansson V, Melsheimer O, Steinbrück A.** Endoprothesenregister Deutschland (EPRD) - Jahresbericht 2019. Arnd 2019. https://www.eprd.de/de/ (Search: EPRD Jahresbericht 2019, last accessed on June 06, 2020 at 11:41h).

189. **Jansson V, Grimberg A, Melsheimer O, Perka C, Steinbrück A.** Orthopaedic registries: the German experience. EFORT Open Reviews 2019; 4(6): 401-408.

190. **Swank AM, Kachelman JB, Bibeau W, Quesada PM, Nyland J, Malkani A, Topp RV.** Prehabilitation before total knee arthroplasty increases strength and function in older adults with severe osteoarthritis. J Strength Cond Res 2011; 25(2):318-325.

191. **Westby MD, Marshall DA, Jones CA.** Development of quality indicators for hip and knee arthroplasty rehabilitation. Osteoarthritis Cartilage 2018; 26(3):370-382.

192. **McMahon M, Block JA.** The risk of contralateral total knee arthroplasty after knee replacement for osteoarthritis. J Rheumatol 2003; 30(8):1822-1824.

Statutory Declaration

I, Louisa Bell, by personally signing this document in lieu of an oath, hereby affirm that I prepared the submitted dissertation on the topic "Interrelationship of periarticular muscle status, electromyographic activity, electromechanical delay and *in vivo* knee joint loads after total knee artroplasty" (English title), "Zusammenhang von periartikulärem Muskelstatus, Elektromyographie, elektromechanischer Verzögerung und *in vivo* Kniebelastungen nach Knietotalendoprothesen-Implantation" (German title), independently and without the support of third parties, and that I used no other sources and aids than those stated.

All parts which are based on the publications or presentations of other authors, either in letter or in spirit, are specified as such in accordance with the citing guidelines. The sections on methodology (in particular regarding practical work, laboratory regulations, statistical processing) and results (in particular regarding figures, charts and tables) are exclusively my responsibility.

My contributions to any publications to this dissertation correspond to those stated in the below joint declaration made together with the supervisor. All publications created within the scope of the dissertation comply with the guidelines of the ICMJE (International Committee of Medical Journal Editors; www.icmje.org) on authorship. In addition, I declare that I am aware of the regulations of Charité – Universitätsmedizin Berlin on ensuring good scientific practice and that I commit to comply with these regulations.

The significance of this statutory declaration and the consequences of a false statutory declaration under criminal law (Sections 156, 161 of the German Criminal Code) are known to me.

14.09.2020   _____

Date   Signature

Curriculum Vitae

Mein Lebenslauf wird aus datenschutzrechtlichen Gründen in der elektronischen Version meiner Arbeit nicht veröffentlicht.

Declaration of Contribution

Louisa Bell contributed the following to the below listed presentations:

1   Bell L, Damm P, Baur ADJ, Winkler T. The effect of knee muscle status on *in vivo* measured joint loadings after total knee arthroplasty: long-term results. Deutscher Kongress für Orthopädie und Unfallchirurgie (DKOU), Berlin, 2019.

  • *Analysis and interpretation of data on in vivo knee joint loads and periarticular muscle status, writing of the abstract and presentation. The presented Figures 9, 10a, 12a, 15a, 24 were created on the basis of my statistical evaluation.*

2   Bell L, Winkler T, Baur ADJ, Perka C, Duda GN, Damm P. Einfluss des allgemeinen Muskelstatus auf die Belastung des Kniegelenks. 13. Endoprothetikkongress Berlin (EKB2020), Berlin, 2020.

  • *Data analysis and interpretation of vivo knee joint loads and skeletal muscle status, writing of the abstract and presentation. The presented Figures 9, 10a, 15a, 24a were created on the basis of my statistical evaluation.*

3   Bell L, Damm P, Baur ADJ, Perka C, Duda GN, Winkler T. Effect of periarticular skeletal muscle status on *in vivo* knee joint loads – an analysis after total knee arthroplasty. 1st Virtual EFORT Congress (VEC), 2020.

  • *Data analysis and interpretation of vivo knee joint loads and periarticular muscle status, writing of the abstract and preparation of e-poster. Figures two to four of the e-poster were created on the basis of my statistical evaluation.*

_____

Signature, date and stamp of supervising university professor / lecturer

_____

Signature of doctoral candidate

Certificate of Statistics

CHARITÉ

CharitéCentrum für Human- und Gesundheitswissenschaften

Charité | Campus Charité Mitte | 10117 Berlin

Institut für Biometrie und klinische Epidemiologie (iBikE)

Direktor: Prof. Dr. Geraldine Rauch

Postanschrift:
Charitéplatz 1 | 10117 Berlin
Besucheranschrift:
Reinhardtstr. 58 | 10117 Berlin

Tel. +49 (0)30 450 562171
geraldine.rauch@charite.de
https://biometrie.charite.de/

Name, Vorname: Bell, Louisa

Emailadresse:

Matrikelnummer:

PromotionsbetreuerIn: PD Dr. Tobias Winkler

Promotionsinstitution / Klinik: Centrum für Muskuloskeletale Chirurgie

Bescheinigung

Hiermit bescheinige ich, dass Frau Louisa Bell innerhalb der Service Unit Biometrie des Instituts für Biometrie und klinische Epidemiologie (iBikE) bei mir eine statistische Beratung zu einem Promotionsvorhaben wahrgenommen hat. Folgende Beratungstermine wurden wahrgenommen:

- Termin 1: *19.12.2018*
- Termin 2: *14.03.2019*
- Termin 3: *20.03.2019*
- Termin 4: *20.12.2019*

Folgende wesentliche Ratschläge hinsichtlich einer sinnvollen Auswertung und Interpretation der Daten wurden während der Beratung erteilt:

- Wilcoxon Test
- t-Test (für verbundene Stichproben)
- ANOVA

Diese Bescheinigung garantiert nicht die richtige Umsetzung der in der Beratung gemachten Vorschläge, die korrekte Durchführung der empfohlenen statistischen Verfahren und die richtige Darstellung und Interpretation der Ergebnisse. Die Verantwortung hierfür obliegt allein dem Promovierenden. Das Institut für Biometrie und klinische Epidemiologie übernimmt hierfür keine Haftung.

Datum: 20.12.2019   Name des Beraters/ der Beraterin:

Unterschrift BeraterIn, Institutsstempel

CHARITÉ
UNIVERSITATSMEDIZIN BERLIN
Institut für Biometrie und Klinische Epidemiologie
Campus Charité Mitte
Charitéplatz 1 | D-10117 Berlin
Besucheranschrift: Rahel-Hirsch-Weg 5

Acknowledgement